UNITED TECHNOLOGIES RESEARCH CENTER

UNITED TECHNOLOGIES™

East Hartford, Connecticut 06108

NASA CR-134982

R76-912038-12

EXPOSURE DAMAGE MECHANISMS FOR KCl WINDOWS IN HIGH POWER LASER SYSTEMS

Final Report

By

P. R. Blaszuk, B. A. Woody, C. O. Hulse, J. W. Davis, J. P. Waters

Prepared for

NATIONAL AERONAUTICS AND SPACE ADMINISTRATION

NASA Lewis Research Center

Contract NAS3-18928

R. A. Lindberg, Project Manager

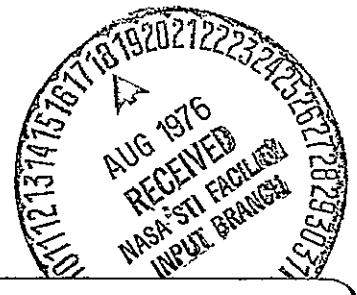

DATE March 1976

NO. OF PAGES 146

COPY NO. _____

UNITED TECHNOLOGIES
RESEARCH CENTER

UNITED TECHNOLOGIES

East Hartford, Connecticut 06108

NASA CR-134982

R76-912038-12

EXPOSURE DAMAGE MECHANISMS FOR KCl WINDOWS IN HIGH POWER LASER SYSTEMS

Final Report

By

P. R. Blaszuk, B. A. Woody, C. O. Hulse, J. W. Davis, J. P. Waters

Prepared for

NATIONAL AERONAUTICS AND SPACE ADMINISTRATION

NASA Lewis Research Center

Contract NAS3-18928

R. A. Lindberg, Project Manager

DATE March 1976

NO. OF PAGES 146

COPY NO. _____

1. Report No	2 Government Accession No	3 Recipient's Catalog No
NASA CR-134982		

4 Title and Subtitle	5 Report Date
EXPOSURE DAMAGE MECHANISMS FOR KCl WINDOWS IN HIGH POWER LASER SYSTEMS	March 15, 1976
	6 Performing Organization Code

7. Author(s)	8 Performing Organization Report No
Blaszuk, P. R. Hulse, C. O. Waters, J. P. Woody, B. A. Davis, J. W.	R76-912038-12
	10 Work Unit No

9. Performing Organization Name and Address	11 Contract or Grant No
United Technologies Research Center Silver Lane East Hartford, CT 06108	NAS3-18928
	13. Type of Report and Period Covered Final Report Nov. 1974-March 1976

12 Sponsoring Agency Name and Address	14 Sponsoring Agency Code
National Aeronautics and Space Administration NASA Lewis Research Center 21000 Brookpark Ave. Cleveland, OH	

15 Supplementary Notes

16 Abstract

This work describes an experimental study of the 10.6 micrometer and 0.6328 micrometer optical properties of single crystal KCl and europium-doped polycrystal KCl subjected to 10.6 micrometer irradiation and high temperature. Significant variations in the optical properties are observed over periods of exposure up to 100 hours. Models are proposed to predict the 10.6 micrometer absorptivity for long exposure periods. Mechanical creep has been detected in both materials at high temperature.

17. Key Words (Suggested by Author(s))	18. Distribution Statement
KCl Damage Laser Window Thermal damage Irradiation damage creep	Unlimited

19. Security Classif. (of this report)	20 Security Classif. (of this page)	21. No of Pages	22 Price*
UNCLASSIFIED	UNCLASSIFIED	146	$3.00

* For sale by the National Technical Information Service, Springfield, Virginia 22161

NASA-C-168 (Rev 10-75)

TABLE OF CONTENTS

FOREWORD

The work described herein was done at the United Technologies Research Center, under NASA Contract NAS3-18928, with Mr. R. A. Lindberg, Materials and Structures Division, NASA-Lewis Research Center, as Project Manager.

SUMMARY

The primary objective of this program was to evaluate the factors that influence the lifetime of alkali-halide windows for use in high-power lasers in a space environment. Projected lifetime requirements for space missions are on the order of 10,000 hours and longer. Data generated under the program, together with supporting analyses, are used both to predict window lifetime and to establish specifications for long-life windows.

The method of approach in the program involves the exposure of alkali-halide test windows to hard vacuum, high temperature, and high 10.6 micrometer flux loading (carbon dioxide laser radiation) and monitoring the optical properties of the test windows. Both the temperature and irradiation exposure tests were conducted with the windows under a pressure preload sufficient to raise the outer fiber stress at the center of the window to 30 percent of the room temperature yield stress for the material. These optical properties along with pertinent mechanical properties have been determined as a function of exposure history for time periods up to 100 hours to provide insight into the mechanisms leading to window damage. These results have been extrapolated to the very long exposure times required for space missions.

Following is a summary of the program which has been conducted to evaluate both single-crystal KCl and europium-doped polycrystal KCl test windows supplied by NASA.

Task I - Material Characterization

The following properties have been measured with the windows in the as-received condition:

1. Single-point determinations of Poisson's ratio at 20, 66, 118, 179 and 250C.

2. Single-point determinations of yield stress in bending at 20, 66, 118, 179 and 250C.

3. Single-point determinations of Young's modulus in bending at 20, 66, 118, 179 and 250C.

4. Triplicate determinations of average surface grain size of europium-doped polycrystal KCl.

5. Single-point determinations of the absorption coefficient, beta, at a wavelength of 10.6 micrometers (CO_2).

6. Multipoint traverse determinations of the index of refraction and extinction moduli at a wavelength of 0.6328 micrometers (He-Ne).

7. Multipoint traverse determinations of the photometric absorption at a wavelength of 0.6328 micrometers (He-Ne).

Task II - Single-Crystal Evaluation

In this task the effects of up to 100-hr CO_2 laser beam exposure of the crystals were evaluated, and the effects of thermal aging in an ultrahigh vacuum were determined for exposure times up to 100 hours and temperatures up to 250°C. The single-crystal windows were subjected to two separate experiments. The first consisted of simultaneous exposure to 10.6 micrometer irradiation and high vacuum loading. The second consisted of operating the windows at elevated temperatures while under a high vacuum loading to determine if thermal aging effects were present.

Laser Beam Exposure

The major elements of this experiment were the development of the exposure chamber and window mounting techniques, the exposure tests, and the crystal evaluation.

Apparatus Requirements

An exposure chamber and window mounts were developed to mount four windows, each with one face exposed to an oil-free ultrahigh vacuum (10^{-8} torr) and the other face exposed to a constant pressure of pure nitrogen. The nitrogen pressure was adjusted so that the total prestress at the center portion of each window was approximately 30 percent of the yield stress. The apparatus included a means of exposing all four windows simultaneously to predetermine power densities of CO_2 laser radiation.

Exposure Tests

The test windows were exposed to cw CO_2 laser beam radiation for cumulative times of 1.5, 4.3, 12.3, 35 and 100 hours. After each successive exposure period the windows were demounted and measurements made of the absorption coefficient, index of refraction and extinction modulus. The power density levels at the four windows were set at 1000 W/cm^2, 1495 W/cm^2, 2236 W/cm^2 and 5000 W/cm^2, respectively. These levels were based on the average intensity in the $1/e^2$ spot of a Gaussian mode beam.

Evaluation

Nondestructive tests of the windows after each exposure period included (1) measurement of the absorption coefficient, β, at 10.6 micrometers using a CO_2 laser absorption calorimeter and (2) measurements of the absorption coefficient and index of refraction in the visible at the 0.6328 micrometer wavelength using a cw He-Ne laser.

Crystal Evaluation

During the course of the experiment, one test window failed by mechanical fracture and another was removed from testing because of the possibility of contamination. The four windows that completed the test cycle showed a slow increase in the 10.6 micrometer absorptivity with considerable fluctuation during the 100-hour test period. A model has been developed to predict the 10.6 micrometer absorptivity as a function of time. No strong correlation between the 10.6 micrometer absorptivity and the visible optical properties was discovered. There are isolated cases where one or the other of the visible properties does show strong correlation to the 10.6 micrometer absorptivity. No correlation between the intensity of irradiation and the rate of increase of the 10.6 micrometer absorptivity was observed.

Thermal Aging of Windows

The major elements of this experiment were the development of the temperature-aging chamber, the aging tests and the crystal evaluation.

Apparatus Requirements

The general requirements for this apparatus were similar to those for the exposure chamber. In this experiment five windows were mounted, each with one face exposed to a 10^{-8} torr oil-free vacuum, and the other face exposed to a pure N_2 pressure sufficient to provide a prestress to 30 percent of yield. In addition, provision was made to heat the crystals to temperatures up to 250°C.

Aging Tests

The five test windows were simultaneously aged for cumulative times of 1.5, 4.3, 12.3, 35 and 100 hrs. The five windows were maintained at temperatures of 20, 66, 118, 179 and 250°C, respectively. Optical measurements of the crystals were made after each successive aging period.

Single-Crystal Evaluation

Testing of the windows exposed at 179° and 250°C was terminated at 4.3 hours of cumulative exposure with the consent of the NASA program manager. Deformation of these windows due to creep was so severe that the possibility of an implosion in the test rig required their removal. An experiment was devised to measure the optical flatness of the remaining test windows and measurements were initiated at the 12.3-hour test point. These measurements showed the presence of creep in all the remaining windows with the exception of the window at 20°C. A model predicting the time and temperature dependence of the radius of curvature of the window has been developed. The 10.6 micrometer absorptivity of the test windows was found to increase with time. The rate of increase of the 10.6 micrometer absorptivity was found to be higher for windows with a low initial 10.6 micrometer absorptivity and to increase with increasing exposure temperature. Models for the rate of increase are presented. There was no general correlation of the 10.6 micrometer and visible optical properties, although in isolated instances strong correlations have been found between the 10.6 micrometer absorptivity and the index of refraction and % transmittance at 0.6328 micrometers.

Task III - Evaluation of Europium-Doped Polycrystal KCl

In this task the experiments performed under Task II with single-crystal KCl were repeated with the europium-doped polycrystal KCl. With respect to the irradiation testing, all four of the europium-doped polycrystal KCl windows survived without incident to the 100-hour test point. As in the single-crystal material, a general increasing trend was observed in the 10.6 micrometer absorptivity. The rate of increase in the 10.6 micrometer absorptivity was found to be dependent on the initial value of absorptivity. As in the single-crystal material, low-absorptivity windows are damaged at a faster rate. No correlation between the rate of increase of absorptivity and intensity was found. A model predicting the temporal variation of the 10.6 micrometer absorptivity has been developed to predict absorptivities at long exposure times. The correlation of the 10.6 micrometer optical properties with the visible optical properties again yields isolated examples of correlated behavior but no general trends for all four windows.

During the course of the thermal aging test of the europium-doped polycrystal KCl, two of the test windows cracked. In both cases the windows remained intact and continued to carry the design pressure preload to the 100-hour point. The 10.6 micrometer absorptivity of the test windows showed a general increase in time with significant fluctuations. Departing from the

previous experiments, the rate of increase of the 10.6 micrometer absorptivity showed no strong correlation with either temperature or the initial value of the 10.6 micrometer absorptivity. The index of refraction at 0.6328 micrometers shows several examples of very strong temporal correlation. Creep was also observed in these test windows but only in the windows tested at 179°C and 250°C. A model predicting the time and temperature dependence of the radius of curvature of the windows undergoing creep has been developed.

Task IV - Prediction of Longer Term Effects

Analysis of the data generated in the previous tasks has allowed the formulation of models that may be used to predict the 10.6 micrometer absorptivity of single-crystal KCl and europium-doped polycrystal KCl for long-term exposure to irradiation. Models for the rate of deflection or change of radius of curvature of the window materials as a function of temperature and time have been developed.

INTRODUCTION

The achievement of reliable high-power, cw, CO_2 lasers has indicated a need for the rapid expansion of the research and development efforts to produce a reliable high-power window material. Many of the potential applications of the high-power CO_2 lasers are such that an aerodynamic window is either technically or financially impractical. This is especially true for anticipated NASA missions which will require long operating times and minimal gas consumption. A measure of the increased efforts to produce reliable material windows can be seen in the growth of the Annual Conference on High-Power Infrared Laser Window Materials sponsored by Air Force Cambridge Research Laboratories. With respect to the alkali-halide materials, divalent ion doping and the creation of a fine grain polycrystalline structure (Ref. 1, 2) have emerged as techniques for greatly enhancing the strength of the halide. Double hardening (the simultaneous use of two hardening techniques) has also been demonstrated (Ref. 3). Reduction in the extrinsic absorptivity of the halides have been made and material with absorptivity essentially at the intrinsic multiphonon level has been produced (Ref. 4, 5). Considerable theoretical work has also been produced, investigating the absorption process itself, such as the work of Sparks (Ref. 6). Investigation of direct damage mechanisms has been confined to a large degree to pulsed systems.

Under Contract NAS3-18928 sponsored by the NASA-Lewis Research Center the United Technologies Research Center has conducted an investigation of the damage mechanisms in alkali-halide window materials for use in high-power lasers. The primary objective of the program was to predict the life expectancy of these windows under conditions that prevail in space. The goal was to predict the window properties for useful lifetimes of 10,000 hours and greater. In this program both single crystal KCl and europium-doped polycrystal KCl were evaluated. The evaluation was made by monitoring selected optical and mechanical properties of the NASA-supplied window materials under conditions of temperature and cw CO_2 laser radiation exposure in a carefully controlled environment.

TECHNICAL PROGRESS SUMMARY

Characterization of KCl Window Optical Parameters at 0.6328 Micrometers

In this part of the program the absorption coefficient, refractive index and extinction coefficient of NASA-supplied KCl laser windows were measured at a wavelength of 0.6328 micrometers as a function of 10.6 micrometer exposure and temperature aging conditions. The initial goals of this effort were to obtain accurate and repeatable data on these optical parameters. The methods employed were restricted to noncontacting techniques to avoid the possibility of window contamination. Additionally, since these materials are hygroscopic, all measurements were performed in a dry, inert gas atmosphere. A technique based on measurement of Brewster's angle was chosen for the refractive index determination, and the absorption coefficient at 0.6328 micrometers was measured by direct comparison with a standard window. Once absorption and index are known, the extinction coefficient can then be calculated using the following equation:

$$k = \frac{\beta\lambda}{4\pi\eta} \qquad (1)$$

where k is the extinction coefficient
β is the absorption coefficient at wavelength
λ is the wavelength of light used (0.6328 micrometers)
η is the index of refraction at wavelength

Refractive Index Measurements

The refractive index measurements were carried out by means of an experimental setup described in Ref. 7 and shown schematically in Fig. 1. This Brewster's angle measurement technique was originally intended to be carried out by first aligning the sample so that the incident beam is reflected directly back upon itself (retroreflected) and then rotating the sample until the reflected beam intensity for "p" polarized light goes to zero. The angle through which the sample is rotated is then equal to Brewster's angle, and the index can be calculated directly from this angle. With this procedure, the initial sample orientation is as important to data accuracy as measurement of the angle at which minimum reflected intensity occurs. Thus, the alignment of the sample was to be performed using accurate retroreflected light and interferometric techniques. However, during the initial checkout and alignment phase of the program, it was determined that the reflected beam intensity was not sufficient to implement this approach.

In a new approach, a four-quadrant, two-axis, position-sensitive photodiode was chosen instead to perform the initial alignment, and its location in the system is indicated in Fig. 2. This device generates two signals one of which is proportional to the deviation of the impinging laser beam from the detector's vertical axis and the other is related to the deviation of the beam from the horizontal axis. To illustrate how initial alignment of the sample is achieved with this device, four different output signals and their corresponding beam positions are presented in Fig. 3. As shown, the signals obtained from the position-sensitive photodetector are for (a) beam centered on both axes, (b) beam unbalanced vertically, (c) beam unbalanced horizontally and (d) beam unbalanced both vertically and horizontally. The amplitude of the square wave is directly proportional to the distance from the center of the light beam to the appropriate axis.

The sensitivity of this method was determined using a glass optical flat mounted in the sample holder and aligning it with respect to the detector by means of the manual rotary and tilt stages. Slight changes in the sample orientation were then made while monitoring the signal from the detector. It was determined in this fashion that a change of 2 arc seconds produced a change in the output signal of about 15 percent. Repetitive trials have shown that errors as small as $\pm$ 1 arc second can be detected using this system for sample positioning. This type of error in determining Brewster's angle for KCl ($n = 1.4800$, $\phi = 55^{\circ}\ 57'\ 15''$) would mean an error in the index of $\pm\ 1.5 \times 10^{-5}$. As will be discussed later, this is approximately an order of magnitude less than the repeatability of the data at any one position, and therefore this alignment procedure will not limit the overall accuracy of the measurement. For initial calibration of the apparatus the detector was mounted at an arbitrary angle with respect to the incident beam (ϕ_m), as shown in Fig. 4. Its value was determined by placing a glass optical flat of known refractive index (as determined by the UTRC abbe refractometer) in the sample holder and adjusting the beam for a null on the position sensor. Then the rotary table was incremented until the angle of minimum reflection was found. Once this angular difference ($\Delta\phi$) between the starting angle ϕ_m and the Brewster angle $\overline{\phi}$ was known, the value of ϕ_m was determined knowing the refractive index as follows:

$$\phi_m = [\arctan (n)] - \Delta\phi \qquad (2)$$

This angle ϕ_m, was determined by the above procedure to be 14.83308°, and is used in all data.

Computer Regression Analysis

While the determination of ϕ_m was being made it also became evident that the reflection coefficient for "p" polarized light did not have a well-defined

minimum, but instead was a fairly wide based parabola. This phenomena is attributed to minute surface imperfections of the sample (grinding and polishing marks as well as impurities imbedded in the surface). In order to determine the position of the minimum value with a high degree of accuracy, a computer regression analysis program for the UTRC PDP-6 computer system was written. This program generates coefficients for polynomials of successively increasing degrees. As each set of coefficients for each polynomial is calculated a least squares analysis provides a measure of how well the generated formula fits the input data. When there is no improvement to the fit between successive polynomials the program terminates. (Almost all data acquired in the research program are successfully explained by a second degree polynomial fit.) The final equation is then differentiated, set equal to zero and solved for the angle at which minimum reflection occurs ($\Delta\phi$). The starting angle ϕ_m is added to ϕ_m and the tangent of the resulting angle is the refractive index of the sample at that position.

N.B.S. Reference Standard

In order to establish traceability to N.B.S., the index of KCl Single Crystal material at 0.6328 micrometerswas measured by N.B.S. using a method which did not require surface contacting fluids. This method, which measures the minimum deviation through a prism did require, however, that the sample be cut in the form of a prism. This was accomplished without affecting the utility of the sample as a reference standard in our system by removing chordal slices from the sample as shown in Fig. 5. The probe beam was then directed into the sample and a measurement made of the minimum deviation angle D_λ. By knowing the wavelength of light and the apex angle of the prism (α) the index at wavelength λ can be calculated from Newton's Formula:

$$n_\lambda = \frac{\sin(\alpha + D\lambda/2)}{\sin(\alpha/2)} \qquad (3)$$

This measurement has been performed and the index found to be $1.48804 \pm 5 \times 10^{-5}$.

Determination of System Accuracy

Before analysis of the NASA samples was performed, a glass optical flat of known refractive index was mounted in the sample holder and a series of three independent measurements were made which yielded a maximum variation in the index of 9.6×10^{-5}. It should be noted, however, that this value applies to glass which was found to have a sharper minimum than KCl. It was later found that a variation of 2×10^{-4} was obtained for repeated measurement at the same location on a KCl sample.

Analysis of NASA Samples

Refractive index data has been accumulated for some of the single crystal material at five positions along a diameter, starting 25.3 mm from the edge, as shown in Fig. 6. It was anticipated that the refractive index would be constant for each sample and slight variations would occur from sample to sample. However, the data show that this is not the case. Some samples such as Samples 1 and 8 exhibit a low index near one edge, rise to a peak near the center and then begin to drop off. However, Samples 5 and 7 appear to have almost a constant index along the diameter (see Tables 5 and 9). In addition, the average index (for the samples tabulated) ranges from a low of 1.4778 to a high of 1.4836 indicating a variation of 0.0058. This value is considerably greater than was first anticipated. Since this variation exceeds the repeatability figure by more than an order of magnitude, it is not likely that this can be attributed to system error.

The point-to-point variation in the index of refraction data obtained to date is considerably larger than was originally anticipated. The measurement of Brewster angle is a surface measurement. The angle at which the magnitude of the "p" polarization wave goes through zero is determined by the change in index at the surface and does not represent an average of the bulk index as does transmission techniques such as the minimum deviation technique used by N.B.S. on the prism sample. We are unable at the present time to determine if the severe fluctuations in index observed in the number 1 sample are purely a surface phenomena or whether the bulk index is actually changing by this amount.

Absorption Coefficient Measurement

Measuring absorption of IR radiation in materials is performed by attaching small thermocouples to the material, suspending it in vacuum and irradiating it with an IR laser emitting 50-200 watts. The temperature rise over a known time period can then be related to the absorption coefficient. In order to perform this measurement at 0.6328 micrometer, a laser of similar power would have to be used. This is not possible with present state-of-the-art He-Ne lasers. The maximum power currently available is 0.05 watts which would require several hours of irradiation to produce only a 0.1°C temperature change. (Radiation and conduction of the thermocouple wires would then constitute a significant source of error.) Bennett et al (Ref. 8), at the Michelson Laboratory have succeeded in measuring absorption of a prism sample with a He-Ne laser. They used a scanning mirror and measured transmitted beam intensity fluctuation as a function of sample thickness. In the present case the KCl material is not in a prism configuration, and therefore, this proven technique is not applicable. The technique used on these samples must therefore be a direct absorption technique which does not require specially prepared prism samples.

As shown in Fig. 7, the system selected for making these absorption measurements consists of a He-Ne laser beam which is split equally into two beams (reference and sample beams). These beams are directed through a chopper which allows passage of the beams alternately through the reference and test samples. The beams are then recombined at the second beamsplitter and impinge upon the photodetector. The photodetector output signal is a low amplitude square wave modulation riding upon a d.c. signal (proportional to laser power). The square wave amplitude is directly related to the differential absorption between the two samples. A lock-in amplifier is used to sense the a.c. component which is in proper phase with respect to the optical chopper. The lock-in selected for this system automatically corrects for any fluctuations in laser output power or photodetector sensitivity eliminating this possible source of error.

Telephone conversations with Drs. R. Foreman and A. Feldman at the N.B.S. indicate that direct N.B.S. traceability of the absorption coefficient at 0.6328 micrometers is not possible. Work presently being carried out in that group is directed toward such capabilities. Currently, neither an absolute power meter of sufficient accuracy nor a vacuum calorimeter of the type required for precision measurements of this type exist. It is anticipated that the current program at N.B.S. will yield data in one to two years, which will make traceability possible at that time, Additional conversations with Dr. J. Harrington at the University of Alabama at Huntsville indicate that measurements of the type required in the present NASA program have not previously been performed. We presently anticipate that the technique of differential absorption measurements previously described should be capable of providing measurements of changes in the absorptivity of the samples down to the level of 1 part in 10^{-4}, but at present have no direct way to calibrate the standard to make the measurement absolute. Bennett (Ref. 8) has developed a technique of obtaining absolute absorptivity, but it requires a prism of the sample material. This approach may provide an absolute reference on which to base the differential measurements.

The high values of absorption encountered with the europium doped polycrystalline KCl at 0.6238 micrometers (see Tables 6 and 12) raise the question of its potential influence on the utility of the material as a 10.6 micron window. The visible absorption experiment measures the forward power transmission ratio. The absorptivity determined by this experiment is a measure of the bulk absorption and scattering in the sample. The absorption and scattering losses are inseparable in this experiment. The power transfer equation for a medium that both absorbs and scatters takes the form

$$\frac{\partial P}{\partial x} = -\beta P - \sigma P \qquad (4)$$

where β is the absorptivity and σ is the scattering coefficient. The forward power transmission experiment determines the sum of β and σ by the solution to Eq. (1) which is

$$-(\beta + \sigma) = \ln \frac{(P \text{ out})}{(P \text{ in})} \qquad (5)$$

where we have neglected the front and back surface reflections. At this point we do not know the actual value of β or σ but only their sum. Visual observation indicate that the europium doped polycrystalline material is an active scattering medium. For the number 6-C test window (see Table 6) the sum of β and σ is 0.82 cm^{-1} at 0.6328 micrometers. The impact of this large extinction rate for the propagating signal at 10.6 micrometers could be estimated if we knew the size of the scattering centers. For example, if the scattering centers are large compared to 10 micrometers in radius, the scattering is the asymptotic form of Mie scattering or nonselective scattering. In this case the scattering loss would be the same in the visible and the infrared. If the scattering centers are small compared to 0.6 micrometers the mechanism is Rayleigh scattering. In this case we can also directly estimate the scattering at 10.6 micrometers from the visible data. The scattering coefficient would be reduced by the ratio of wavelengths to the fourth power. A scattering coefficient of 0.82 cm^{-1} at 0.6328 micrometers would be reduced to 8.3×10^{-6} cm^{-1} at 10.6 micrometers. If the scattering center size is intermediate between these extremes the mechanism would be Mie scattering. Calculations of the scattering coefficient would require a measure of scatterer size distribution, number density and index of refraction. The other potential approach would be a direct measurement of the 10.6 micrometer scattering.

On the basis of the large losses at .6328 micrometers and the fact that the 10.6 micrometer loss is relatively small, we can eliminate nonselective scattering as the mechanism. We cannot at this point determine if the observed scatter is Rayleigh or Mie.

10.6 Micrometer Absorption Measurements

The 10.6 micrometer absorptivity of the single crystal KCl samples has been determined by calorimetric techniques. Figure 8 shows the calorimeter chamber, sample mount, focusing optics and water calorimeter used to carry out the measurements. Under operating conditions, the chamber is purged with dry nitrogen to avoid contamination of the sample windows. The sample is mounted in an aluminum mounting ring which is suspended from four thin wires. The field stops shown in Fig. 8 were included to minimize the possibility of scattered radiation generated by imperfections in the focusing lens and reflections from the water calorimeter from reaching the thermocouples.

The measurements of sample temperature were made with a set of eight copper-constantan thermocouples which are connected in series electrically. Four of the thermocouples are mounted on the aluminum ring which holds the sample, and four are attached to the chamber wall. The two sets of four thermocouples are connected so that the induced emfs oppose each other. Thus the measured quantity is at a voltage proportional to the temperature difference between the chamber interior and the sample. The chamber interior temperature is determined by two principal factors. The first is the temperature of the room and the second is the temperature of the cooling water in the water calorimeter that absorbs the beam transmitted through the sample. The cooling water is maintained at the temperature of the room by an active regulating system. This technique has been found to minimize the time required for a sample to equilibrate when it is introduced into the chamber. Even with these precautions there are still diurnal fluctuations in the sample chamber temperature difference. These can be seen in Fig. 9 as a baseline drift before the sample was irradiated.

Figure 9 shows typical data of the temperature rise of a sample window under irradiation. The output of the thermocouple network is fed to a Hewlett Packard HP-425 microvoltmeter and the recorder output of the voltmeter is used to drive the strip chart recorder. The transmitted power is determined in a similar manner using another voltmeter and recorder. The 10.6 micrometer signal used to irradiate the sample was provided by a CRL Model 41 laser operating at the 30 to 40 watt power level.

The calculation of the absorptivity of the individual windows has been carried out using a minor modification of the analysis of Weil (Ref. 10) who has derived the following expression for the time rate of change of temperature of an absorbing body under the assumption that the radiation is coherent.

$$\frac{\partial T}{\partial t} = \frac{\beta L P_T}{mc_p} \left(\frac{n^2+1}{2n} \right). \qquad (6)$$

Equation 6 assumes that the radiation is incident normal to the surface of a parallel sided sample and relates the temperature to the transmitted power P_T, the absorptivity β, path length L and index of refraction n of the material. The product mc_p is the heat capacity. The two major assumptions inherent in Eq. 6 are that the product βL be small compared to unity and that the rate of heat loss by the body is small during irradiation. The magnitude restriction on βL is required in the analysis of Ref. 10 to allow the linearization of the exponential propagation constant for the wave. Weil assumes that this is satisfied for values of $\beta L < 0.01$ and in our experiments the value is on the order of 10^{-3} or less. Examination of the data in Fig. 9 shows that the rate of heat loss after the

irradiation is terminated is of the same order as the rate of heat addition (i.e., the sample does not remain isothermal after irradiation). The correction for the nonzero rate of heat loss due to conduction through the sample support wires and by free convection is carried out using the formalism of Hass et al (Ref. 9) who have shown that the correction for finite heat loss takes the form

$$mc_p \left[\frac{\partial T}{\partial t} \Big|_{T_1,t_1} - \frac{\partial T}{\partial t} \Big|_{T_1,t_2} \right] = \beta L P_T \frac{(1+n^2)}{2n} \qquad (7)$$

when the partial derivatives of the temperature are evaluated at the same temperature T_1 at time t_1 during irradiation and t_2 during the cooling cycle. This technique also cancels out any linear component in the baseline drift. The two partial derivatives of temperature are shown as M_1 and M_2 respectively in Fig. 9.

The heat capacity which appears in Eqs. 6 and 7 represents the total heat capacity of the body and in our case this is the sum of the window heat capacity plus the heat capacity of the mounting ring. The mounting ring is constructed of aluminum and weighs 0.066 kg. The heat capacity of the ring and window was taken to be 143.5 J/K°. The mounting ring represents about 40 percent of the total heat capacity and is designed to allow rapid heat transfer to the thermocouples without the use of heat transfer compounds, which might contaminate the window. The responsivity (i.e., the ΔT for unit power absorbed) could be increased by eliminating the ring but we would then be faced with the problem of mounting the thermocouples directly on the sample.

The accuracy of measurement of the 10.6 micrometer absorptivity of the test windows has been improved significantly. The initial absorptivity measurements of the single crystal KCl showed a run-to-run variation in the measured value of more than 20 percent in some cases. The major cause of the variation was traced to the reference thermocouples which were being affected by small-scale fluctuations in the room temperature. When these thermocouples were insulated to prevent the room temperature fluctuations from reaching them, the variation was reduced to a few percent. The reference thermocouples were attached to the calorimeter cover plate which also served as the sample support. Insulation of this cover plate with 5 cm thick fiberglass insulation in the form of a cover box was sufficient to produce the reduction in the run-to-run repeatability.

Window Visual Condition

Initial visual inspection of the single crystal KCl windows was carried out as the windows were unpacked for the absorptivity measurements. The optical

surfaces of the windows were of good quality and almost completely free of scratches and digs. The edges of some of the windows are a potential problem area. There appears to have been a variation in the technique of cutting the windows to size. All the windows appear to have been cut with a string saw. One group appears to have been cut with a very wet string. This group had the typical large scale irregularities associated with string wander but on a smaller scale the edge is quite smooth. The other group had a similar appearance with respect to the large scale irregularities but on a small scale they were relatively rough, giving the appearance of having been cut with a very dry string. Several of these windows had a series of cracks extending radially inward from the edge. Almost all the cracks lie in planes parallel to the optical faces of the windows, with a typical size on the order of 1 mm x 1 mm and a maximum size in Sample 3, where one crack reached about 4 mm radially inward and was about 8 mm in azimuthal extent at the outside edge. Figure 10 shows a photograph of Sample 3. The extensive crack on the left hand edge at the 8 o'clock position is not a single crack but a series of unconnected smaller cracks at different heights in the window. The foreshortening effect of photographing at an acute angle makes them appear to merge.

Irradiation Testing

The irradiation testing of the single crystal KCl and polycrystal europium doped KCl was carried out to the 100 hour level for both sets of test windows. The test windows were characterized optically at the prescribed test intervals of 0, 1.5, 4.3, 12.3, 35, and 100 hours. During the course of the testing, one of the single crystal KCl windows failed under load and one was removed from the test sequence because of the possibility of contamination. The europium doped polycrystal KCl windows completed the test cycle without incident. The flux levels selected for testing were sufficient to induce significant changes in the optical properties of the test windows over the 100 hour test period.

Irradiation Chamber Design

In summary, the basic purpose of the chamber is to allow the simultaneous exposure of four test windows to 10.6 micrometer radiation in the intensity range from 1 kW/cm^2 to 5 kW/cm^2 with the windows under a pressure-induced prestress to 30 percent of yield and with one face of each window exposed to a 10^{-8} Torr oil-free vacuum. The following sections describe the basic optical train and the construction of both the pressure and vacuum systems.

Optical System

Design calculations were made for the optical system that will provide the 10.6 micrometer illumination for the irradiation testing phase. An f/12 single element focusing system was selected as the initial design candidate for simultaneous irradiation of all four test windows. Assuming a working free aperture of 2 cm for the input beam, a diffraction limited focal spot of 0.024 cm diameter would be produced. The only primary aberration of importance in this case is spherical aberration, which is a function of the material index of refraction. If we assume an index of refraction of 1.5 and an object at infinity (collimated input beam), the optimum lens shape is a plano-convex lens, and the angular spherical aberration (ASA) is given by Ref. 11 as

$$ASA = 0.7y^3\phi^3 \tag{8}$$

where y is the free semi-aperture and ϕ the reciprocal focal length. The transverse spherical aberration (TSA) can be obtained by multiplying (8) by the focal length giving:

$$TSA = 0.7\ y^3\phi^2 \quad . \tag{9}$$

For this lens the TSA is approximately 0.0012 cm in diameter. This is so small compared to the diffraction limited spot size of 0.024 cm that the system is essentially diffraction limited near the focal point, and the Fresnel zone intensity distributions at points away from the focal plane can be obtained using the analysis of Sherman (Ref. 12).

The test windows were located such that the desired intensity levels of 1000, 1495, 2236 and 5000 watts/cm^2 could be obtained with an input power of 1 kW. The spot radii by geometric calculations for the four intensity levels were 0.564 cm, 0.462 cm, 0.378 cm and 0.252 cm, respectively.

Using the baseline optical design, a series of calculations of the state of stress of the windows to be subjected to 10.6 micrometer radiation was initiated. The calculations consider the azimuthal hoop stress developed at the outside edge of the window. From previous experience this is usually the location of highest stress due to the thermal loading of the window. The calculations indicate a tensile stress of 1200 KPa (175 psi) for all four windows. These stress levels were calculated assuming a 1 kW beam power level and a bulk absorptivity of 0.001 cm^{-1}. Separate calculations of the pressure induced stress have also been made. Assuming a value of Poisson's ratio of 0.3 (a more exact value is obtained as part of Task I), the requirement for a 685 KPa (100 psi) pressure induced stress at the center of the window produces an additional 275 KPa (40 psi)

of azimuthal tensile stress at the outside vacuum edge of the window. This outside vacuum edge stress is 1475 KPa (205 psi). This level did not present any appreciable problem for the polytran material with its yield strength of approximately 21,000 KPa (300 psi), but it did lead to plastic flow and brittle failure in some single crystal samples, since the yield strength in this material is in the range of 1400 KPa (200 psi) to 2800 KPa (400 psi). This problem is further complicated by the possibility of brittle failure. McClintock (Ref. 13), has found a brittle to ductile transition at about 21°C. Below the transition temperature the polycrystalline material tested was found to be sensitive to the presence of cracks and flaws which produced brittle failure at stresses well below yield of the base material. These authors did not examine single crystal material, but the possibility of similar behavior in the single crystal material should not be discounted. For our test configuration, the maximum stress occurs at the point of least certainty with respect to the presence of small cracks and flaws, because the maximum stress occurs at the saw cut outside edge of the window.

Pressure Chamber Design

The two half-cylinder pressure chambers that were used to provide the pressure induced prestress can best be seen in the section drawing c-c of Fig. 11. The left half cylinder, which serves as the pressure chamber to prestress test windows one and four in the test train, also provides the mounting surfaces for the input focusing element and the calorimeter that will be used to provide continuous power monitoring during the irradiation testing. The right hand half-cylinder, which provides the pressure prestress on test windows two and three, also contains the beam turning optics. The turning optics subassembly were secured to the main vacuum chamber with a combination of bolts and precision dowel pins. The dowel pins have been included to allow precise relocation of the previous mounting position. This is required since the optics will be demounted several times in the course of the irradiation test sequence. The pressure chamber has been designed to operate at pressure to 630 KPa (90 psi). The actual required pressure for the strongest material, the europium-doped polycrystalline material, should be approximately 280 KPa (40 psia) for a simply supported window. The uncertainty here is in terms of Poisson's ratio which was determined as part of the Task I characterization. For the purposes of the initial design calculations we assumed a value of 0.3 for Poisson's ratio.

Vacuum System

In order to provide the cleanest possible vacuum environment, the main vacuum chamber was machined from a single block of stainless steel. The only weld that is exposed to the vacuum is the interior weld that secures the chamber to the eight inch conflat flange. This serves to reduce the problem of weld outgassing

to a minimum. The pumping station consists of a set of three molecular absorption pumps, to provide the rough vacuum pumping without danger of hydrocarbon contamination of the test windows, and a 500 ℓ/sec vac-ion pump to provide the high vacuum pumping capacity to bring the chamber pressure below 10^{-8} mm Hg. The vacuum seal to the test windows was made with a fluorocarbon O-ring manufactured by the Parker Seal Company. This material is reported to be capable of providing a high vacuum seal with as little as 15 percent compression. The seal configuration is designed so that the O-ring is held in slight precompression with the same pressure on either side of the window. When the vacuum chamber is pumped down, the pressure load on the window compresses the O-ring and draws the window free of the retaining ring, thus producing a simply supported mount that applies no bending moments to the edge of the window.

The irradiation test facility was designed to allow simultaneous irradiation of four test windows at different flux levels while imposing a predetermined pressure stress on all four windows. Figures 12 and 13 show the irradiation test chamber with and without the pressure preload chambers.

The four test windows were exposed to the ultra-high vacuum which was maintained in the central chamber. Typical operating pressures in the UHV portion of the system range from 10^{-8} Torr to 5×10^{-9} Torr. The pressures were measured both with the vac-ion pump itself and with a nude ion gage located between the test cell and the vac-ion pump.

The test windows were exposed at power densities ranging from 5000 W/cm^2 to 1000 W/cm^2. The exposure levels for the individual windows are tabulated below.

Power Density	KCl Single Crystal	KCl Europium Doped Polycrystal
1000 w/cm^2	4-9	6-C
1495 w/cm^2	7	5-C
2236 w/cm^2	8-6	1-C
5000 w/cm^2	5	4-C

During the course of the irradiation testing of the single crystal windows two separate events have occurred that require documentation. At t = 0.9 hours during the first irradiation cycle one of the transfer mirrors over heated. We estimate the mirror reached a minimum temperature of 230°C, the melting point of the solder used to attach the mirror to its base. The mirror moved and a sharp decrease in throughput power was observed. The test was stopped at this point. During this period, the pressure in the UHV system and the preload chamber remained constant. Examination of the various O-ring seals and components showed no visible signs of damage. It was subsequently determined that a mirror in the optical train had moved, and the beam irradiated a tapped hole in the mirror mount. The hole acted as a radiation trap and caused the heating of the mount. Remedial action included reassembly of the loose mirror mount, refastening the transfer mirrors to their bases with a silver braze (MP ≈ 570°C), plugging the tapped holes that could act as radiation traps and forced water cooling the transfer mirrors. The test was resumed and carried to the 1.5 hr point without further incident. Optical test data on the window closest to the transfer mirror (single crystal #8) that moved showed a significant change in the properties of the window. Window #5 which shared the pressure preload chamber with #8 showed considerably less change in optical properties. Windows #7 and #4 which were in the other preload chamber showed no major changes in optical properties.

At exposure time 2.1 hours in the single crystal KCl testing, the irradiation was stopped due to a sudden rise in the UHV system pressure. Window #4 had cracked. The pressure preload chamber was removed and the crack, shown in Fig. 14 was photographed. The crack remained stable for about one hour. When the UHV system was being bled to atmospheric pressure the crack propagated to the outside edge of the window. Calculations of the stress distribution indicate that maximum stress occurs at the outside edge of the window. This includes the composite stress field due to pressure and thermal stress. For the crack to have initiated where it did required the presence of a flaw or micro-crack to act as a stress riser in the interior portion of the window.

The influence of flaws on the strength of KCl has been considered by others (Refs. 13 and 14) who have shown that even in small samples the presence of flaws can cause considerable variation in the observed yield. This effect becomes particularly important in the case of large samples if there is a distribution in flaw strengths in the material. The probability of encountering a weaker limiting flaw increases with the size of the test piece. The only present technique that would provide assurance of a minimum flaw strength would be a proof test such as that developed by Ref. 13.

The single crystal KCl and europium doped polycrystal KCl were irradiated alternately to allow the optical measurements to be made on all eight test windows at each of the prescribed test intervals. The 10.6 micrometer absorptivity for the test windows as a function of exposure time is presented in Tables 1 and 2. This data is presented graphically in Figs. 15 through 24. The visible optical data giving the variation in the visible index of refraction and percent transmission loss are presented in Tables 3 through 6.

Thermal Aging

The thermal aging test of the single crystal KCl and europium doped polycrystal KCl was carried out through the 100 hour time period. In this test two separate sets of windows, one set of single crystal KCl and one set of europium doped polycrystal KCl were aged at various temperatures with a pressure preload to determine the presence of thermal degradation effects in the window materials. The pressure preload was set at 30 percent of the yield strength of the windows. The temperature range investigated was from room temperature (20°C) to 250°C. Significant changes in the optical properties of the test windows indicate that elevated temperature operation of these windows may not be practical. Creep has been observed in both the single crystal KCl and europium doped polycrystal KCl at elevated temperature.

The 250°C and 179°C single crystal KCl test windows were discontinued at 4.3 hours due to excessive deformation of the windows. Centerline deflections on the order of several mm were observed. An experiment aimed at determining the rate of deflection was devised. Measurements of the surface flatness of the individual were initiated at the 12.3 hour test point. The single crystal KCl windows showed some deflection with time, with the possible exception of the room temperature sample. The europium doped polycrystal KCl material faired significantly better. The test windows at 20°C, 66°C, and 118°C showed no detectable deflection. The 179°C test window showed a very slight deflection as did the 250°C window.

The thermal aging test was conducted in the test chamber shown in Fig. 25. The chamber was designed to allow the simultaneous testing of both the single crystal KCl and europium doped polycrystal KCl. Since these two sets of test windows required different pressure loads to produce the desired stress level (30 percent of yield stress), the chamber was designed with two independent pressure chambers sharing a common high vacuum chamber. This allowed the parallel testing of both sets of test windows. The individual windows were tested at temperatures of 20°C, 66°C, 118°C, 179°C, 250°C. The individual windows were mounted in individual test fixtures shown schematically in Fig. 26. The table

below identifies the specific windows tested at each temperature. The quartz

Sample		Test Temperature
13	8-C	20° C
14	14-C	66° C
2	15-C	118° C
10	7-C	179° C
1	12-C	250° C

serves to minimize the heat conduction to the chamber walls and provides an optically smooth sealing surface for the O-ring seals. The shield and heater mechanism are designed to completely enclose the test window with the exception of a small hole in the shield that allowed the equalization of the pressure on both sides of the shield. The shield is required to eliminate convective cooling of the test window on the pressure loaded side. The initial design calculations showed that if edge heating alone was employed, high stress levels would be induced in the window because of the convective cooling of the pressure loaded face. The shield as presently designed uses both edge heating and convective heating from the shield to maintain the test windows at the desired temperature. The O-ring seals used in this test chamber are designed in the same manner as those employed in the irradiation with the exception that the O-ring material was selected to produce an O-ring with a "Shore A" hardness of 50 to 55 at the operating temperature of the individual O-ring. The three low temperature test windows operated at temperatures of 20°C, 66°C, and 118°C used Parker fluorocarbon O-rings. The test windows operated at 179°C and 250°C used O-rings made of a perfluoroelastomer marketed by E. I. DuPont DeNemours and Co. under the trade name ECD-006 perfluoroelastomer. Appendix II is a preprint of an article to be published in the "Journal of Vacuum Science and Technology" which provides data on the high vacuum properties of the material. This work was performed under Corporate sponsorship.

The individual windows in each set were aged at temperatures of 20°C, 66°C, 118°C, 179°C and 250°C for cumulative times of 1.5 hrs, 4.3 hrs, 12.3 hrs, 35 hrs, and 100 hrs. At each of these times, the windows were subjected to the same set of optical measurements. The absorptivity at 10.6 micrometers (β) was determined as previously described. The index of refraction and percent transmission loss were determined at a wavelength of 0.6328 micrometers. The 10.6 micrometer absorptivity of the windows as a function of time is presented in Table 7. Graphical presentations of the individual β history of each window are shown in Figs. 27 through 36. The radius of curvature measurements are shown in Table 8. Tables 9 through 12 present the visible optical properties as a function of aging time.

The exposure cycles were conducted in the following fashion. The individual heaters were energized at a preset voltage. This voltage having been previously established by calibration runs using quartz windows in place of the KCl test windows. When the temperature of the 250°C test windows reached 90 percent of the final value, the exposure time count was begun. The heaters remained energized for the required exposure period and were then turned off. Figure 37 shows a typical temperature plot for test window #12-C at 250°C for the time period from 35 hrs to 100 hrs.

During the course of the testing, two windows were removed from the test cycle due to extensive creep and the possibility of implosion of these windows into the high vacuum chamber. Test window 8-C which was tested at 20°C cracked during the period from t = 35 hrs to t = 100 hrs. It is shown in Fig. 38. The cracks occurred on the compression loaded side of the window and did not penetrate the vacuum seal. The presence of the cracks was not discovered until the system was disassembled at the 100 hour point. Test window 12-C which was tested at 250°C cracked at 96 hrs cumulative exposure and these cracks penetrated the vacuum system. The dry nitrogen preload gas leaking through the crack forced a shut-down of the vac-ion pump. The system was suited to the cryogenic pumps which maintained the vacuum at the 1 mm Hg level to the 100 hr point. The automatic pressure regulation maintained the preload pressure on the europium doped poly-crystal KCl window. Despite this shut-down of the vac-ion pump, we believe the remaining windows were essentially unaffected by the cracking of window 12-C. The cryogenic pumps maintained a low enough pressure so that the ΔP across the window was essentially unchanged and the gas leak into the vacuum system was the same gas the pressure side of the windows was exposed to, so that contamination should not be a problem. Figure 39 shows window 12-C at the 100 hour point. Despite the extensive cracks in both windows neither failed catastrophically.

DATA ANALYSIS

The data obtained in the irradiation and thermal aging experiments have been subjected to standard linear regression analysis to determine the degree of correlation between the measured optical properties of the test windows and the major experimental variables. The data were analyzed in four groups. The potential correlations investigated include the temporal variation of the 10.6 micrometer absorptivity (β), the temporal variation of index of refraction (n) and the temporal variation of the percent transmission loss (% T). The relation between the 10.6 micrometer absorptivity and the visible optical parameters were also investigated. For the irradiation experiments the relationship between the 10.6 micrometer absorptivity (β) and the incident intensity and power were investigated. For the thermal aging experiments the relationship between the 10.6 micrometer absorptivity and temperature was investigated. An additional experiment has shown the presence of creep in the thermal aging experiment. These data were analyzed to yield a prediction of the time rate of change of the window curvature.

The method of presentation of the analysis in this section is to take the tabular data presented in the experimental section of the report and reduce the data by linear regression to obtain a least squares fit to the data. The linear equations are presented in terms of the form of a straight line $y = a_o + a_1 x$ and two other parameters are given, namely, the number of data points used in the calculation of the least squares fit or the system degrees of freedom (DF) which is two less than the number of data points and the coefficient of determination r_d^2. The coefficient of determination or its square root r_d, the correlation coefficient, may be used to determine the relative "goodness of fit" of the data to a straight line. The coefficient of determination has a value of 1 if the data is an exact linear function and decreases to zero as the correlation of the data decreases. The small insert table shown below may be used to illustrate the interaction of the coefficient of determination and the number of data points available. The table was constructed by Ref. 20 assuming that a set of data (N points) has a zero correlation. The table gives the probability of finding a set of random numbers that would have a linear correlation with a coefficient of determination greater than r_d^2. For example, consider a set of 6 data points (DF = 4) which exhibits a coefficient of determination of 0.777. The table shows that a set of 6 random data points exhibiting this large a correlation would occur 2 times in 100 by chance. Alternately, there is a 98 percent probability that the data set is correlated.

Probability of a Larger r_d^2

DF.	0.10	0.05	0.02	0.01
1	.976	.994	1	
2	.81	.9025	.9104	.9801
3	.698	.7078	.872	.919
4	.531	.6577	.777	.840
5	.447	.568	.693	.763
10	.247	.332	.433	.501
16	.160	.219	.294	.348
20	.130	.179	.242	.288
25	.104	.145	.198	.237

Single Crystal KCl Irradiation

Single Crystal KCl Absorptivity

The single crystal windows subjected to irradiation did not all complete the test cycle of 100 hours. One window (#4) broke and another (#8) was removed from the test cycle because of the possibility of contamination. The linear curve fits obtained for this variation of the 10.6 micrometer absorptivity (β) with time are given below

Window	β =	$a_o(cm^{-1})$	$+a_1 \frac{cm^{-1}}{hr} t$	DF	r_d^2
7		0.00114	$2.29(10^{-6})$	4	0.102
5		0.000976	$.78(10^{-6})$	4	0.014
8		0.00103	$158.\ (10^{-6})$	1	0.398
4		0.000640	$26.7\ (10^{-6})$	0	1.0
9		0.000980	$.70(10^{-6})$	3	0.114
6		0.000537	$4.31(10^{-6})$	2	0.723

The data show a poor correlation indicating large variations from linear behavior. All the samples do show a positive slope if we eliminated from consideration the window that was believed to be contaminated (#8) and the window which broke (#4), both of which show very high relative values of a_1. The remaining data sets for windows which survived the test duration were then analyzed to determine if there was any correlation between the rate of

increase of $\beta_{10.6}$ and intensity of the irradiating field or the initial value of β. The resulting equations are

$$\frac{\partial \beta_{10.6}}{\partial t} = .36 \quad (10^{-4}) - 1.86 \quad (10^{-5}) I \frac{W}{cm^2} \tag{10}$$

with DF = 2 and $r_d^2 = .00198$

$$\frac{\partial \beta_{10.6}}{\partial t} = 6.35(10^{-6}) - 4.77(10^{-3})\ \beta_o \tag{11}$$

with DF = 2 and $r_d^2 = .53$

Two points of note arise from these equations. First, there seems to be no direct correlation with intensity. Second there appears to be a relatively strong correlation with the initial value of the 10.6 micrometer absorptivity (β_o). Also it may be noted that the variation of $\frac{\partial \beta 10.6}{\partial t}$ involves a negative dependence on β_o, i.e., $\frac{\partial \beta 10.6}{\partial t}$ decreases as β_o increases. Since the data field used to generate the fit ranged only from $0.00054 \leq \beta_o \leq 0.00114$, the presence of a zero in the relationship at $\beta = 0.00135$ and the prediction of negative values of $\frac{\partial \beta 10.6}{\partial t}$ above that should not be considered greatly significant.

The apparent variation of the rate of change of β with β_o in the single crystal KCl window suggests a technique to correlate all of the individual data. The form investigated is a normalization of β as

$$\frac{\beta - \beta_o}{a+b\ \beta_o} = a_o + a_1 x \tag{12}$$

The variable x has been investigated for x = t and x = ℓn t. The resulting curve fits to all the data available for windows 7, 5, 9 and 6 are

$$\frac{\beta - \beta_o}{a+b\ \beta_o} = 9.54 \times 10^{-4} + 1.523 \times 10^{-6} t, \ DF = 19, \ r_d^2 = 0.0417 \tag{13}$$

and

$$\frac{\beta - \beta_o}{a+b\ \beta_o} = 6.4799 + 32.328\ \ell nt; \ DF = 15, \ r_d^2 = 0.145 \tag{14}$$

where the constants of normalization were selected as $a = 6.35 \times 10^{-6}$ and $b = -4.77 \times 10^{-3}$. The logarithmic time form fit shows slightly less than 90

percent probability of correlation. Using this form a value of β at 10^4 hours of 0.00154 cm^{-1} would be predicted assuming a β_o of 0.001 cm^{-1}. A scatterplot of the data and fit is presented in Fig. 40.

Single Crystal KCl Visible Optical Properties under Irradiations

Similar analysis has been applied to the visible optical data. We have attempted to correlate the variation of the average index of refraction and the average percent transmission loss at 0.6328 micrometers with time of irradiation. The direct correlations with time were computed using the average value of index of refraction $(\Sigma N_i)/n$ and average percent transmission loss $(\Sigma \%T_i)/n$. The variations in the index of refraction obtained were

Window	$(\Sigma N_i)/n =$	a_o	+	$a_1 X$	DF	r_d^2
4		1.4860	-	$2.733(10^{-3})t$	0	1
5		1.4824	+	$8.371(10^{-5})t$	4	0.416
7		1.4807	-	$4.130(10^{-6})t$	4	0.0013
8		1.4837	+	$2.678(10^{-3})t$	1	0.734
6		1.4866	+	$2.78\ (10^{-6})t$	2	0.312
9		1.4867	+	$1.929(10^{-7})t$	2	0.0078

Only two samples showed significant variation in time. These were window 4 which failed during testing and window 8 which was removed from testing because it was believed to be contaminated. The remaining samples show very little organized behavior in time and very small changes in the average index of refraction over the time period of observation.

The average transmission loss $(\Sigma \%T_i)/n$ which was computed by averaging the measured transmission loss at the 5 positions on the sample surface was also correlated with time. The results of the linear regression fit are

Window	$(\Sigma \%T_i)/n$	a_o	+	$a_1 X$	DF	r_d^2
4		0.776	+	0.0056t	0	1
5		0.573	+	0.0100t	4	0.616
7		0.827	+	0.00624t	4	0.27
8		1.926	+	0.997t	1	0.82
6		-0.515	+	0.00559t	1	0.935
9		0.0302	-	$3.48(10^{-4})t$	2	0.033

Sample 8 again shows a radical increase in time. The remaining samples show a general increase over the 100 hour test period. It should be noted that a negative value of a_o does not indicate a power gain but that the window in question had a lower transmission loss than the reference sample.

Coupling Effects

To investigate the possibility of coupling effects between the visible (0.6378 micrometers) parameters and the 10.6 micrometer absorptivity, the cross correlation of these parameters has been computed. Since the 10.6 micrometer absorptivity was determined in the center of the window, the values of index of refraction and percent transmission loss were taken at the number 4 test position (the center of the window). The results of the regression analysis are presented as a pair of equations linking the 10.6 micrometer absorptivity and the visible properties. As in the previous paragraphs the system degree of freedom (DF) and the coefficient of determination are also presented.

Window	$\beta_{10.6}$ = a_o	+	a_1X	DF	r_d^2
7	$\beta_{10.6}$ = 0.05550	-	.03663N	4	0.581
	$\beta_{10.6}$ = 0.001146	+	$5.65(10^{-5})$%T	4	0.015
5	$\beta_{10.6}$ = 0.012104	-	$7.473(10^{-3})$N	4	0.0134
	$\beta_{10.6}$ = $9.905(10^{-4})$	+	$8.444(10^{-6})$%T	4	0.00043
8	$\beta_{10.6}$ = 0.086235	+	.058744N	1	0.974
	$\beta_{10.6}$ = 0.000433	+	.00026%T	1	0.999
4	Insufficient Data			0	1
				0	1
9	$\beta_{10.6}$ = -2.607823	-	1.75454N	2	0.604
	%T = 0.008120	-	82.706β	2	0.0024
6	$\beta_{10.6}$ = 0.072252	+	.049654N	2	0.0017
	$\beta_{10.6}$ = Insufficient data				

The reversal of dependent and independent variables in some of the equations is an artifact of the computer program used. It occurs in cases where the originally selected independent variable has negative valves. The program automatically reverses the variables. No significant correlation has been found between the visable and 10.6 micrometer properties.

Europium-Doped Polycrystal KCl Under Irradiation

10.6 Micrometer Absorptivity

A similar analysis has been applied to the europium doped polycrystal KCl subjected to 10.6 micrometer irradiation. All four of these windows completed the 100 hour irradiation without incident.

Window	$\beta_{10.6} = a_o\ (cm^{-1})$		$a_1 \frac{cm^{-1}}{hr} t$	DF	r_d^2
4-C	0.00163	+	$2.87(10^{-6})$	5	0.0143
5-C	0.00137	+	$34.5\ (10^{-6})$	5	0.75711
6-C	0.00408	-	$18.8\ (10^{-6})$	4	0.2495
1-C	0.00151	+	$5.48(10^{-6})$	5	0.4382

As in the case of the single crystal material the relationship between $\frac{\partial \beta_{10.6}}{\partial t}$, the intensity and β_o have been investigated. The resultant linear regression fits are

$$\frac{\partial \beta_{10.6}}{\partial t} = 5.79 \times 10^{-6} - 9.13 \times 10^{-11} I;\ DF = 2;\ r_d^2 = 0.5 \times 10^{-6} \quad (15)$$

$$\frac{\partial \beta_{10.6}}{\partial t} = 34.8 \times 10^{-6} - 13.5 \times 10^{3}\ \beta_o;\ DF = 2;\ r_d^2 = 0.638 \quad (16)$$

As in the single crystal samples almost no correlation is found with the intensity and a moderately strong correlation is found with the initial value of β_o. The change in $\frac{\partial \beta_{10.6}}{\partial t}$ is again found to decrease with increasing β_o. In the case of window 6-C which had the highest value of β_o of the test windows used in the irradiation experiments the average slope of the β-time data is found to be negative.

Analysis of the four europium doped polycrystal KCl window as individuals shows an increasing rate of damage with decreasing β_o. The same normalization parameter used with the single crystal window was again employed in an attempt to correlate all the data. The linear regression fits for the linear and log time fits are

$$\frac{\beta - \beta_o}{a + b\ \beta_o} = -36.778 + 1.5895\ t;\ DF = 24;\ r_d^2 = 0.1732 \quad (17)$$

and

$$\frac{\beta - \beta_o}{a + b\ \beta_o} = -67.403 + 29.319\ \ell n\ t;\ DF = 20;\ r_d^2 = 0.09109 \quad (18)$$

where $a = 34.8 \times 10^{-6}$ and $b = -13.5 \times 10^{-3}$. The linear time fit indicates a probability of correlation in excess of 95 percent. The log time can be improved by discarding data points that fall well below the mass of the data on the scatter plot shown in Fig. 41. The fit that results takes the form

$$\frac{\beta - \beta_o}{a+b\ \beta_o} = -16.9105 + 13.655\ \ell n\ t;\ DF = 18;\ r_d^2 = 0.14603 \qquad (19)$$

Visible Optical Parameters

The visible optical data on the europium doped polycrystal KCl subjected to irradiation has been analyzed in the same manner as the single crystal material. The correlations between the visible properties and time and cross correlation between the visible and 10.6 micrometer properties are presented below

Window	$(\Sigma N_i)/n =$	a_o	+	$a_1 X$	DF	r_d^2
1-C		1.4858	-	$1.182 \times 10^{-5} t$	6	0.293
4-C		1.48537	-	$1.802 \times 10^{-6} t$	6	0.0363
5-C		1.48236	+	$9.305 \times 10^{-4} t$	4	0.997
6-C		1.48713	+	$5.840 \times 10^{-6} t$	6	0.121

Window	$(\Sigma \%T_i)/n =$	a_o	+	$a_1 X$	DF	r_d^2
1-C		10.02	-	$0.758 \times 10^{-4} t$	6	0.212
4-C		33.5	-	0.0286t	6	0.126
5-C		29.0	+	0.0879t	6	0.412
6-C		45.6	-	0.0454t	6	0.223

No strong correlation is found in general. Window 5-C shows strong correlation with the visable index of refraction.

Cross Coupling Effects

The potential correlation of the 10.6 micrometer absorptivity and the index of refraction and % Transmission at .6328 micrometer has been investigated for the europium doped polycrystal KCl windows. The resulting linear regression fit equations are

		DF	r_d^2
4-C	$\beta_{10.6} = -.374603 + .253395N$	4	.16
	$\beta_{10.6} = .0093218 - 2.343x10^{-4}\%T$	4	.35
5-C	$\beta_{10.6} = .0371377 - .02382N$	2	.743
	$\beta_{10.6} = .001020 + 3.768x10^{-5}\%T$	4	.342
6-C	$\beta_{10.6} = -.743275 + .502036N$	4	.185
	$\beta_{10.6} = .002453 + 2.5276x10^{-5}\%T$	4	.0048
1-C	$\beta_{10.6} = -.1262730 + .08595N$	4	.065
	$\beta_{10.6} = .001856 - 2.2307x10^{-5}\%T$	4	.01

No strong cross correlation of the 10.6 micrometer and visable parameters were found.

Single Crystal KCl Thermal Aging Test

10.6 Micrometer Absorptivity

The single crystal KCl windows subjected to thermal aging showed considerable changes during the course of the 100 hour test period. Two of the windows did not complete the test sequence. Large scale deformation of the test windows at 250°C and 179°C forced their removal from the test. As in the previous paragraphs detailing the analysis of the irradiation testing, the 10.6 micrometer absorptivity data of the individual windows were reduced by linear regression. The high temperature test windows (1 and 10) were removed from the test cycle at 4.3 hours so that sufficient data is available to subject these windows to analysis and so they are also presented in the group

Window	Temp.C	$\beta_{10.6}$ =	a_o		a_1X	DF	r_d^2
1	--	$\beta_{10.6}$ =	0.000278	+	.000420t	1	0.958
10	--	=	0.000450	+	.000232t	1	0.997
2	--	=	0.00156	+	$1.72(10^{-6})t$	4	0.0024
14	--	=	0.001266	+	$5.88(10^{-5})t$	4	0.663
13	--	=	0.000835	+	$5.31(10^{-5})t$	4	0.953

In this experiment there appears to be a reasonably good correlation between the 10.6 micrometer absorptivity and the exposure time. In the equations above, the windows are presented in order of decreasing temperature and two additional correlation relations have been calculated. These are the temperature dependence of the time rate of change of 10.6 micrometer absorptivity and

the dependence of the time rate of change of 10.6 micrometer absorptivity on the initial value of β. The derived relationships are

		a_o		$a_1 T$	DF	r_d^2	
$\frac{\partial \beta_{10.6}}{\partial t}$	=	$-5.637(10^{-5})$	+	$1.651(10^{-6})T$	3	0.758	(20)
$\frac{\partial \beta_{10.6}}{\partial t}$	=	$4.012(10^{-4})$	-	$0.283\ \beta_o$	3	0.731	(21)

In this case there appears to be a strong probability of correlation of the rate of change of the 10.6 micrometer absorptivity with temperature and with β_o. The time rate of change of absorptivity is found to increase with temperature and is also found to decrease with increasing β_o as did the irradiation test specimens.

Visible Optical Parameters

The variation in the average index of refraction at 0.6328 micrometers $(\Sigma N_i)/n$ and the average percent transmission loss, $(\Sigma \%T_i)/n$, at the same wavelength have been calculated in the same fashion as in the irradiation experiments. These results are presented in order of decreasing test temperature

Window	$(\Sigma N_i)/n = a_o$		$a_1 X$	DF	r_d^2
1	= 1.48449	+	$1.727(10^{-3})t$	1	0.64
10	= 1.48510	+	$5.73\ (10^{-3})t$	0	1.0
2	= 1.48632	+	$3.369(10^{-5})t$	4	0.68
14	= 1.48734	-	$1.28\ (10^{-5})t$	4	0.099
13	= 1.48596	+	$2.178(10^{-4})t$	4	0.925

Window	$(\Sigma \%T_i)/n = a_o$		$a_1 X$	DF	r_d^2
1	= 2.37	-	1.35t	1	0.089
10	= -0.180	+	0.55t	1	0.887
2	= -0.132	+	0.049t	4	0.960
14	= 2.89	+	0.204t	4	0.399
13	= 130	+	$1.26(10^{-3})t$	4	0.0062

There are individual windows that appear to have strong temporal dependence. The percent transmission loss in window 2 and the index of refraction of window 13 display a high degree of correlation. The rate of increase of the percent transmission loss appears to be temperature sensitive from the above relationships. The least squares fit to this parameter is

		a_o	+	a_1X	DF	r_d^2
$\frac{\partial(\%T)}{\partial t}$	=	-0.267	+	0.00551T	3	0.811 (22)

which shows a high degree of correlation with the temperature.

Cross Coupling Effects

The possibility of coupling between the visible optical properties and the 10.6 micrometer absorptivity has been investigated using the technique described in the section on the irradiation testing. The linear regression equations relating the visible index of refraction and the percent transmission loss at the center of the window with the 10.6 micrometer absorptivity is given below

indow			a_o	+	a_1X	DF	r_d^2
1	$\beta_{10.6}$	=	- .27788	+	0.187882N	1	0.47
	$\beta_{10.6}$	=	$-2.547(10^{-5})$	+	$1.892(10^4)\%T$	1	0.825
10	$\beta_{10.6}$	=	- .184804	+	0.12470N	1	0.554
	%T	=	-1.6530	+	$3.5366(10^3)\beta_{10.6}$	1	0.846
2	$\beta_{10.6}$	=	- .16968	+	0.11523N	2	0.016
	%T	=	1.19544	+	$289.4\beta_{10.6}$	4	0.021
14	$\beta_{10.6}$	=	.49174	-	0.32932N	2	0.0209
	$\beta_{10.6}$	=	.00226	+	$5.87(10^{-5})\%T$	4	0.073
13	$\beta_{10.6}$	=	- .144022	+	0.097627N	3	0.825
	%T	=	.236	-	41.55β	4	0.0098

There is no general trend to indicate a strong correlation. The three cases which show strong correlation 1 ($\beta_{10.6}$, %T), 10(%T, $\beta_{10.6}$) and 13 ($\beta_{10.6}$, N) appear to result from even stronger correlation of the individual properties with time.

Temperature Dependence of 10.6 Micrometer Absorptivity

The strong temperature dependence of the single crystal KCl time rate of change of 10.6 micrometer absorptivity suggests an exponential relationship between the rate of increase of absorptivity and temperature. To this end we have plotted the natural log of the time rate of change of β versus absolute temperature in Fig. 42. The data has been fit in two ways. Using all the data the best fit becomes

$$\ell n \left(\frac{\partial \beta}{\partial t} \times 10^6 \right) = -0.2991 + 0.01077\ T;\ DF = 3\ r_d^2 = 0.210 \qquad (23)$$

The coefficient of variation can be reduced considerably by excluding the data point at 391°K. This produces a fit with the following form

$$\ell n \left(\frac{\partial \beta}{\partial t} \times 10^6 \right) = 0.9903 + 0.00967\ T;\ DF = 2\ r_d^2 = 0.977 \qquad (24)$$

Using this expression it was possible to obtain a fit to all the absorptivity data for the single crystal KCl windows that were thermally aged. The data and the fit curve are presented in Fig. 43. The resulting least squares fit takes the form

$$\frac{(\beta - \beta_o) \times 10^6}{\exp\ (0.9903 + 0.009675\ T)} = -7.1379 + 13.1408\ \ell nt. \qquad (25)$$

with DF = 17 and $r_d^2 = 0.3577$. The probability of a correlation is slightly greater than 99 in 100.

Europium Doped Polycrystal KCl under Thermal Aging

10.6 Micrometer Absorptivity

The europium doped polycrystal KCl subjected to thermal aging has been analyzed in the same manner as the single crystal KCl. The 10.6 micrometer absorptivity of the test windows has been analyzed and the results presented below. The results are arranged in order of decreasing test temperature.

Window	$\beta_{10.6}$ =	a_o	+	a_1X	DF	r_d^2	T. C°
12-C	=	0.00213	+	$2.93(10^{-5})t$	4	0.582	250
7-C	=	0.00173	+	$5.37(10^{-5})t$	4	0.494	179
15-C	=	0.00142	+	$1.78(10^{-5})t$	4	0.317	116
14-C	=	0.00148	+	$1.83(10^{-5})t$	4	0.605	66
8-C	=	0.00215	+	$4.55(10^{-5})t$	4	0.774	20

The temperature dependence of the rate of change of 10.6 micrometer absorptivity and the variation with β_o have been calculated for this set of windows and are given below

	DF	r_d^2	
$\frac{\partial \beta_{10.6}}{\partial t} = 3.17 \times 10^{-5} + 9.58 \times 10^{-9} T$	3	0.0029	(26)

and

$\frac{\partial \beta_{10.6}}{\partial t} = 1.215 \times 10^{-5} + 2.529 \times 10^{-2} \beta_o$	3	0.294	(27)

There is no strong correlation in either case.

Visible Optical Parameters

The variation of the visible optical properties of the europium doped polycrystal KCl windows have been computed using the average values of both the index of refraction and the percent transmission loss at 0.6328 micrometers.

Window	$(\Sigma N_i)/n$ =	a_o	+	a_1X	DF	r_d^2	T. Co
12-C	=	1.4909	+	$8.32(10^{-5})t$	4	0.493	250
7-C	=	1.48735	+	$6.64(10^{-5})t$	4	0.837	179
15-C	=	1.48722	-	$1.86(10^{-5})t$	4	0.0788	116
14-C	=	1.49112	-	$1.43(10^{-3})t$	2	0.868	66
8-C	=	1.48624	+	$3.18(10^{-4})t$	4	0.983	200
	$(\Sigma \%T_i)/n$						
12-C	=	49.0	-	$1.66(10^{-2})t$	4	0.0077	260
7-C	=	42.6	-	$5.40(10^{-2})t$	4	0.262	179
15-C	=	10.2	+	0.018	4	0.1784	116
14-C	=	38.9	-	$8.07(10^{-3})t$	4	0.0067	66
8-C	=	34.5	+	$3.78(10^{-2})t$	4	0.086	20

The index of refraction data shows several cases of highly ordered behavior in time. The percent transmission loss (%T) shows no particular ordered behavior. However, window 15-C which is of more recent manufacture shows a considerably smaller transmission loss than the remainder of the group.

Cross Coupling Effects

The 10.6 micrometer absorptivity visible index of refraction and visible percent transmission loss have been analyzed to determine the presence of coupling between the properties at 10.6 micrometers and 0.6328 micrometers. These equations were computed using the values of index of refraction and percent transmission loss measured at the center of the window.

Window	$\beta_{10.6}$	=	a_o	+	$a_1 X$	DF	r_d^2
12-C		=	-0.3112745	+	0.210281N	4	0.613
		=	0.00331	-	$8.26(10^{-6})$%T	4	0.0013
7-C		=	1.86990	+	1.25750N	0	1.0
		=	0.026467	-	.0006552%T	4	0.367
15-C		=	-0.0684964	+	0.047360N	4	0.0277
		=	0.00254	-	$6.86(10^{-5})$%T	4	0.0046
14-C		=	-0.532483	+	0.353744N	1	0.56
		=	-0.001632	+	$8.485(10^{-5})$%T	4	0.179
8-C		=	-0.203302	+	0.138203N	4	0.807
		=	-0.068438	+	0.002392%T	4	0.315

No general trend of cross correlation is observed for either set of parameters.

Temperature Dependence of 10.6 Micrometer Absorptivity

The europium doped polycrystal KCl showed no significant temperature dependence in the time rate of change of absorptivity. The least square fit to the entire data set produced an equation of the form

$$\frac{\beta - \beta_o}{\beta_o} = -0.050905 + 0.44507 \ln(t) \qquad (28)$$

DF = 24 $\qquad r_d^2 = 0.250$

The correlation coefficient for this fit, $r_d = 0.5$, in a system with 24 degrees of freedom indicates a 99 percent probability of correlation. A scatter plot of the data set and the fit curve are presented in Fig. 44.

Creep in Single Crystal KCl and Europium Doped Polycrystal KCl

The measurements of the optical surface flatness that were initiated at the 12.3 hour test point on the thermal aging test have been reduced to yield the time and temperature of the radius of curvature r_c. It was more convenient to fit the reciprocal radius of curvature in (meters^{-1}). As in the previous calculations the time (t) is expressed in hours and the temperature is in centigrade degrees. In fitting the data it was assumed that all windows had an infinite radius of curvature at time t = 0. The single crystal KCl least squares fits are

Window	$1/r_c$ =	a_o +	a_1X	DF	r_d^2
13 (20C°)	$1/r_c$ =	0.022698 +	0.000269t	2	0.303
14 (66C°)	$1/r_c$ =	0.01632 +	0.000983t	2	0.916
2 (118C°)	$1/r_c$ =	0.239 +	0.0119t	2	0.789

The temperature dependence of the time rate of change of radius of curvature was found to be

		DF	r_d^2
$\frac{\partial(1/r_c)}{\partial t}$	= - 0.00362 + 0.000115T	1	0.826 (29)

With the eruopium doped polycrystal KCl no creep was detected in the three low temperature windows (20C°, 66C°, 118C°). The data for the high temperature windows was reduced to the following

Window	$1/r_c$ =	a_o +	a_1X	DF	r_d^2
7-C (179C°)	$1/r_c$ =	0.012307 +	0.000210t	2	0.476
12-C (250C°)	$1/r_c$ =	0.01943 +	0.000515t	2	0.679

Since no distortion of the 118C° test window was observed the reciprocal radius of curvature was set to zero and using that value as a data point the relationship between the rate of change of the reciprocal radius of curvature and temperature was calculated

		DF	r_d^2	
$\frac{\partial(1/r_c)}{\partial t}$	= $-4.713 \times 10^{-4} + 3.91 \times 10^{-6}T$	1	.996	(30)

Mechanical Testing

The measurements of Young's Modulus, yield stress and Poisson's ratio were made in four-point bending with a span of 3.81 cm and a cross head speed of 0.0127 cm/min. The yield strength, Young's Modulus and Poisson's ratio for the as-received single crystal material are presented in Table 16. The same data for the as-received europium-doped polycrystal material is presented in Table 15. Room temperature measurements of the Modulus of Elasticity, Poisson's ratio and yield strength for the irradiated and thermal aged material are presented in Tables 16 and 17.

The temperature-dependence of the modulus of elasticity, Poisson's ratio and yield stress are shown for the as-received materials in Figs. 45 through 50.

Grain Size Measurements

The grain size of the europium-doped polycrystal KCl has been determined for both the as-received material and on all the samples subjected to irradiation and thermal aging. The material preparation technique consisted of a water etch to remove surface damage followed by an alcohol rinse. The samples were then etched using the technique developed by Slack (Ref. 17) as improved by Moran (Ref. 18). The etch was a two-component mix. The first part consisted of 95 volume percent ethyl alcohol solution, 25% saturated with $BaBr_2$. The remaining 5 volume percent of the solution was methanol containing 100 gm of $BaBr_2$ per liter.

Figure 51 illustrates that there was quite a large variation in grain size. It appears some areas here have recrystallized while others have not. The three photographs selected for measurement were selected as more typical and away from the outside edge of the window. Three lines were drawn on each picture and the average intercept length ($\bar{L}$) measured over a large number of grains using the equation developed by Mendelson (Ref. 19) for the average grain size ($\bar{D}$).

$$\bar{D} = 1.570\ \bar{L}$$

The measurements resulted in values of 18.3, 25.7 and 19.9 microns (average 21.3×10^{-4} cm) on the as-received material.

The grain size measurements for the polycrystal europium-doped KCl after irradiation and thermal aging were made in the same manner previously described. Grain size in all samples was quite varied. Typical areas were selected in the center section of each window. Figure 52, a 100 x picture of window 12-C, shows an example where contiguous large and small grain size material can be seen together. Another point to note is that, when grains grew or coarsening occurred, not all boundaries grew or moved together. Some remained stuck within the larger grains and some apparently left behind residues (impurities?) which formed subgrain boundaries. Windows 1C, 5C and 6C, for example, reveal subgrain boundaries. For counting grain boundary intersections, this distinction was noted. If the boundaries etched lightly compared to the more obvious grain boundaries, they were not counted for purposes of grain size determination.

Figures 53 and 54 show the irradiated samples at t = 100 hr. Figures 55, 56 and 57 show the thermal aged samples at t = 100 hr and Table 13 shows the measured grain size.

DISCUSSION OF RESULTS

This section is subdivided into three parts in order to present the material in as clear a fashion as possible. The single crystal KCl window performance and the europium-doped polycrystal KCl window performance comprise the first two sections. The third section details areas that appear to require more investigation and considers other potential window materials that were outside the scope of this program.

Single Crystal KCl Windows

The single crystal KCl windows that were subjected to irradiation have shown a general tendency to increase in absorptivity with exposure time. This behavior does not appear to be a function of the exposure intensity over the range of intensity tested (1 kW/cm^2 to 5 kW/cm^2). It also does not correlate with the thermal-induced stress caused by the radial heat flow of the absorbed laser power. This self-induced thermal stress would increase directly with the product of the absorptivity and the power transmitted through the window, as shown in Appendix I. There is a correlation between the rate of increase of the absorptivity and the initial absorptivity. The windows with lower initial values of absorptivity are damaged at a faster rate. Since the calorimetry experiment used to measure the 10.6 micrometer absorptivity cannot separate the contributions of surface and bulk absorptivity, it is not possible at this point to determine which component of the total absorptivity is increasing or if, in fact, both components are increasing. Arguments that the surface contribution is the more likely candidate to increase are plausible, but at this point we cannot establish this as fact. A statistical model for the rate of increase of absorptivity has been developed.

In the course of both the irradiation and thermal aging tests, periodic behavior was observed in the absorptivity of some of the test windows. The cyclic rise above the mean growth rate is of critical importance to the high-power window designer. The safety margin selected must be large enough to prevent the window from being deformed by self-induced thermal stress. By way of illustration, consider a single crystal KCl window 10 cm in diameter with a critical stress of 400 psi (2800 KPa). If the window has an illuminated area of 7 cm and an absorptivity of 0.001 cm^{-1}, the window will be at yield stress in azimuthal tension at the outside edge at a throughput power of 3 kW. This azimuthal tensile stress is the result of the thermal gradient caused by heat

flow to the outside edge of the window. The details of this analysis are presented in Appendix I. Thus, if peaking on the order of a factor of 2 is expected in the absorptivity variation with time, the safety factor must be increased accordingly above the mean growth rate to allow for this.

The calculation of the maximum allowable throughput power for a single crystal KCl window for operation to 10^4 hrs can be made using the statistically derived growth of β (Eq. (14)). This equation predicts that a single crystal window with an initial β of .001 cm^{-1} will, at 10^4 hrs, have a β of .00154 cm^{-1}. This increase in β will reduce the maximum permissible power throughput. Using the analysis of Appendix I and assuming a beam diameter of 7 cm incident on a 10 cm diameter window with edge cooling, the maximum permissible power the window can transmit at t = 0 (β = .001 cm^{-1}) is 3 kW. At this power level the azimuthal tensile stress is 400 psi (2800 KPa). At t = 10^4 hrs (β = .00154 cm^{-1}) the power throughput must be reduced to 1.95 kW to maintain a maximum stress of 400 psi (2800 KPa). It should be noted that no safety factors are included in this analysis.

It is of considerable interest to the system designer to determine the nature of the mechanism producing the increase in the 10.6 micrometer absorptivity. If the increases observed are due to surface absorption, it is possible to reduce the impact of the increase by appropriate design of the window. If the cooling method is restricted to conduction cooling through the edge, an increase in bulk absorptivity will uniformly increase the radial heat flow and the resultant thermal stress is independent of window thickness. If the surface absorptivity of the sample increases, the designer has the option of increasing the thickness of the window, which has the effect of lessening the thermal resistance to heat flow from the optical surfaces to the cooled cylindrical edge of the window, thus reducing the stress increase.

The index of refraction measurements, which were made at 0.6328 micrometers, are due to the nature of the technique, measurements of the surface properties of the window. The technique of measurement employed determines the change in index of refraction at the air-surface interface. The considerable variation in the index of refraction during the course of the irradiation and thermal aging indicates that significant changes are taking place at the surface of the samples. No general correlation between the 10.6 micrometer absorptivity and the visible index of refraction has been observed. However, isolated samples have shown strong correlation between the visible optical properties and the 10.6 micrometer absorptivity.

Mechanical creep has been detected in the single crystal KCl windows that were subjected to thermal aging at temperatures of 66°C and higher. The windows tested at 179°C and 250°C deflected sufficiently to warrant their removal from the test sequence to prevent a possible implosion in the test cell. A model predicting the rate of creep as a function of temperature has been developed.

During the course of the irradiation testing, one of the single crystal KCl windows failed. The failure was unusual in that a crack developed in the center of the window. Calculations of the stress distribution in the windows indicate maximum stress is developed at the edge of the window. For the window to crack at the position observed, a flaw of sufficient size to initiate crack growth must have been present in the material. As a corollary of this observation, the probability of survival of the windows could be improved by careful attention to the edge conditions. Irregularities in the edge should be polished out to prevent them from acting as stress risers.

Europium-Doped Polycrystal KCl

The europium-doped polycrystal KCl windows survived the irradiation exposure test without incident. As in the case of the single crystal KCl windows, the europium-doped polycrystal KCl shows a general increase in absorption with time. This group of windows showed a correlation between the rate of increase of absorptivity and the initial value of absorptivity. The windows with a lower value of initial 10.6 micrometer absorptivity were damaged at a faster rate. As in the test with the single crystal KCl windows, individual windows displayed periodic variations about the mean growth curve. The previous comments concerning the design of a high-power window are equally applicable to these specimens.

The maximum allowable transmitted power for the europium doped polycrystal KCl has been calculated in the same fashion as the previous single crystal KCl calculations. We have assumed a 7 cm diameter uniform intensity beam incident on a 10 cm diameter window. We have ignored the effect of pressure loading which can be added by linear superposition. The initial value of β was assumed to be .001 cm^{-1}. Equation 19 was used to predict the value of β at 10^4 hrs. This was calculated to be .0033 cm^{-1}. The analysis of Appendix I was used to calculate the maximum power the window could transmit based on the assumed beam geometry and at t = 0 the window would transmit 22.5 kW with the outer fiber tensile stress at a level of 3000 psi (21 MPa). At 10^4 hrs the value of β increases to .0033 cm^{-1} reducing the allowable transmitted power to 6.82 kW. As in the single crystal KCl case presented previously, no safety factor has been included in the analysis.

The mechanical creep observed in the single crystal material did not present a great problem in the thermal aging of the europium-doped polycrystal material. The windows aged at 179°C and 250°C showed evidence of creep and an analytical model has been developed to predict the rate of creep, No creep was detected in the windows operated at 118°C and below.

During the course of the thermal aging test, the mean absorptivity of the samples increased in time but no temperature-dependence was detected in the rate of change of 10.6 micrometer absorptivity. The single crystal windows subjected to identical aging temperature showed an exponential dependence on temperature in the growth rate of the 10.6 micrometer absorptivity. The cyclic behavior of the 10.6 micrometer absorptivity observed in the single crystal KCl during thermal aging has also been observed in the europium-doped polycrystal KCl.

The possibility that the cyclic variation in the 10.6 micrometer absorptivity is related to changes in the sample surfaces due to a combination of stress conditions is significant in the light of recent work by Soileau, et al (Ref. 15), who have shown that slow polishing (period of weeks) with its resultant stressing of the sample could drastically increase the surface absorptivity. A single crystal KCl sample so polished was found to have a total absorptance on the order of 0.006 cm^{-1}. A rapid HCl etch of the same sample to remove the surface damage layer was found not only to destroy the good optical figure but also to reduce the total 10.6 micrometer absorptance to 0.00077 cm^{-1}.

Recommendations for Future Study

Several areas of investigation immediately suggest themselves. The first is the development of a measurement technique that will permit the separation of the surface and bulk absorptivities in windows of conventional geometries. Techniques based on a long cylinder sample geometry are presently available. Another area that appears to require consideration is the question of surface damage in the windows as a result of the optical polishing operations. The question that arises is, does the damaged layer tend to grow at stress levels that are well below the average yield strength of the undamaged bulk material and, more important, does the surface absorption also tend to grow under these conditions.

Alternate window materials that appear worthy of consideration are zinc selenide and the reactive-atmosphere-grown KBr produced recently by Rice, et al (Ref. 16) at NRL, who have grown KBr single crystals with 10.6 micrometer absorptivities on the order of 6×10^{-5} cm^{-1} by growing the crystals in a CCl_4 atmosphere.

As a result of experience gained in the course of this effort, certain improvements appear possible with the visible optical diagnostics. Calibration of the index of refraction measuring system was performed using a single fixed point (the NBS-calibrated sample) and a linear extrapolation based on this value was used. A more precise calibration of the equipment could be obtained if several samples covering the refractive index range of about 1.4700 to 1.5100 and spaced at intervals of about 0.0100 were available. These would also serve as a secondary check on the constancy of the index of each sample. That is, if the index of a calibration sample started to change due to hydration or stress annealing or some other mechanism, it should become immediately evident.

While the bulk absorption (transmission loss) at 0.6328 micrometers was measured directly, the index values obtained are strictly surface measurements and are valid only at the surface. This is a direct consequence of the geometry of the sample and the requirement for a noncontacting measurement. A slight modification of the sample geometry made by polishing two one-inch-wide flats (at accurately known angles to each other) on the edge of the sample would permit use of the minimum deviation method (see Fig. 5) (this was done to the reference sample so that a precise index value could be obtained by NBS). This method has the desirable feature of being a true bulk measurement and still being a noncontacting method (after the flat surfaces are polished). This method would require only a very slight modification of the laser and thermal aging fixtures, and would also have the advantage of not being affected by such things as surface quality and localized variations in the index.

The previously-mentioned diffraction and sample curvature effects may provide information relating to sample lifetime and beam quality effects. The diffraction patterns observed may contain information about crystal nucleation, growth and orientation. If such information were obtainable in this manner, a simple, noncontacting, in situ measurement of window quality may be possible.

CONCLUSIONS

The purpose of this program has been to investigate the long-term effects of exposing single crystal KCl and europium-doped polycrystal KCl to 10.6 micrometer irradiation and high temperature to determine the impact of these parameters on potential high-power laser window designs using these materials. Single crystal KCl and europium-doped polycrystal KCl windows were exposed to flux densities ranging from 1 kW/cm^2 to 5 kW/cm^2 for time periods of 100 hours. Periodic measurements of the optical properties of the test windows during the exposure period indicate a slow growth in the 10.6 micrometer absorptivity. This slow growth is accompanied by cyclic fluctuations above the average or mean value. The periodic excursions will require the use of larger safety factors in a high-power system design to prevent self-induced thermal stress failure of the windows.

The single crystal KCl as received would be capable of transmitting a 3 kW beam. This figure is based on assuming an initial value of β of .001 cm^{-1}. The calculation assumes a 10 cm diameter window illuminated with a 7 cm diameter beam of uniform intensity and that the window is edge-cooled by conduction. At this power level the outer fiber azimuthal tensile stress is equal to the material yield stress of 400 psi (2800 KPa). The absorptivity increases with time and the predicted value at $t = 10^4$ hrs was found to be .00154 cm^{-1} based initial assumed value of .001 cm^{-1}. This increase in absorptivity requires a reduction in the transmitted power to 1.95 kW. No safety factors are included in this analysis and no consideration has been given to the possibility of flaws in the volume that would cause failure to initiate at a point other than the outside edge. Some form of proof test would be required to eliminate this potential source of in-service failure.

The europium doped polycrystal KCl will transmit a considerably higher power beam than the single crystal material. This gain is realized because of the increased strength of the material (typically 3000 Psi (21 MPa)). The maximum transmitted power for a beam and window geometry as described previously for the single crystal material would be 22.5 kW for an initial β of .001 cm^{-1}. The 10.6 micro-meter absorptivity of the europium doped polycrystal material was found to increase more rapidly with time than the single crystal material. The predicted value of β at 10^4 hrs was .0033 cm^{-1} assuming an initial value of .001 cm^{-1}. Thus at 10^4 hrs the maximum transmitted power is reduced to 6.82 kW. As in the previous case no safety margin is included. The calculations of allowable transmitted power have not considered distortion of the beam due to thermal and stress optic effects or the possibility of local flaws causing premature (sub yield stress) failure of the windows. Allowable power loadings could also be increased by use of convection face cooling techniques.

Exposure of single crystal KCl and europium-doped polycrystal KCl to elevated temperature and pressure loading has shown the presence of mechanical creep in both types of windows. The europium-doped polycrystal material has proved to be significantly more resistant than the single crystal material. Periodic measurements of the optical properties of the test windows during the course of the 100-hour thermal aging has shown a general increase in the 10.6 micrometer absorptivity of the test windows. In the single crystal KCl material the rate of increase of 10.6 micrometer absorptivity is found to have an exponential temperature-dependence, increasing drastically at higher temperatures. The europimm-doped polycrystal KCl did not display any temperature-dependence in the rate of increase of 10.6 micrometer absorptivity over the temperature range from room temperature to 250°C.

On the basis of this work, it appeared possible to operate either single crystal KCl or europium-doped polycrystal KCl windows for long operating times as 10.6 micrometer windows provided sufficient safety margin is left in the design to accommodate the temporal growth of the window absorptivity.

TABLE 1

SINGLE CRYSTAL KCL ABSORPTIVITY AT
10.6 MICROMETERS AFTER
10.6 MICROMETER IRRADIATION

(absorptivity-cm^{-1})

Sample	10.6 Micrometer Laser Test Time						@ Power Density = watts/cm^2
	t=0 hrs	t=1.5 hrs	t=4.3 hrs	t=12.3 hrs	5=35 hrs	t=100 hrs	
7	0.00105	0.00101	0.00096	0.00129	0.00171	.00120	1495
5	0.00062	0.00087	0.00107	0.00139	0.00104	.00099	5000
8	0.00071	0.00175	0.00154	Discontinued			2236
4	0.00064	0.00068	Failed at 2.1 hrs				1000
9	Replaced 4 at t=2.1 hrs (0.00104)		0.00093	0.00106	0.00089	.00108	1000
6	Replaced 8 at t=4.3 hrs		0.00044	0.00073	0.00060	.00096	2236

TABLE 2

EUROPIUM-DOPED POLYCRYSTAL KCL ABSORPTIVITY AT
10.6 MICROMETERS AFTER
10.6 MICROMETER IRRADIATION

(absorptivity-cm^{-1})

Sample	10.6 Micrometer Laser Test Time						@ Power Density = watts/cm^2
	t=0 hrs	t=1.5 hrs	t=4.3 hrs	t=12.3 hrs	t=35 hrs	t=100 hrs	
4-C	0.00067 0.00068	0.00129	0.00158	0.00343	0.00145	.00181	5000
5-C	0.00195	0.00180	0.00170	0.00153 0.00162	0.00115	.00534	1495
6-C	0.00301	0.00313	0.00440	0.00618	0.00276	.00214	1000
1-C	0.00121	0.00130	0.00185	0.00170	0.00187	.00195 .0020	2236

TABLE 3

KCl SINGLE CRYSTAL REFRACTIVE INDEX
AFTER 10.6 MICROMETER IRRADIATION

(@ .6328 micrometers)

Sample	10.6 Micrometer Laser Test Time						@ Power Density = watts/cm^2
	t=0 hrs	t=1.5 hrs	t=4.3 hrs	t=12.3 hrs	t=35 hrs	t=100 hrs	
4-1	1.4846	1.4815					1000
-3	1.4870	1.4823					
-4	1.4864	1.4814	Failed During 4.3 Hour Irradiation				
-5	1.4854	1.4827					
-7	1.4865	1.4816					
5-1	1.4869	1.4840	1.4846	1.4851	1.4867	1.4813	5000
-3	1.4863	1.4836	1.4843	1.4851	1.4883	1.4941	
-4	1.4868	1.4828	1.4830	1.4849	1.4865	1.4935	
-5	1.4870	1.4838	1.4840	1.4870	1.4847	1.4982	
-7	1.4866	1.4834	1.4834	1.4837	1.4834	1.4905	
7-1	1.4861	1.4802	1.4800	1.4808	1.4823	1.4879	1495
-3	1.4871	1.4888	1.4871	1.4763	1.4776	1.4791	
-4	1.4873	1.4879	1.4853	1.4739	1.4768	1.4828	
-5	1.4874	1.4876	1.4683	1.4730	1.4751	1.4803	
-7	1.4874	1.4714	1.4729	1.4770	1.4687	*	
8-1	1.4800	1.4963	1.4957				2236
-3	1.4813	1.5007	1.5061				
-4	1.4814	1.4916	1.4933	Discontinued at t = 4.3 hrs			
-5	1.4812	1.4882	1.4925				
-7	1.4815	1.4818	1.4814				
6-1			1.4863	1.4872	1.4894	1.4872	2236
-3			1.4859	1.4867	1.4875	1.4884	
-4	Not Irradiated		1.4866	1.4866	1.4862	1.4865	
-5			1.4863	1.4863	1.4856	1.4867	
-7			1.4870	1.4868	1.4857	1.4853	
9-1			1.4866	1.4861	1.4865	1.4868	1000
-3			1.4862	1.4884	1.4862	1.4857	
-4			1.4869	1.4867	1.4869	1.4865	
-5			1.4868	1.4874	1.4868	1.4869	
-7			1.4867	1.4855	1.4867	1.4878	

TABLE 4

KCl SINGLE CRYSTAL PERCENT TRANSMISSION LOSS AFTER 10.6 MICROMETER IRRADIATION

(@ 0.6328 Micrometers)

Sample	10.6 Micrometer Laser Test Time						@ Power Density = watts/cm^2
	t=0 hrs	t=1.5 hrs	t=4.3 hrs	t=12.3 hrs	t=35 hrs	t=100 hrs	
4-1	1.05	-.13					1000
-3	.79	3.08					
-4	.75	-.10	Failed During 4.3 Hour Irradiation				
-5	.67	1.00					
-7	.62	.45					
5-1	.50	.09	.24	.43	-.11	.86	5000
-3	.41	.53	.87	-.01	.42	2.37	
-4	.43	.18	1.38	.23	.47	1.63	
-5	.81	.41	.70	.12	1.08	.60	
-7	2.02	1.46	1.66	.52	1.50	3.03	
7-1	.92	.74	1.42	.68	1.19	1.23	1495
-3	.77	.06	1.18	.43	1.09	.95	
-4	.92	.25	1.49	.42	1.19	1.85	
-5	1.12	.16	2.00	.74	1.47	1.50	
-7	.83	.51	1.16	.47	1.4	1.45	
8-1	1.37	6.86	10.17				2236
-3	1.28	8.39	11.32				
-4	1.06	5.03	4.13				
-5	1.11	2.17	2.06				
-7	1.04	.45	1.37				
6-1			-	-.61	-.31	-.10	2236
-3			-	-.84	-.37	.17	
-4	Not Irradiated		-	-.67	-.39	-.27	
-5			-	-.62	-.20	-.15	
-7			-	-.11	-.30	.11	
9-1			.47	.12	.15	.36	1000
-3			-.01	.11	-.33	.03	
-4			-.14	.11	-.06	-.27	
-5			.08	.11	-.33	-.16	
-7			-.30	.12	.13	-.15	

TABLE 5

EUROPIUM DOPED POLYCRYSTAL KCl REFRACTIVE INDEX AFTER
10.6 MICROMETER IRRADIATION

(@ .6328 micrometers)

Sample	10.6 Micrometer Laser Test Time						@ Power Density = watts/cm^2
	t=0 hrs	t=1.5 hrs	t=4.3 hrs	t=12.3 hrs	t=35 hrs	t=100 hrs	
1-C-1	1.4830	1.4832	1.4828	1.4827	1.4813	1.4811	2236
-3	1.4868	1.4877	1.4868	1.4883	1.4836	1.4833	
-4	1.4876	1.4877	1.4887	1.4899	1.4873	1.4881	
-5	1.4875	1.4870	1.4875	1.4879	1.4900	1.4882	
-7	1.4803	1.4873	1.4873	1.4767	1.4829	1.4834	
4-C-1	1.4862	1.4861	1.4842	1.4824	1.4846	1.4844	5000
-3	1.4862	1.4869	1.4847	1.4875	1.4839	1.4839	
-4	1.4859	1.4860	1.4836	1.4871	1.4836	1.4842	
-5	1.4854	1.4864	1.4884	1.4829	1.4877	1.4867	
-7	1.4829	1.4848	1.4836	1.4861	1.4874	1.4870	
5-C-1	1.4855	1.4847	1.4915	1.4986	1.4788*	*	1495
-3	1.4825	1.4833	1.4907	1.5074	- *	*	
-4	1.4813	1.4827	1.4836	1.4940	- *	*	
-5	1.4819	1.4838	1.4828	1.4807	- *	*	
-7	1.4823	1.4832	1.4826	1.4891	1.4763*	*	
6-C-1	1.4864	1.4865	1.4879	1.4871	1.4862	1.4871	1000
-3	1.4875	1.4873	1.4873	1.4907	1.4874	1.4882	
-4	1.4865	1.4871	1.4865	1.4896	1.4887	1.4878	
-5	1.4863	1.4866	1.4865	1.4882	1.4873	1.4877	
-7	1.4863	1.4868	1.4866	1.4864	1.4871	1.4872	

*strong glare-data unreliable

TABLE 6

EUROPIUM DOPED POLYCRYSTAL KCl PERCENT TRANSMISSION LOSS AFTER 10.6 MICROMETER IRRADIATION

(@ .6328 micrometers)

Sample	10.6 Micrometer Laser Test Time						@ Power Density
	t=0 hrs	t=1.5 hrs	t=4.3 hrs	t-12.3 hrs	t=35 hrs	t=100 hrs	= watts/cm^2
1-C-1	7	7	7	6	7	6	2236
-3	8	8	9	6	6	8	
-4	8	11	11	8	9	8	
-5	9	12	13	9	8	9	
-7	17	17	18	17	18	16	
4-C-1	30	32	33	26	27	26	5000
-3	33	36	38	29	30	30	
-4	33	31	36	29	33	33	
-5	35	36	40	29	36	35	
-7	35	37	42	30	32	33	
5-C-1	24	26	29	28	33	30	1495
-3	28	27	29	37	41	40	
-4	29	26	29	38	42	38	
-5	25	26	29	37	38	34	
-7	25	26	28	33	35	35	
6-C-1	40	42	47	40	43	39	1000
-3	45	48	53	42	43	42	
-4	44	47	53	42	44	43	
-5	46	48	58	44	45	45	
-7	43	45	50	38	41	39	

TABLE 7

10.6 MICROMETER ABSORPTIVITY OF WINDOWS
FOR THERMAL AGING TEST

Europium Doped Polycrystal KCl

(absorptivity-cm^{-1})

Sample	Thermal Aging Test Time						Thermal Aging Temperature °C
	t=0 hrs	t=1.5 hrs	t=4.3 hrs	t=12.3 hrs	t=35 hrs	t=100 hrs	
12-C	0.00182	.00302	.00111	.00208	.00462	.00464	250°C
7-C	0.00553	.001506	.00089	.00095	.00172	.00798	179°C
15-C	0.00086	.00135	.00340	.00075	.00142	.00345	118°C
14-C	0.00080	.00128	.00176	.00179	.00309	.00295	66°C
8-C	0.00125	.00170 .00166	.00212	.00453	.00387	.00646	20°C
			Single Crystal KCl				
1	0.00042	.00069	.00216				250°C
10	0.00047	.00077	.00146				179°C
2	0.00047	.00076	.00127	.00429	.00139	.00152	118°C
14	0.00065	.00096	.00444	.00129	.00152	.00775	66°C
13	0.00095	.00097	.00118	.00184	.00175	.00641	20°C

TABLE 8

THERMAL AGING TEST WINDOW
RADIUS OF CURVATURE
(r_c meters)

	12.3 hrs.	35 hrs.	100 hrs.	Thermal Aging Temperature °C
Single Crystal KCl				
13	23 ± 6	23 ± 6	23 ± 6	20°C
14	23 ± 6	18 ± 3+	9 ± 1+	66°C
2	$2.6 \pm .2$	$1.0 \pm .1$+	$.8 \pm .1$+	118°C
Europium doped Polycrystal KCl				
8-C	> 40	> 40	> 40++	20°C
14-C	> 40	> 40	> 40	66°C
15-C	> 40	> 40	> 40	118°C
7-C	$40. \pm 10$	$40. \pm 10$	33 ± 7	179°C
12-C	23 ± 6	23 ± 6	15 ± 2	250°C

* Window cracked at 96 hrs.

\+ Windows show considerable small scale irregularities on surface. Step type discontinuities with a depth on the order of 1/4 to 1/2 fringe of visable light.

++ Window cracked between 35 and 100 hours but cracks did not penetrate vacuum surface.

TABLE 9

KCl SINGLE CRYSTAL REFRACTIVE INDEX AFTER THERMAL AGING

(@ .6328 micrometers)

Sample	Thermal Aging Test Time						Thermal Aging Temperature°C
	t=0 hrs	t=1.5 hrs	t=4.3 hrs	t=12.3 hrs	t=35 hrs	t=100 hrs	
1-1	1.4787	1.4309	1.6173*				250°C
-3	1.4809	1.4943	1.4857				
-4	1.4822	1.4865	1.4871				
-5	1.4848	1.4883	1.4943				
-7	1.4858	1.4917	1.4962				
2-1	1.4848	1.4874	1.4874	1.4870	1.4888	1.4896	118°C
-3	1.4858	1.4864	1.4872	**	**	**	
-	1.4851	1.4898	1.4869*	1.4876	**	**	
-5	1.4843	1.4894	1.4856	1.4860	**	**	
-7	1.4849	1.4860	1.4855	1.4853	1.4868	**	
10-1	1.4850	1.4942	1.4907*				179°C
-3	1.4852	1.4953	1.4939*				
-4	1.4857	1.4909	1.4910*				
-5	1.4846	1.4948	1.4905*				
-7	1.4848	1.4935	1.4879*				
13-1	1.4855	1.4885	1.4864	1.4898	1.4911	**	20°C
-3	1.4852	1.4862	1.4872	1.4903	1.4940	**	
-4	1.4854	1.4866	1.4868	1.4911	1.4952	**	
-5	1.4852	1.4853	1.4873	1.4904	1.4931	**	
-7	1.4840	1.4858	1.4856	1.4889	1.4920	**	
14-1	1.4867	1.4867	1.4873	1.4866	**	**	66°C
-3	1.4864	1.4890	1.4877	1.4869	**	**	
-4	1.4867	1.4881	1.4873	1.4884	**	**	
-5	1.4879	4.4896	1.4864	1.4903	**	**	
-7	1.4862	1.4871	1.4855	1.4853	1.4868	1.4852	

** Diffraction in reflected beam prevents initialization of system for Index Run

* Initialization not reliable due to diffraction effects.

TABLE 10

KCl SINGLE CRYSTAL PERCENT TRANSMISSION
LOSS AFTER THERMAL AGING

(@ .6328 micrometers)

Sample	Thermal Aging Time						
	t=0 hrs	t=1.5 hrs	t=4.3 hrs	t-12.3 hrs	t=35 hrs	t-100 hrs	Thermal Aging Temperature°C
1-1	1.64	3.57	.86				250°C
-3	5.17	8.60	11.47				
-4	1.27	6.17	10.25				
-5	.35	6.99	12.36				
-7	-.38	2.52	4.03				
10-1	-.46	.49	.99				179°C
-3	-.49	1.26	2.16				
-4	-.59	1.93	3.25				
-5	-.55	.69	2.55				
-7	-.41	.34	1.23				
2-1	-.67	.39	-.48	.05	.33	2.82	118°C
-3	-.73	.76	.57	--	3.88	5.12	
-4	-.64	.57	.38	1.12	3.34	6.35	
-5	-.64	.35	.21	1.05	3.45	5.63	
-7	-.36	.07	-.26	.17	.30	2.92	
14-1	-.37	.46	.20	.36	22.46	12.43	66°C
-3	-.16	.24	.80	.56	31.41	21.03	
-4	-.19	.30	.77	1.31	30.89	17.94	
-5	-.37	.09	.90	.84	36.04	17.33	
-7	-.31	.03	.41	3.40	27.46	16.68	
13-1	-.55	.33	.22	.99	.46	-.23	20°C
-3	-.58	.03	-.04	.24	1.92	-.19	
-4	-.55	.31	.21	-.10	1.87	-.25	
-5	-.52	.02	.37	.14	2.08	.16	
-7	-.34	-.09	.21	.24	.09	-.23	

* Compared to reference sample

TABLE 11

EUROPIUM DOPED POLYCRYSTAL KCl REFRACTIVE INDEX
AFTER THERMAL AGING

(@ .6328 micrometers)

Sample	Thermal Aging Time						
	t=0 hrs	t=1.5 hrs	t=4.3 hrs	t=12.3 hrs	t=35 hrs	t=100 hrs	Thermal Aging Temperature °C
12-C-1	1.4903	1.4937	1.4918	1.4958	1.5011	1.4978	250°C
-3	1.4903@	1.4921	1.4896	1.4911	1.4996	1.4995	
-4	1.4889	1.4886	1:4903	1.4954	1.5013	1.4993	
-5	1.4870	1.4925	1.4894	1.4988	1.5036	1.4971	
-7	1.4893	1.4912	1.4900	1.4914	1.4931	1.4968	
7-C-1	1.4879	1.4875	1.485 6	1.4869	1.4900	1.4989	179°C
-3	1.4877	1.4876	1.4874	1.4865	1.4910	1.4894	
-4	1.4914	1.4882	**	**	**	**	
-5	1.4876	1.4873	1.4862	1.4865	1.4926	**	
-7	1.4864	1.4854	1.4852	1.4918	1.4922	1.4922	
15-C-1	1.4858	1.4873	1.4949	1.4854	1.4860	1.4856	118°C
-3	1.4846	1.4857	1.4872	1.4813	1.4845	1.4838	
-4	1.4848	1.4920	1.4903	1.4813	1.4849	1.4823	
-5	1.4859	1.4933	1.4873	1.4841	1.4894	1.4863	
-7	1.4845	1.4908	1.4869	1.4853	1.4950	1.4879	
14-C-1	1.4878	1.4890	1.4885	**	**	**	66°C
-3	1.4879	1.4903	1.4887	1.4721	**	**	
-4	1.4875	1.4871	1.4890	**	**	**	
-5	1.4885	1.4897	1.4892	**	**	**	
-7	1.4881	1.4931	1.4886	**	**	**	
8-C-1	1.4861	1.4894	1.4874	1.4946	1.4992	1.5181	20°C
-3	1.4869	1.4976	1.4876	1.4936	1.5000	1.5206	
-4	1.4851	1.4889	1.4873	1.4925	1.4961	1.5204	
-5	1.4839	1.4866	1.4878	1.4924	1.4969	1.5222	
-7	1.4846	1.4810	1.4806	1.4856	1.4869	1.5109	

@ 3 x normal reflectivity

TABLE 12

EUROPIUM DOPED POLYCRYSTAL KCl PERCENT TRANSMISSION * LOSS AFTER THERMAL AGING

(@ .6328 micrometers)

Sample	Thermal Aging Time						Thermal Aging Temperature °C
	t=0 hrs	t=1.5 hrs	t=4.3 hrs	t=12.3 hrs	t=35 hrs	t=100 hrs	
12-C-1	31	47	46	46	47	37	250°C
-3	32	42	41	50	44	34	
-4	42	57	57	55	57	46	
-5	43	54	55	63	67	52	
-7	32	54	55	60	61	52	
7-C-1	49	46	46	48	52	38	179°C
-3	38	52	36	40	51	32	
-4	37	35	35	37	39	31	
-5	35	34	36	37	40	31	
-7	39	48	48	51	54	43	
15-C-1	9	8	8	9	10	8	118°C
-3	8	8	8	10	10	9	
-4	8	9	9	11	11	10	
-5	8	11	12	13	14	12	
-7	9	16	17	17	18	17	
14-C-1	30	29	30	34	36	32	66°C
-3	35	38	39	46	46	38	
-4	39	39	40	48	48	39	
-5	37	38	39	50	52	40	
-7	40	36	37	38	38	30	
8-C-1	30	30	30	34	35	28	20°C
-3	36	34	33	41	44	35	
-4	30	29	29	37	38	34	
-5	31	30	30	49	49	43	
-7	33	33	33	41	47	37	

* Compared to reference sample

TABLE 13

EUROPIUM-DOPED POLYCRYSTAL KCl

Average Grain Size in Exposed Material
(t = 100 hr)

IRRADIATION

Window	Average Grain Size (Micrometers)	Irradiation Level
6-C	33.2	1000 w/cm^2
5-C	15.4	1495 w/cm^2
1-C	119.6	2236 w/cm^2
4-C	15.0	5000 w/cm^2

THERMAL AGING

Window	Average Grain Size (Micrometers)	Temperature
8-C	21.7	20°C
14-C	37.9	66°C
15-C	33.6	118°C
7-C	53.8	179°C
12-C	30.6	250°C

TABLE 14

SINGLE CRYSTAL KCl
(as received material)

Sample	Temperature °C	E(GPa)	μ	σ_{yield} (MPa)
3-3	20			2.54
3-5	118			1.98
3-6	179			2.51
12-3	66			3.05
12-4	250			2.07
12-1	20	24.5	.110	
12-1	66	23.4	.116	
12-1	118	24.1	.122	
12-2	179	29.9	.253	
12-2	250	34.5	.263	
12-3	66			3.05
12-4	250			2.07

TABLE 15

EUROPIUM-DOPED POLYCRYSTAL KCl
(as received material)

Sample	Temperature (°C)	E(GPa)	μ	σ_{yield} (MPa)
2-C-1	20	32.3	.273	
	66	30	.399	
	118	28.4	.300	
	179	19.6	.495	
	250	21.0	.485	
2-C-2	20	19.1	.410	
	66	17.5	.398	
	118	17.3	.388	
	179	17.4	.386	
	250	18.4	.395	
2-C-3	179			11.7
2-C-4	250			12.3
2-C-5	66		brittle failure	
3-C-1	20			13.9
3-C-2	66			12.2
3-C-3	118			13.5
3-C-4	179			16.4
3-C-5	250			11.4
3-C-6	66		brittle failure	

TABLE 16

SINGLE CRYSTAL KCl POST EXPOSURE
MECHANICAL PROPERTIES (Measured at 20°C)

Irradiation Test (t = 100 hrs)

Sample	I(w/cm^2)**	E(GPa)	μ	σ_{yield} (MPa)
9	1000	31.6	.083	1.19
7	1495	60.8	.231	3.81
6	2236	13.4	.095	.97
5	5000	18.6	.121	.81

Thermal Aging Test (t = 100 hrs)

Sample	Temperature (°C)**	E(GPa)	μ	σ_{yield} (MPa)
13	20	41.0	.144	not available
14	66	51.4	.457	1.61
2	118	70.3	.204	.68
10*	179	24.6	.419	7.31
1*	250	38.3	.102	1.63

*Data shown is on samples as removed at t = 4.3 hrs.
**Exposure level

TABLE 17

EUROPIUM-DOPED POLYCRYSTAL KCl

Irradiation Test (t = 100 hrs)

Sample	Test Intensity (w/cm^2)	E(GPa)*	μ*	σ_{yield} (MPa) *
6-C	1000	59.0	.334	26.9
5-C	1495	25.2	.349	16.5
1-C	2236	24.1	.276	6.81
4-C	5000	18.2	.306	9.65

Thermal Aging Test (t = 100 hrs)

Sample	Test Temperature (°C)	E(GPa)*	μ*	σ_{yield} (MPa) *
8-C	20	27.5	.279	11.9
14-C	66	52.3	.472	16.4
15-C	118	37.3	.197	7.13
7-C	179	46.5	.213	17.6
12-C	250	19.3	.287	19.0

* Measured values were obtained at 20°C after 100 hours of exposure at the Test Intensity or Test Temperature shown.

FIG. 1

BREWSTER ANGLE DETERMINATION

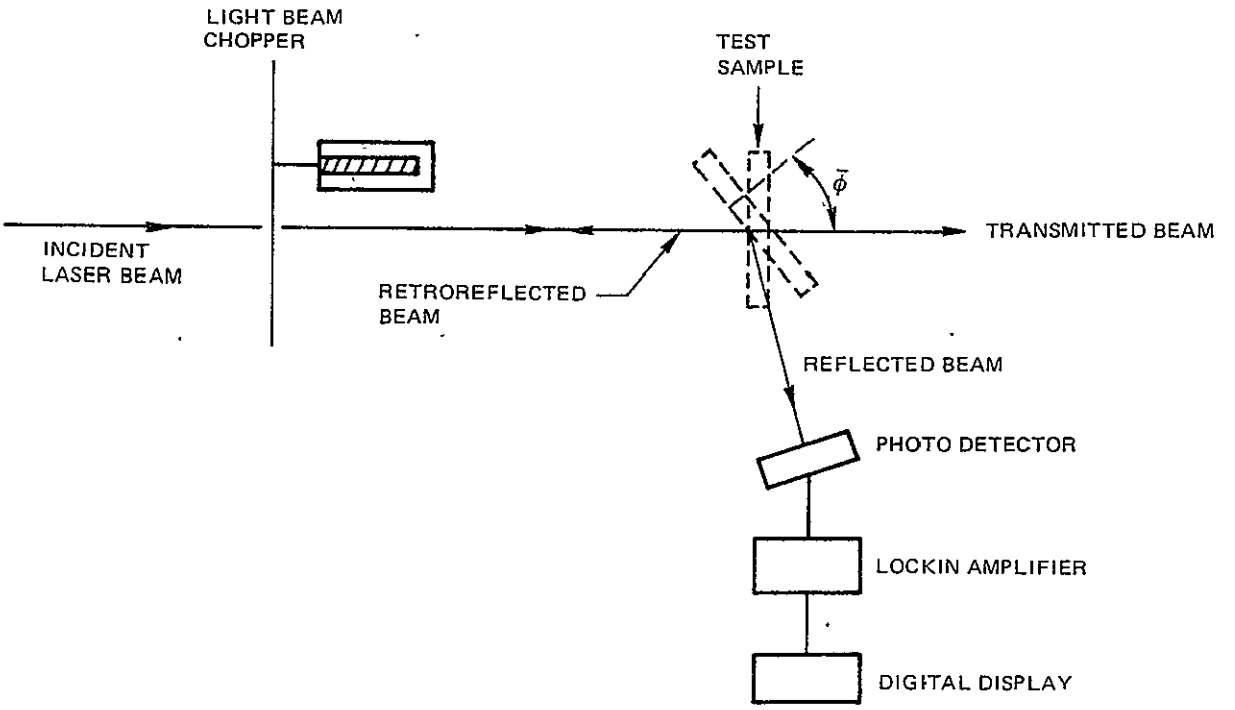

R05–75–5

POSITION SENSING PHOTODETECTOR INSTALLATION

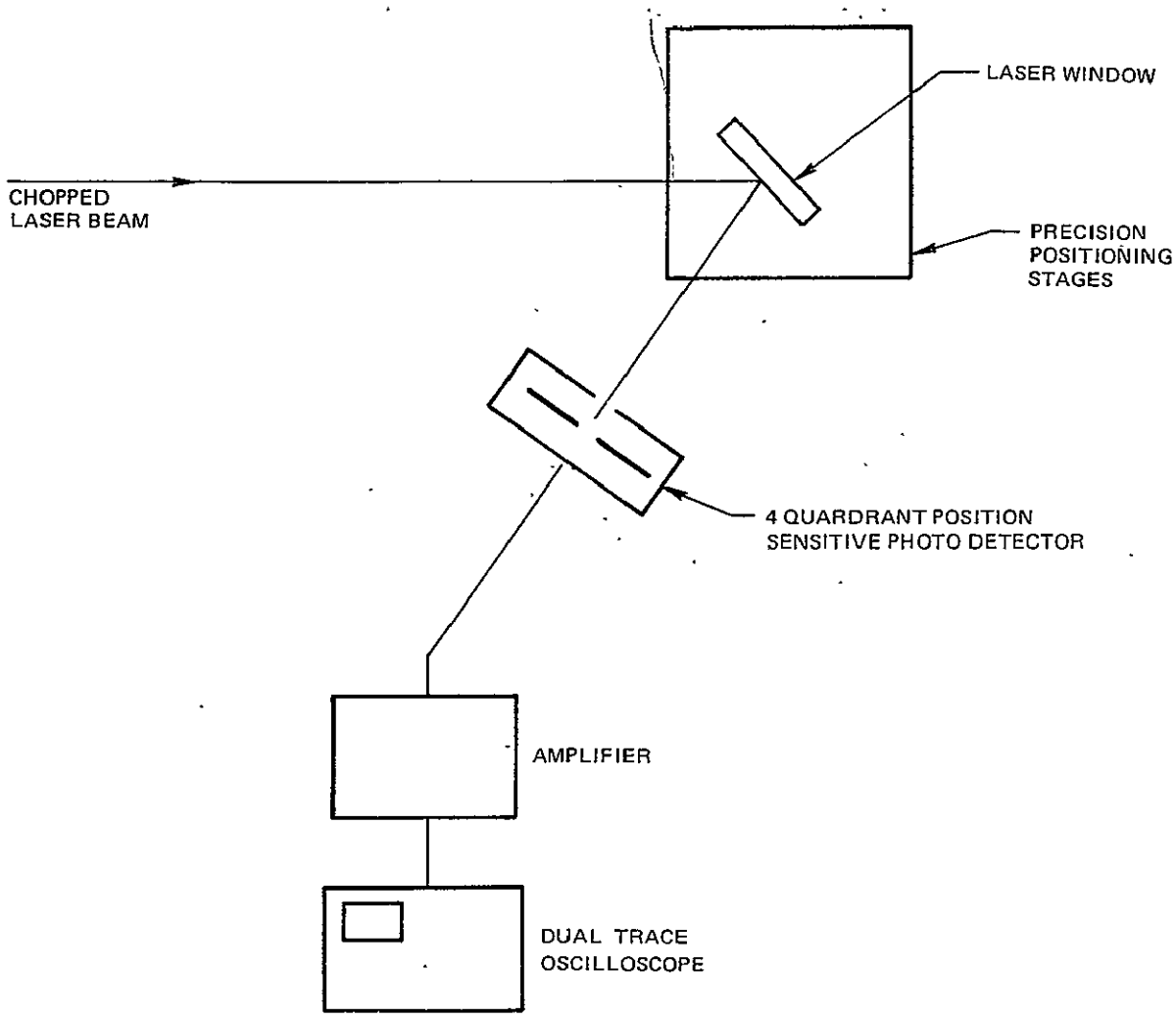

R05–75–4

INITIAL POSITION SENSOR SYSTEM OPERATION

(a) BEAM CENTERED

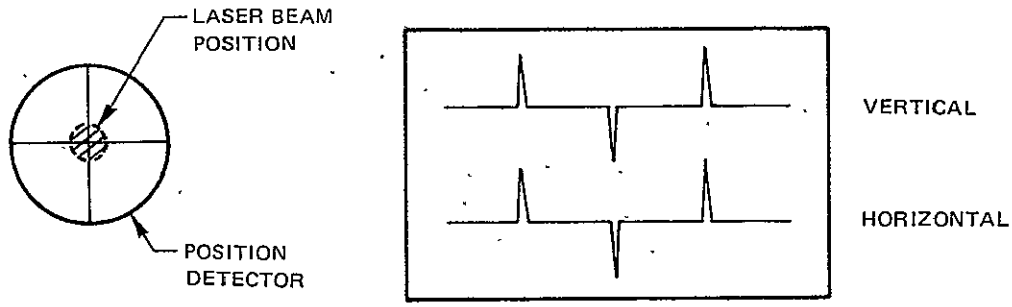

(b) BEAM UNBALANCED VERTICALLY

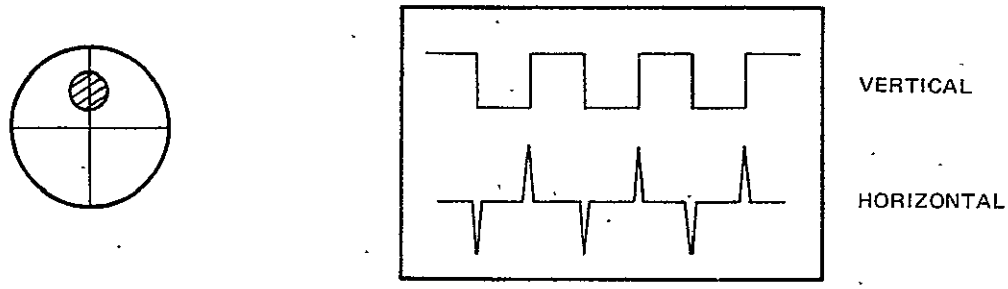

(c) BEAM UNBALANCED HORIZONTALLY

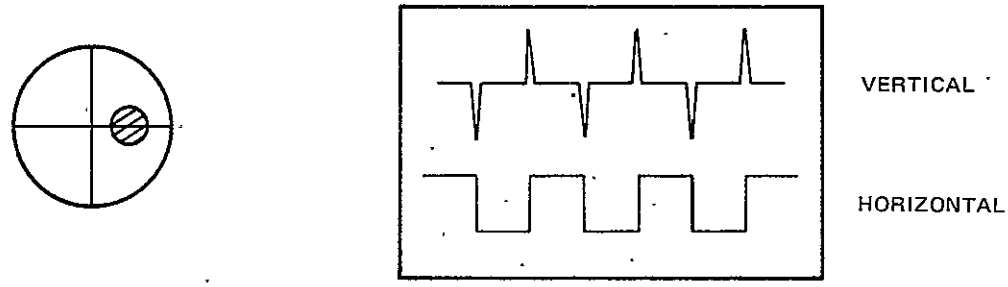

(d) BEAM UNBALANCED HORIZONTALLY AND VERTICALLY

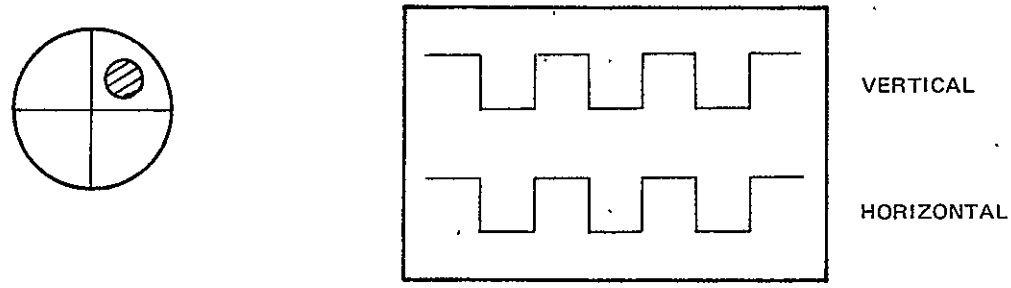

FIG. 4

REFRACTOMETER GEOMETRY

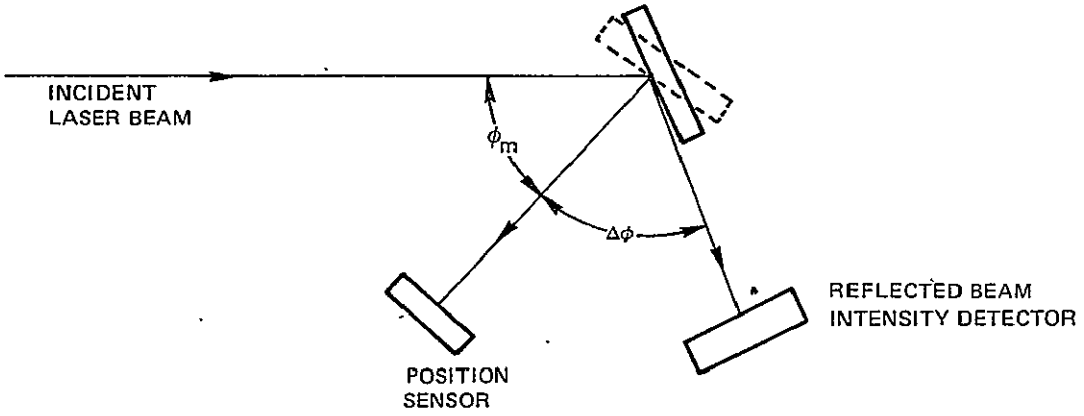

R05–75–3

GEOMETRY FOR MINIMUM DEVIATION REFRACTOMETRY

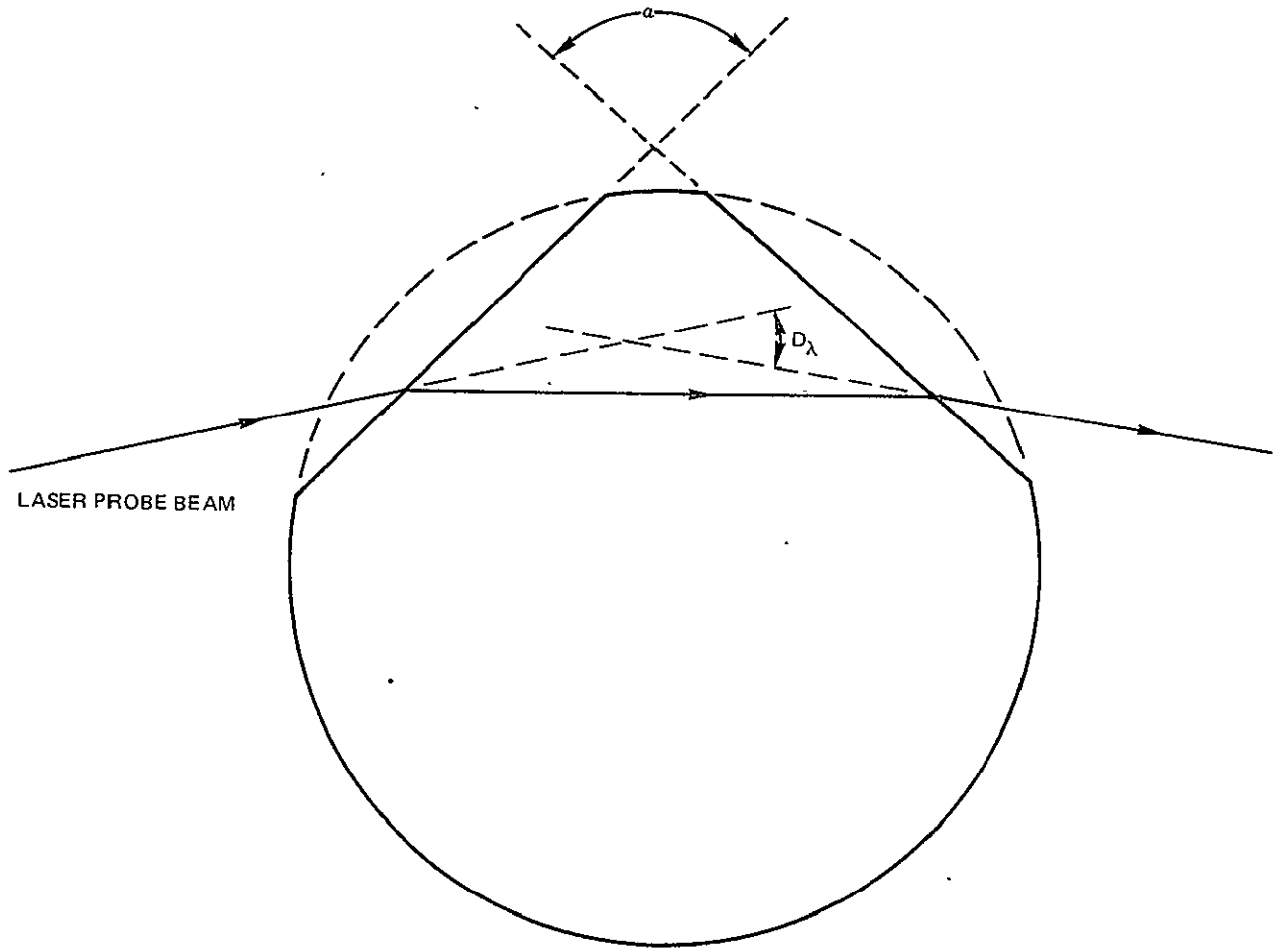

R05–75–2

FIG. 6

FIG. 7

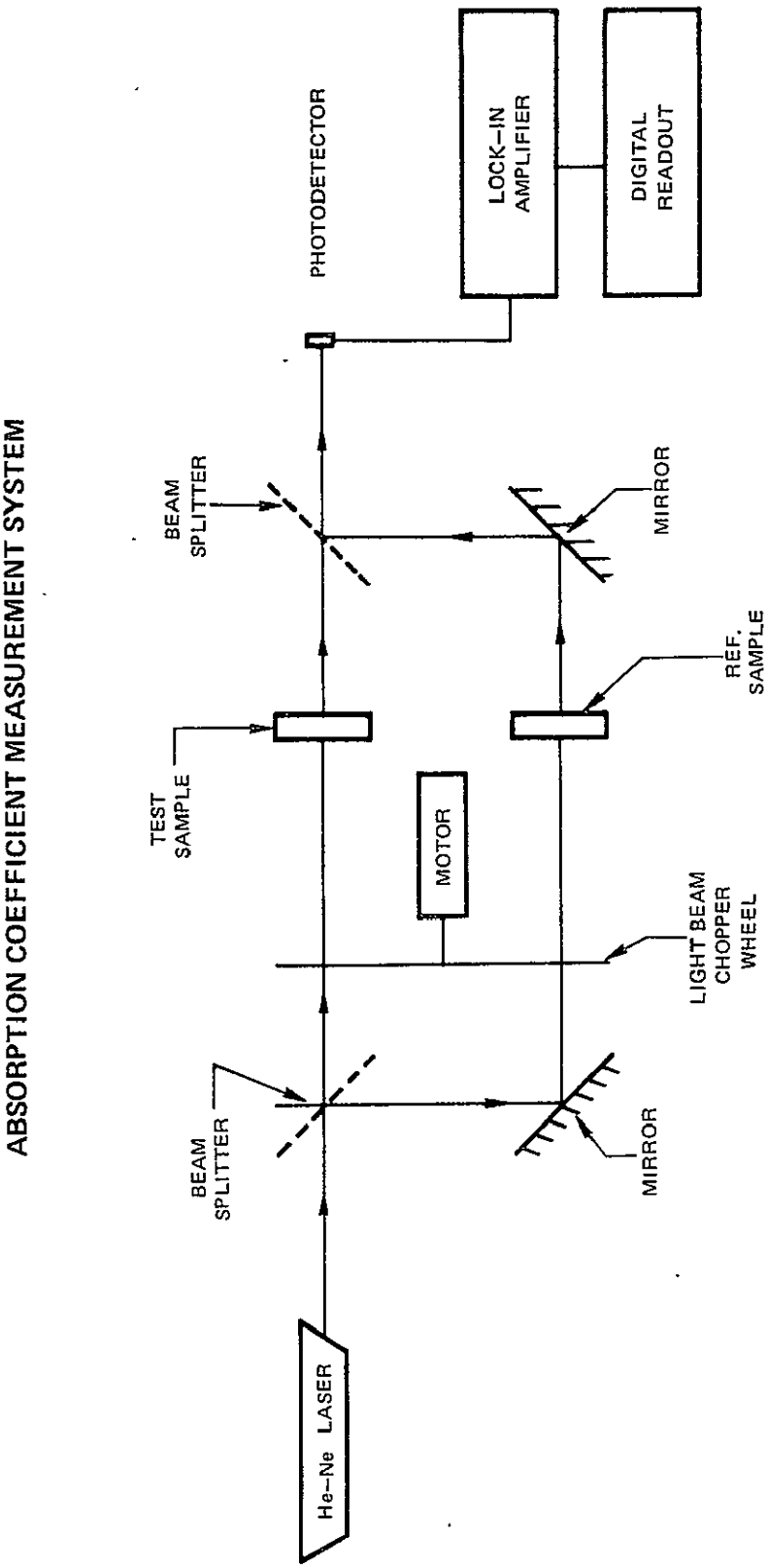
ABSORPTION COEFFICIENT MEASUREMENT SYSTEM
He-Ne LASER
BEAM SPLITTER
BEAM SPLITTER
MIRROR
MIRROR
TEST SAMPLE
REF. SAMPLE
MOTOR
LIGHT BEAM CHOPPER WHEEL
PHOTODETECTOR
LOCK-IN AMPLIFIER
DIGITAL READOUT

RO2–28–3

10.6 MICRO–METER ABSORPTION CALORIMETER

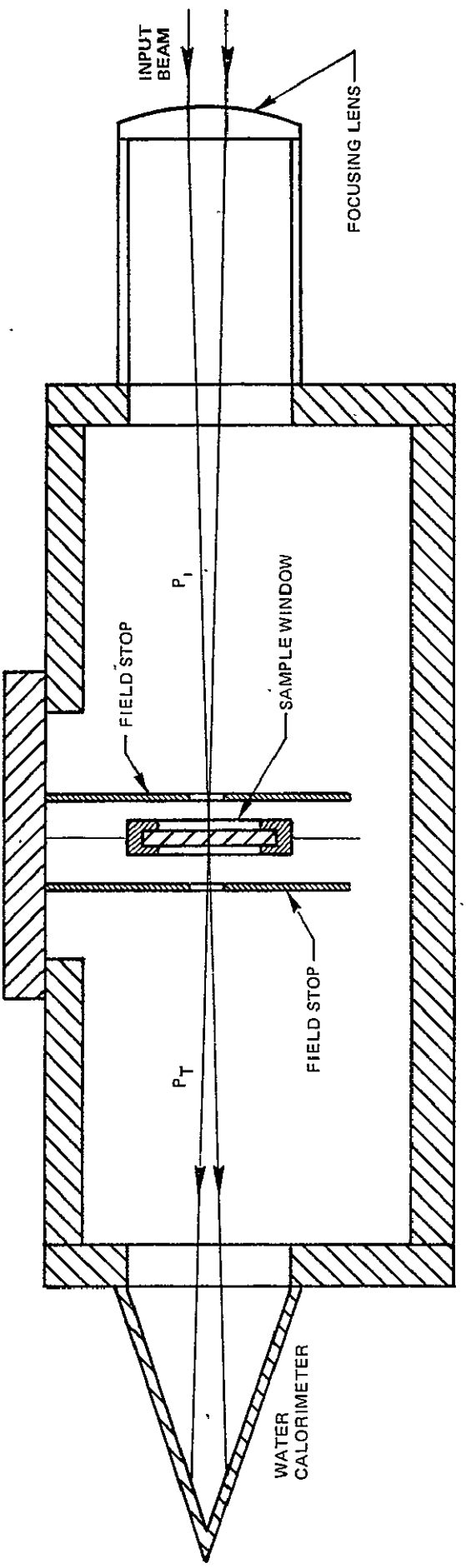

FIG. 9

NASA SINGLE CRYSTAL # 1

P_T = 33.6 WATTS

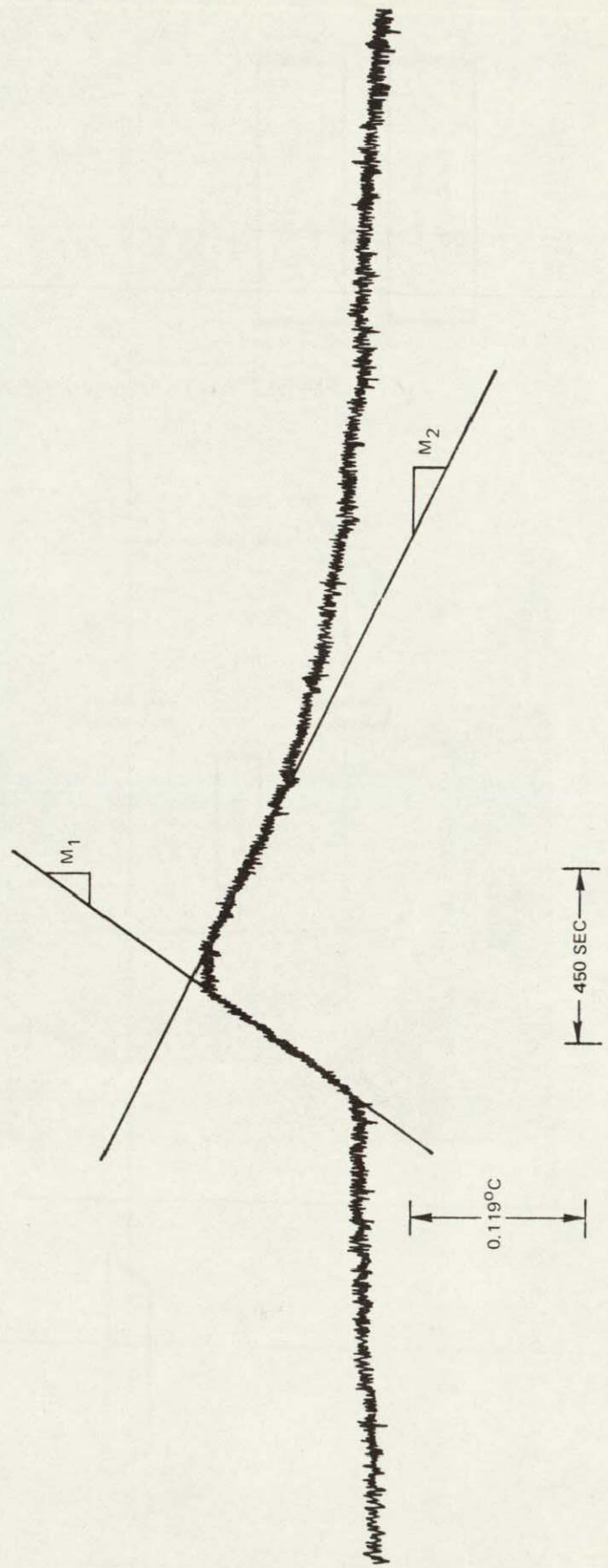

R05–18–2

FIG. 10

SINGLE CRYSTAL WINDOW

SAMPLE #3

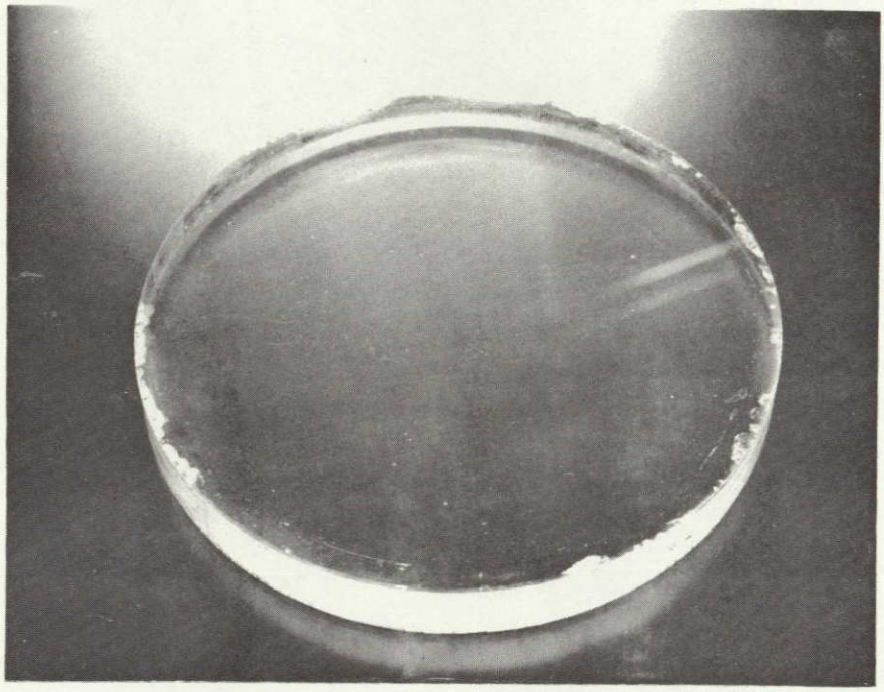

R05–104–1

FIG. 11

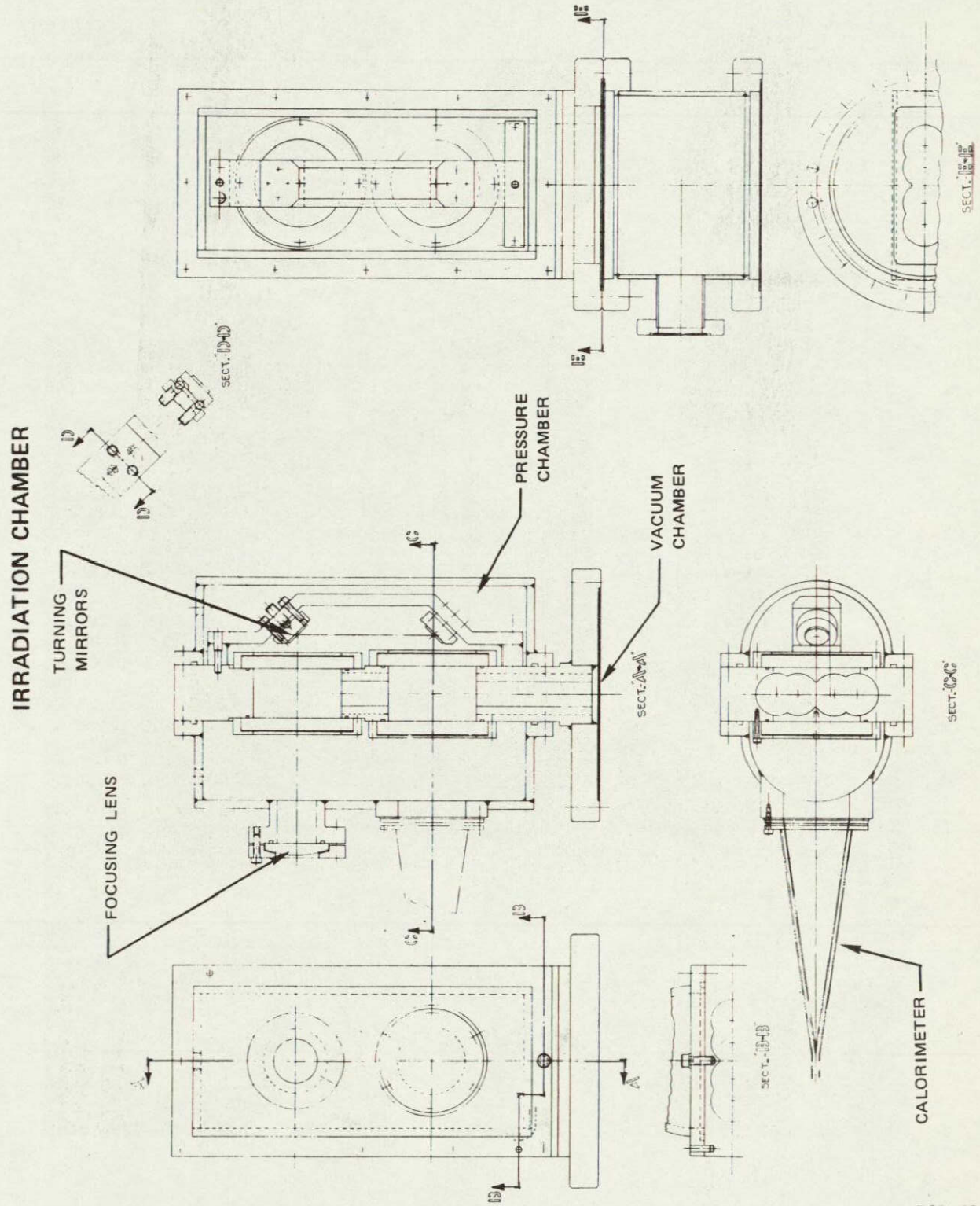
IRRADIATION CHAMBER
TURNING MIRRORS
FOCUSING LENS
PRESSURE CHAMBER
VACUUM CHAMBER
CALORIMETER
R02–60–1

FIG. 12

IRRADIATION TEST FACILITY

(PRESSURE CHAMBER COVERS IN POSITION)

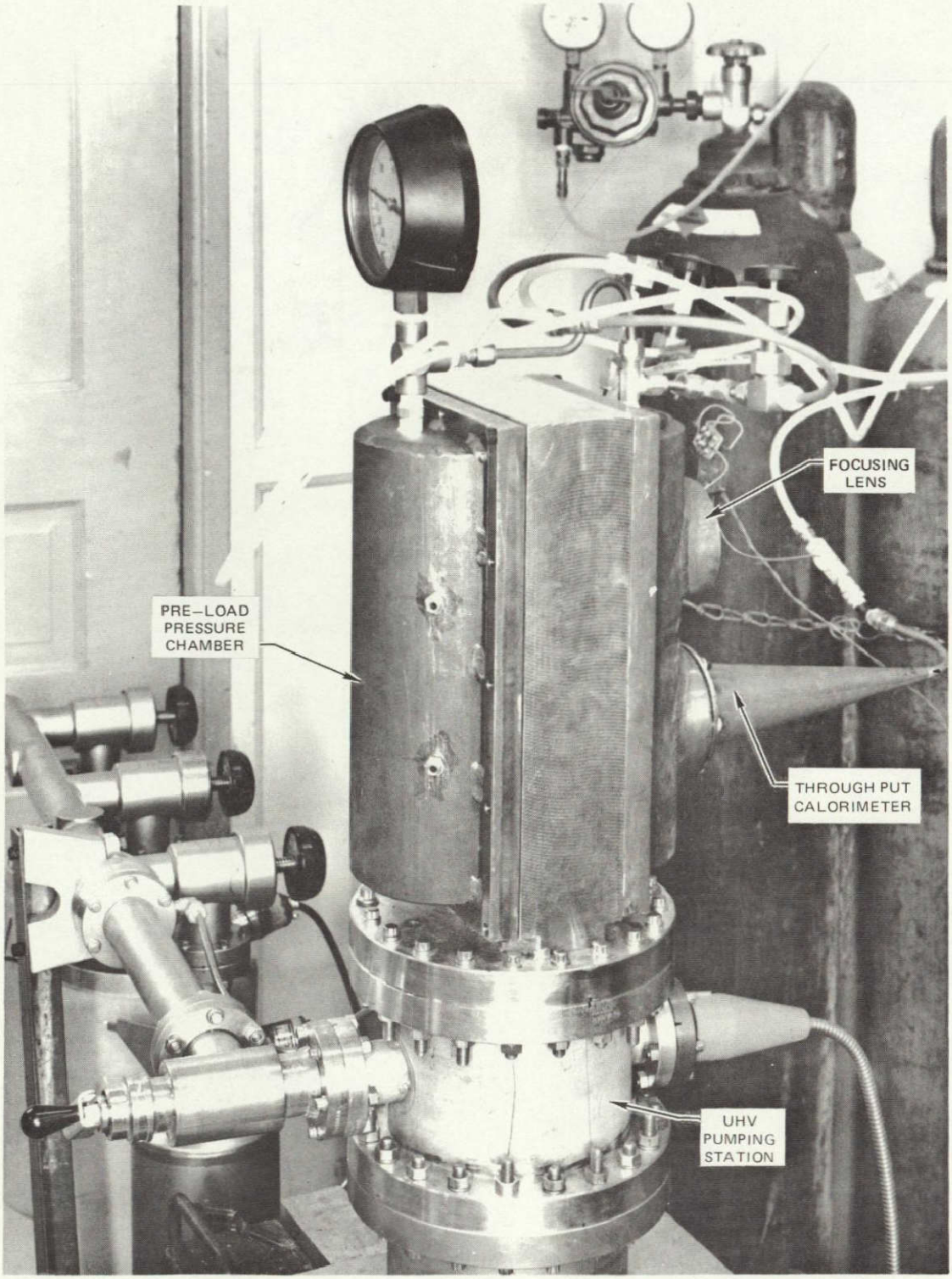

FIG. 13

IRRADIATION TEST FACILITY

(PRESSURE CHAMBER COVERS REMOVED)

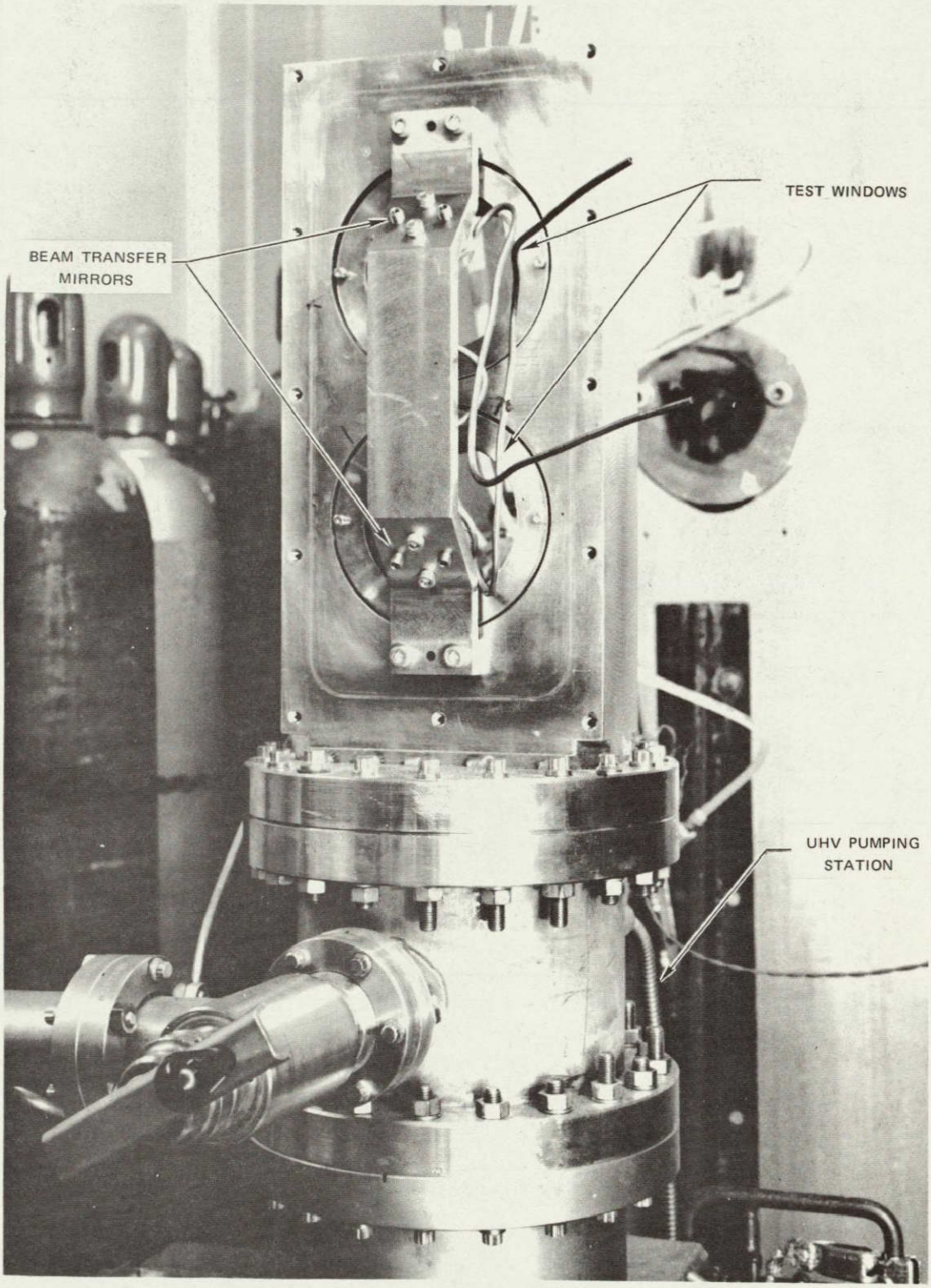

R08-73-8

FIG. 14

SINGLE CRYSTAL KCl WINDOW

AFTER 2.1 HRS AT 1000 WATTS/CM^2

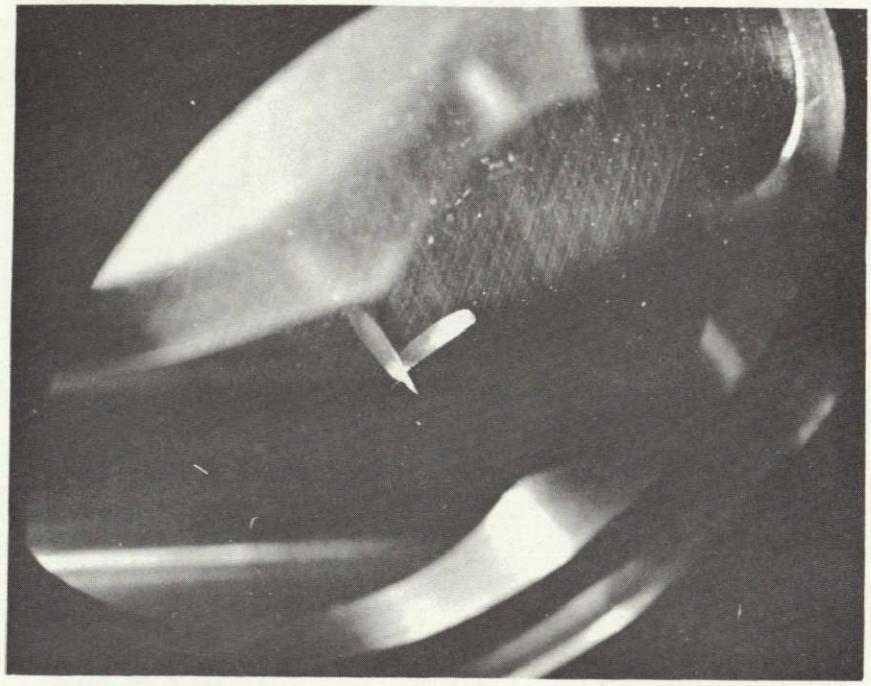

R08–73–4

FIG. 15

SINGLE CRYSTAL KCL 10.6 MICROMETER ABSORPTIVITY VS TIME OF IRRADIATION

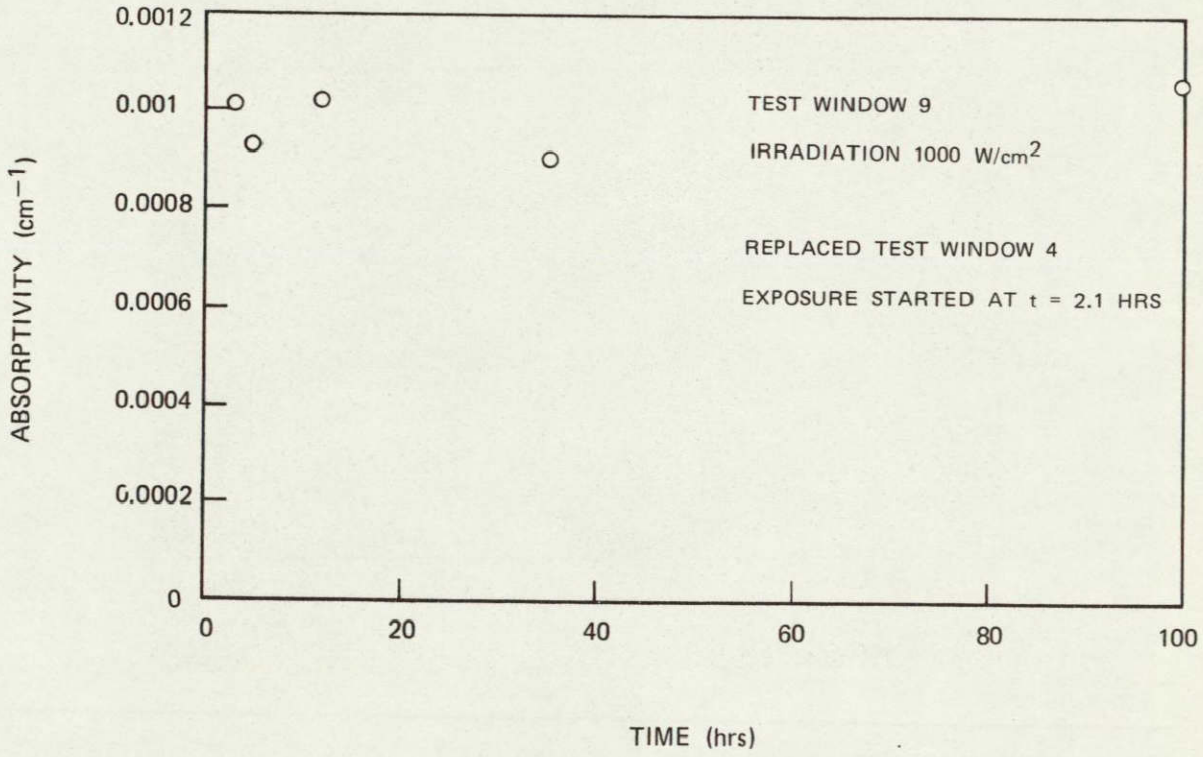

76–02–85–6

FIG. 16

SINGLE CRYSTAL KCL 10.6 MICROMETER ABSORPTIVITY VS TIME OF IRRADIATION

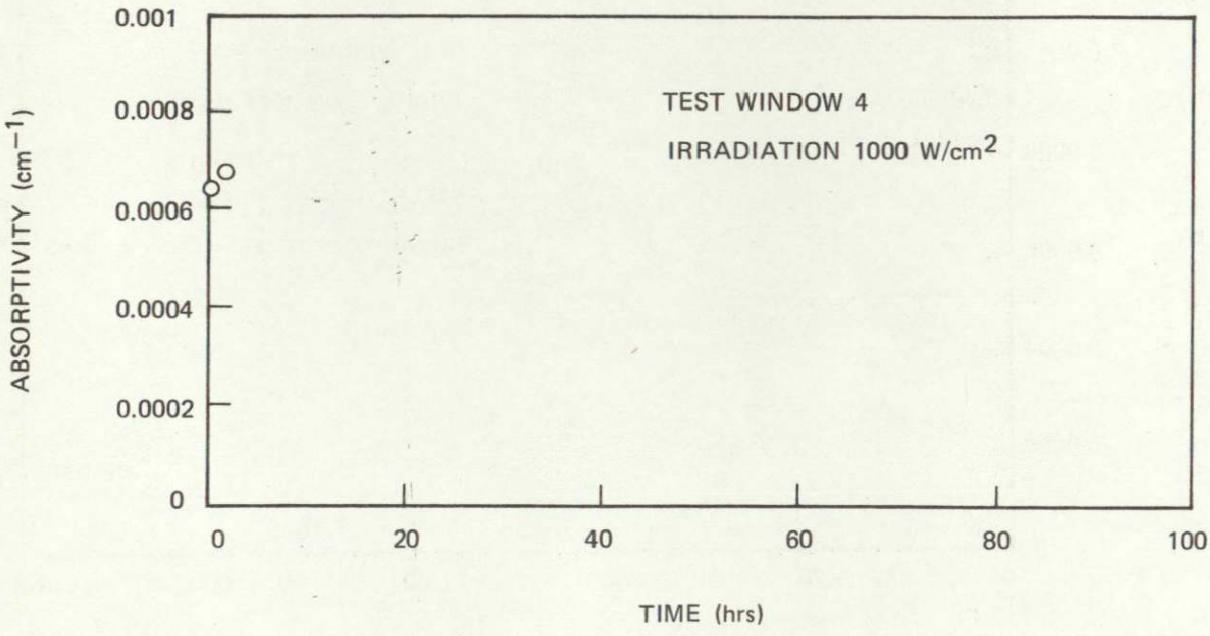

76–02–85–20

FIG. 17

SINGLE CRYSTAL KCL 10.6 MICROMETER ABSORPTIVITY VS TIME OF IRRADIATION

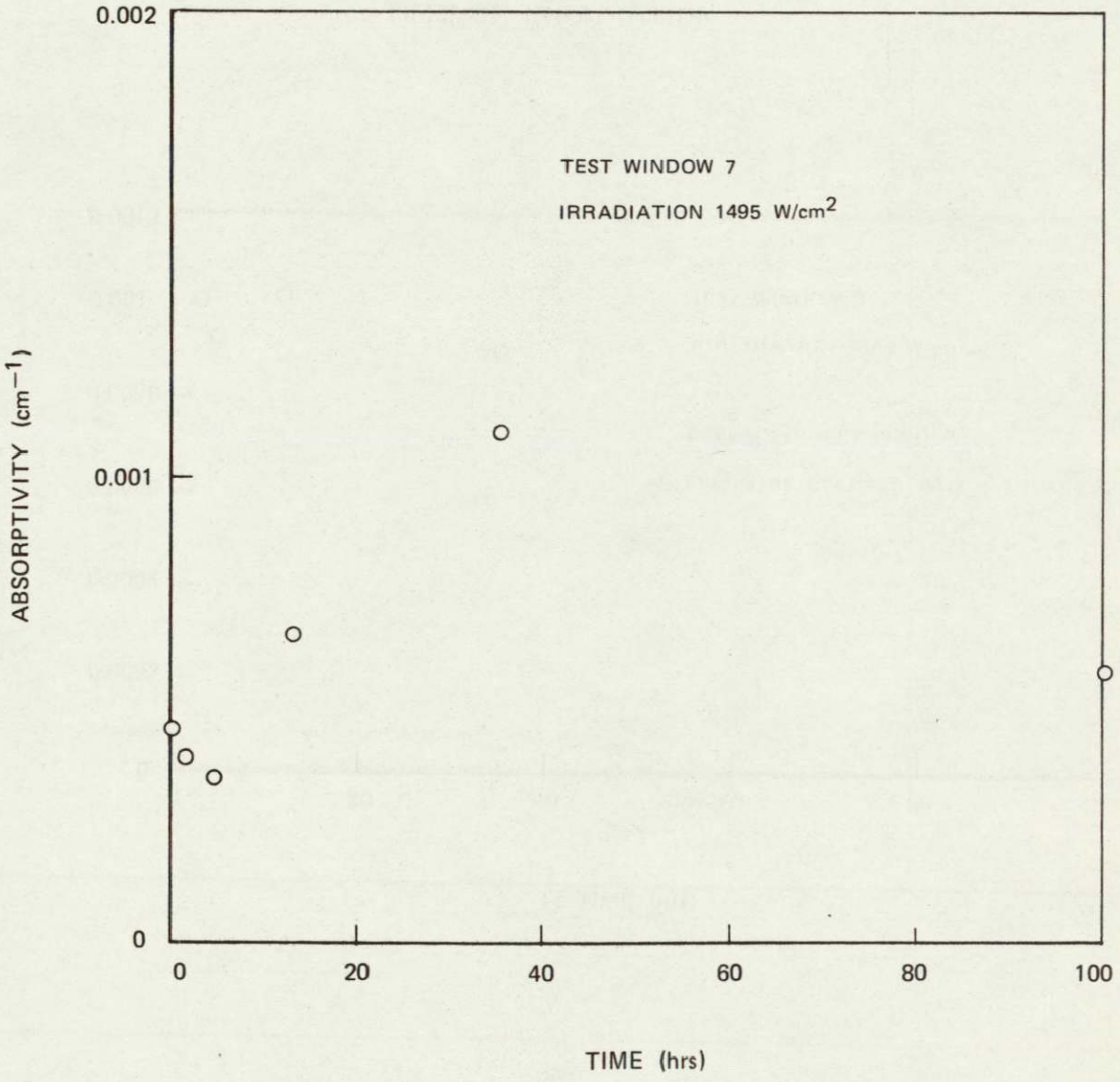

76–02–85–10

FIG. 18

SINGLE CRYSTAL KCl 10.6 MICROMETER ABSORPTIVITY VS TIME OF IRRADIATION

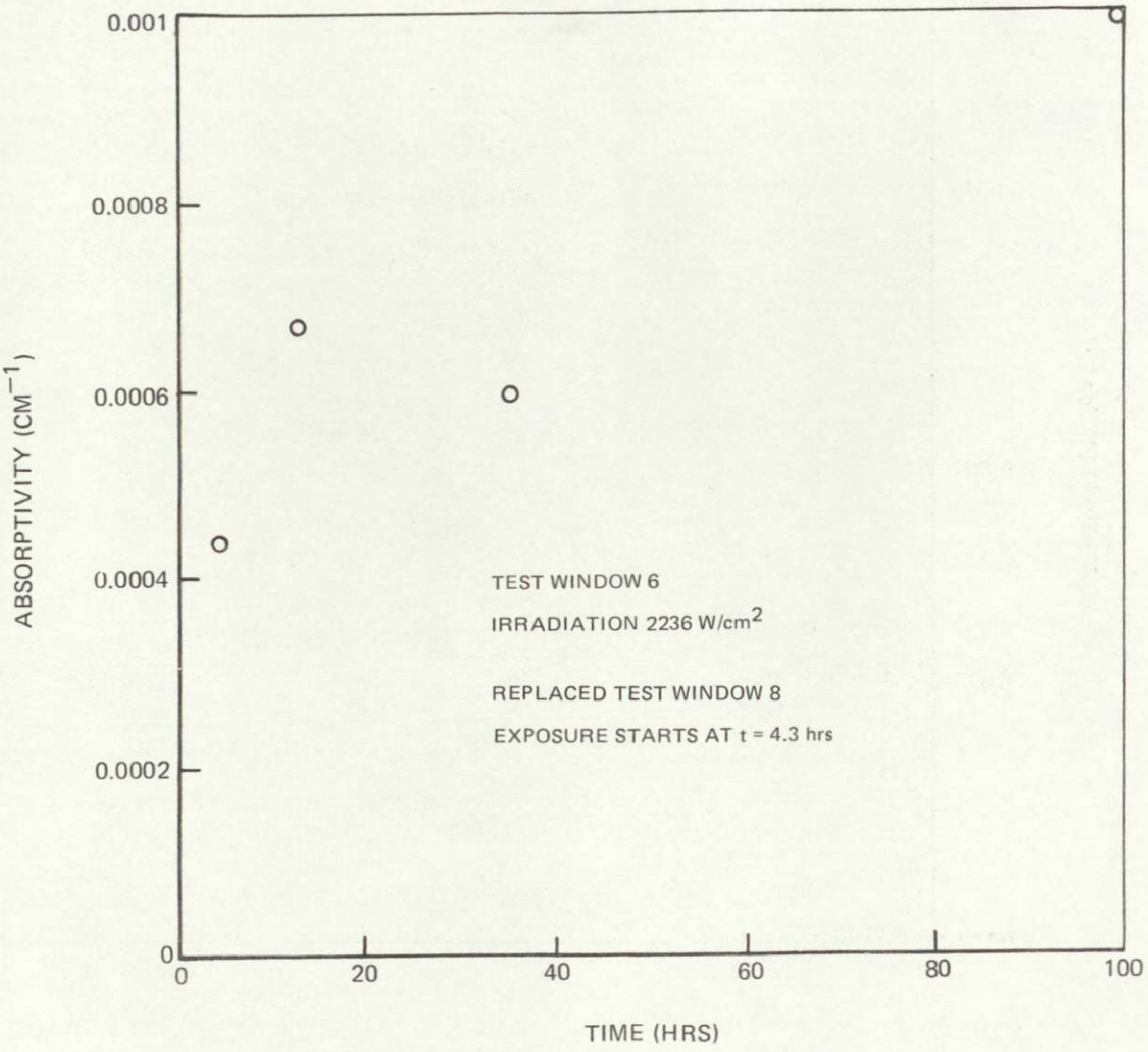

76–03–234–3

SINGLE CRYSTAL KCL 10.6 MICROMETER ABSORPTIVITY VS TIME OF IRRADIATION

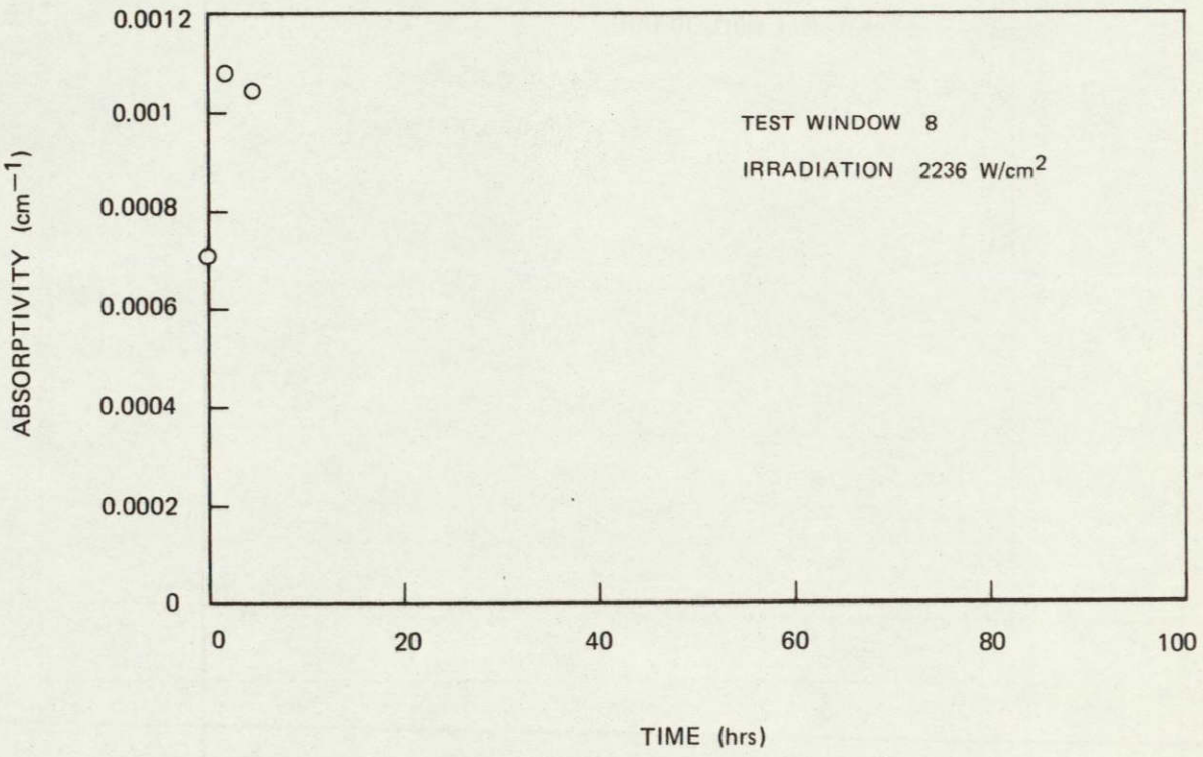

76–02–85–19

FIG. 20

SINGLE CRYSTAL KCL 10.6 MICROMETER ABSORPTIVITY VS TIME OF IRRADIATION

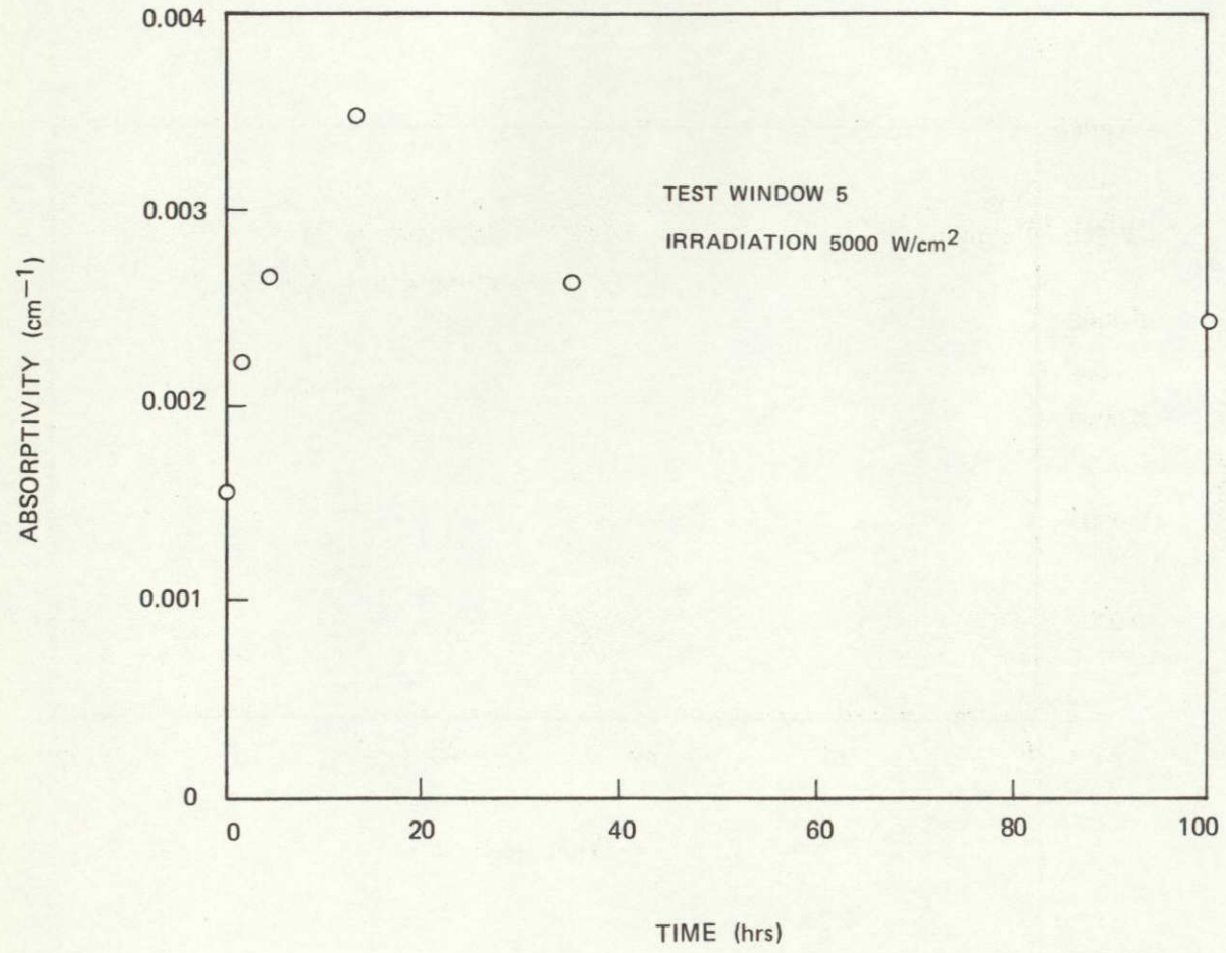

76–02–85–14

FIG. 21

EUROPIUM DOPED POLYCRYSTAL KCL 10.6 MICROMETER ABSORPTIVITY VS TIME OF IRRADIATION

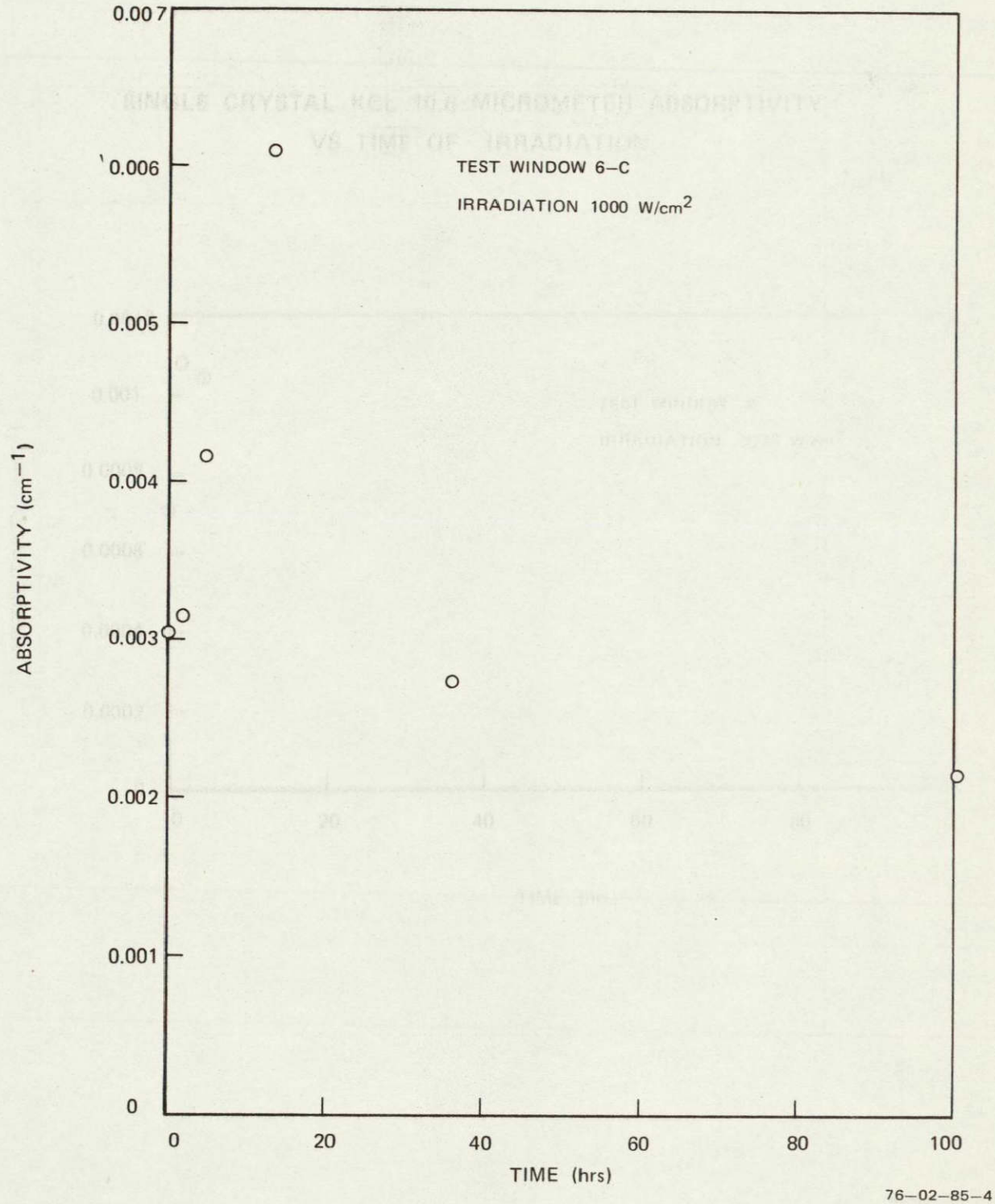

FIG. 22

EUROPIUM DOPED POLYCRYSTAL KCL 10.6 MICROMETER ABSORPTIVITY VS TIME OF IRRADIATION

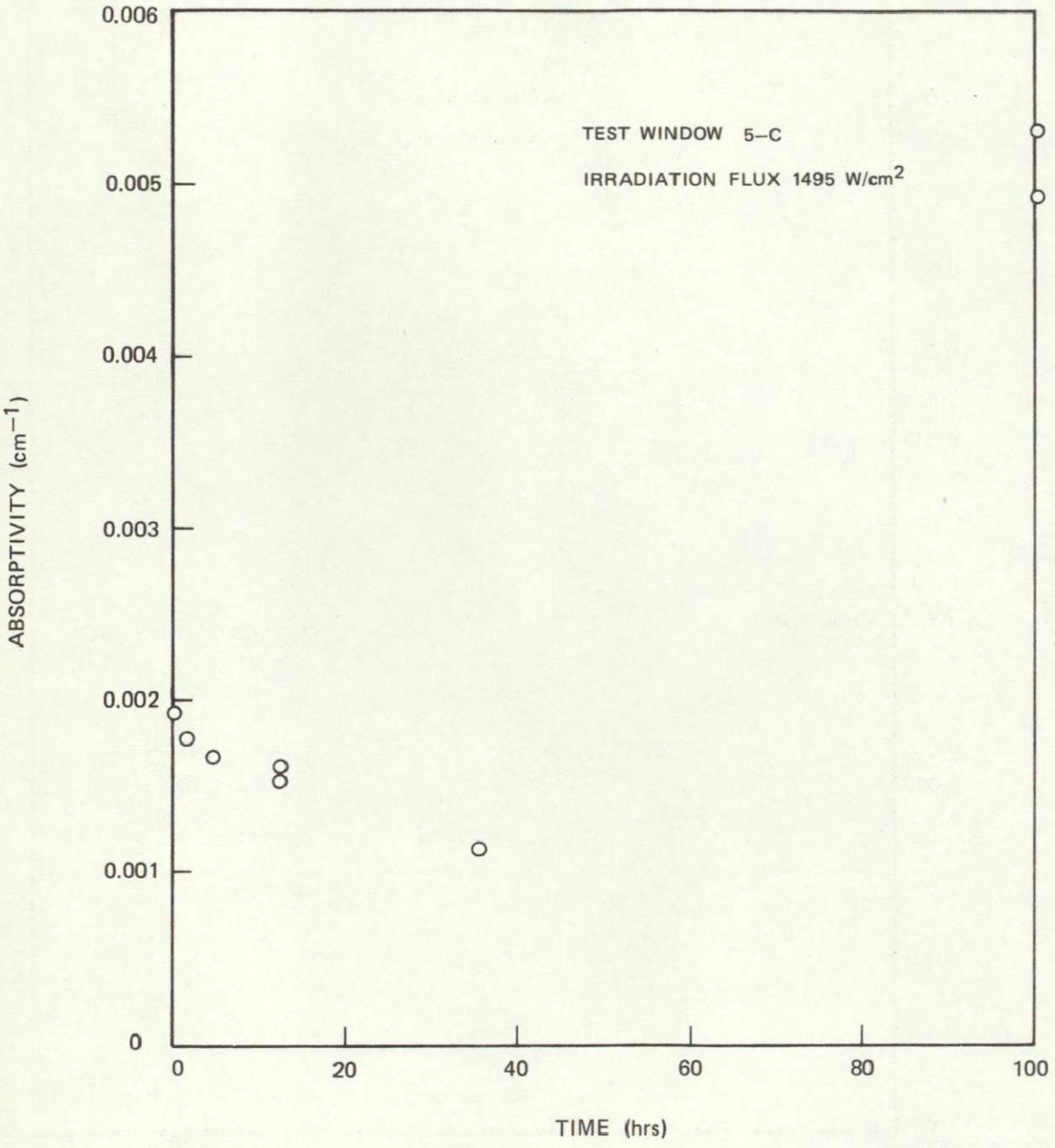

76–02–85–7

FIG. 23

EUROPIUM DOPED POLYCRYSTAL KCL 10.6 MICROMETER ABSORPTIVITY VS TIME OF IRRADIATION

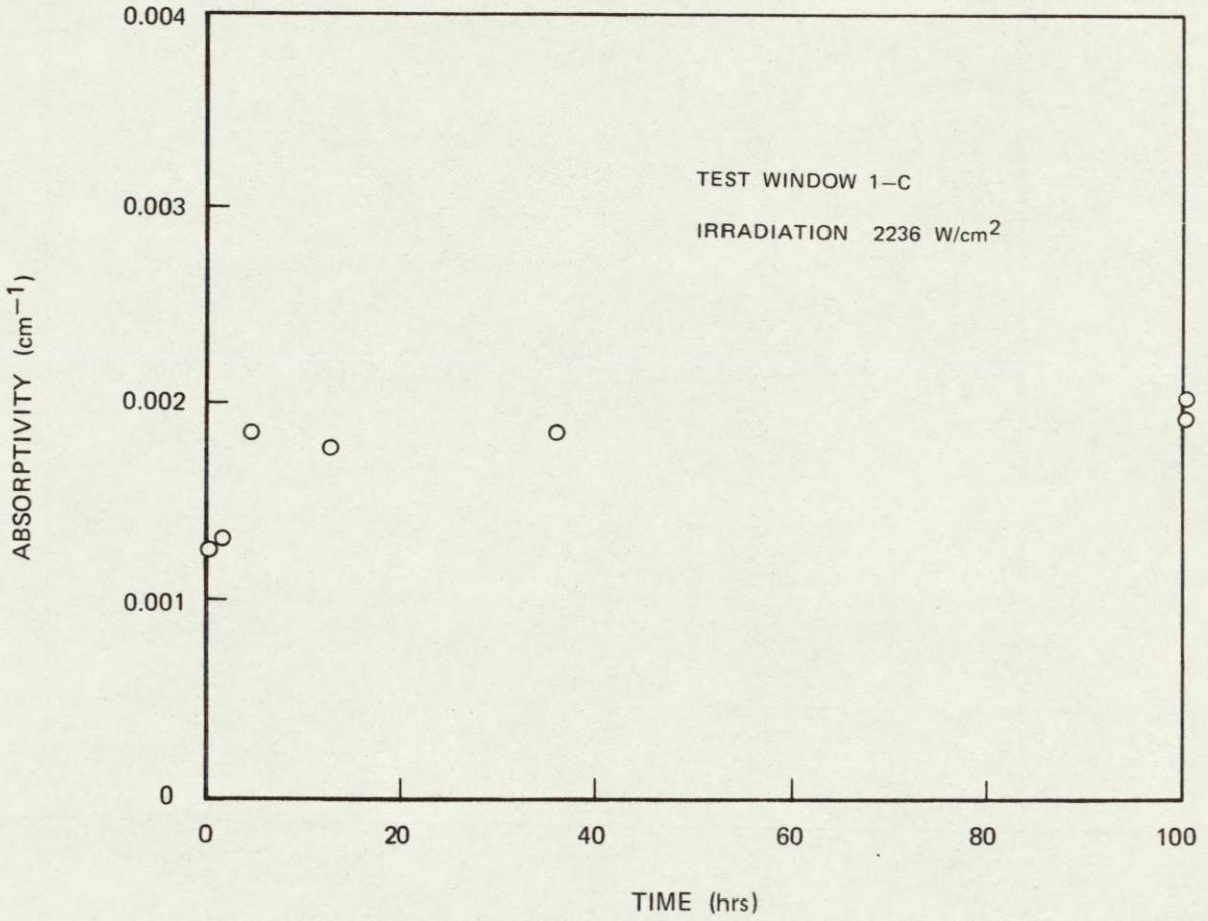

76–02–85–9

FIG 24

EUROPIUM DOPED POLYCRESTAL KCL 10.6 MICROMETER ABSORPTIVITY VS TIME OF IRRADIATION

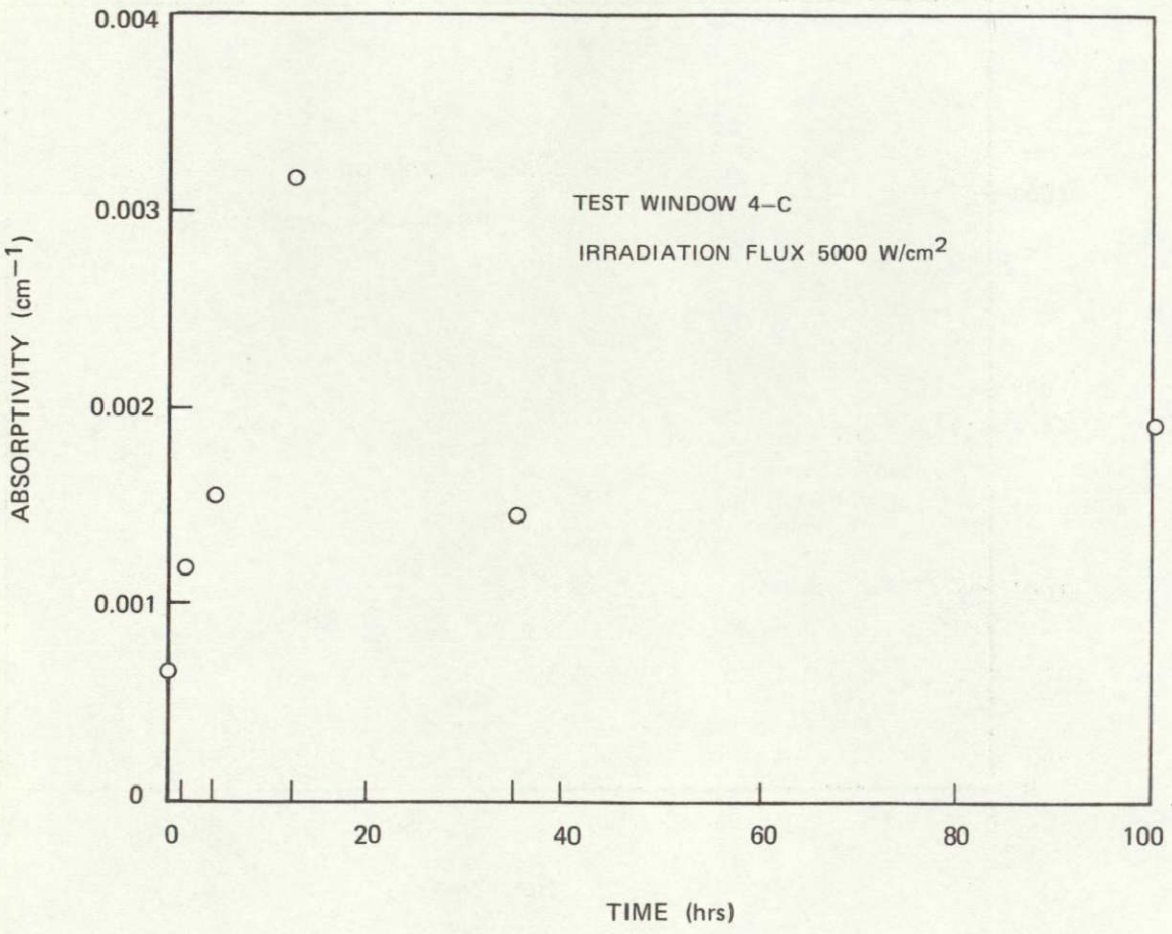

76–02–85–1

FIG. 25

THERMAL AGING CHAMBER

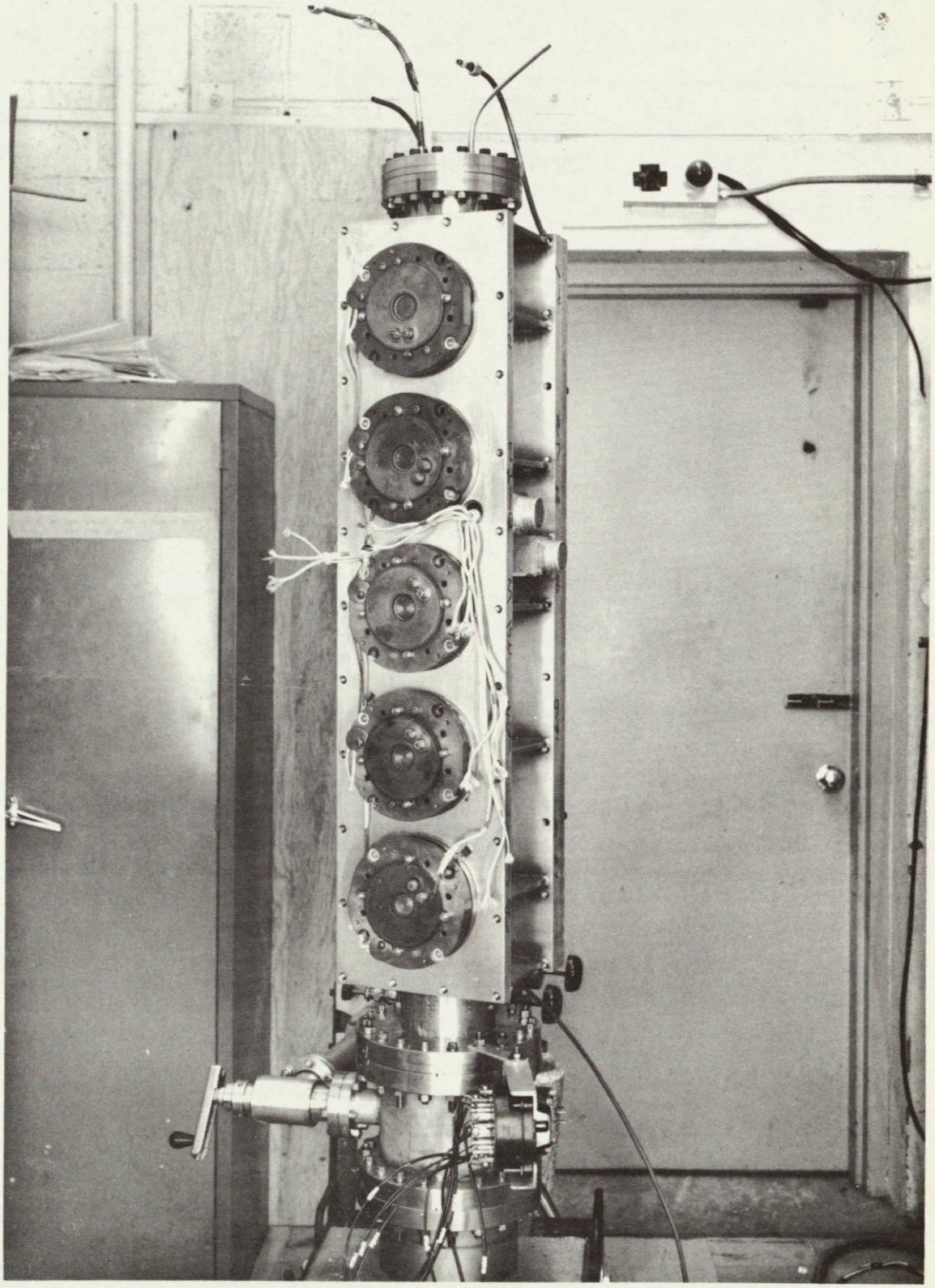

FIG. 26

THERMAL AGING CHAMBER FIXTURE

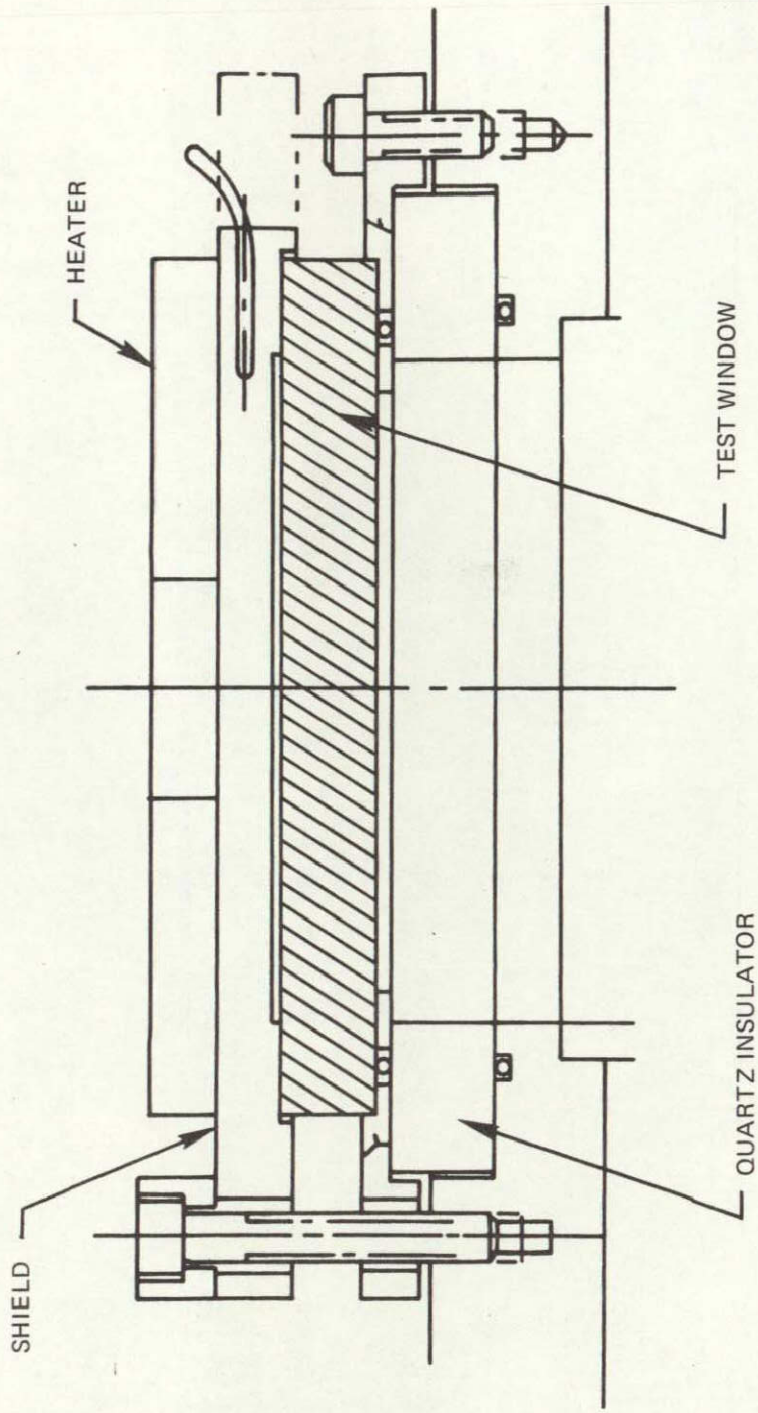

76–02–101–1

FIG. 27

SINGLE CRYSTAL KCL 10.6 MICROMETER ABSORPTIVITY VS THERMAL AGING TIME

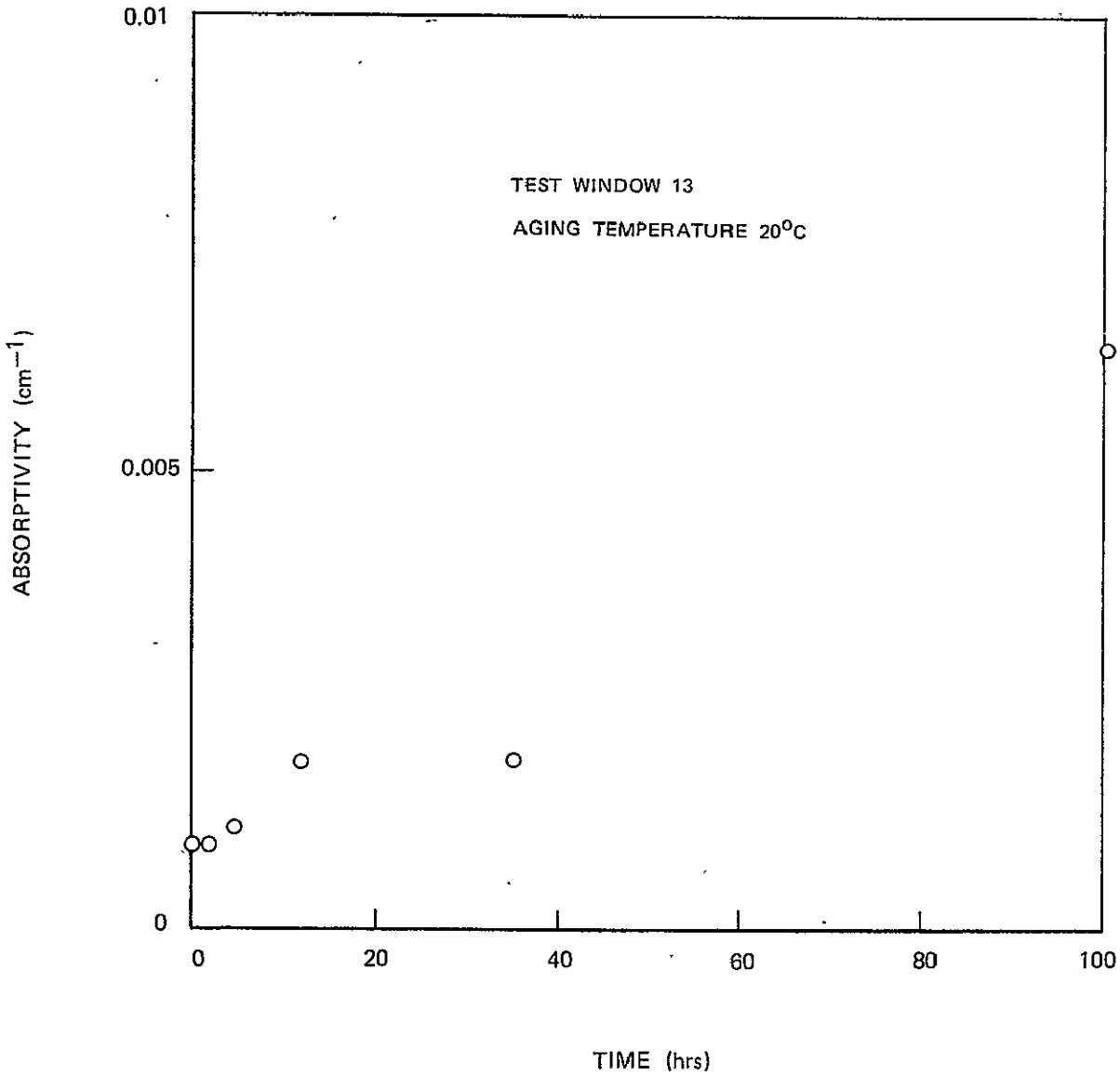

76–02–85–5

FIG. 28

SINGLE CRYSTAL KCL 10.6 MICROMETER ABSORPTIVITY VS THERMAL AGING TIME

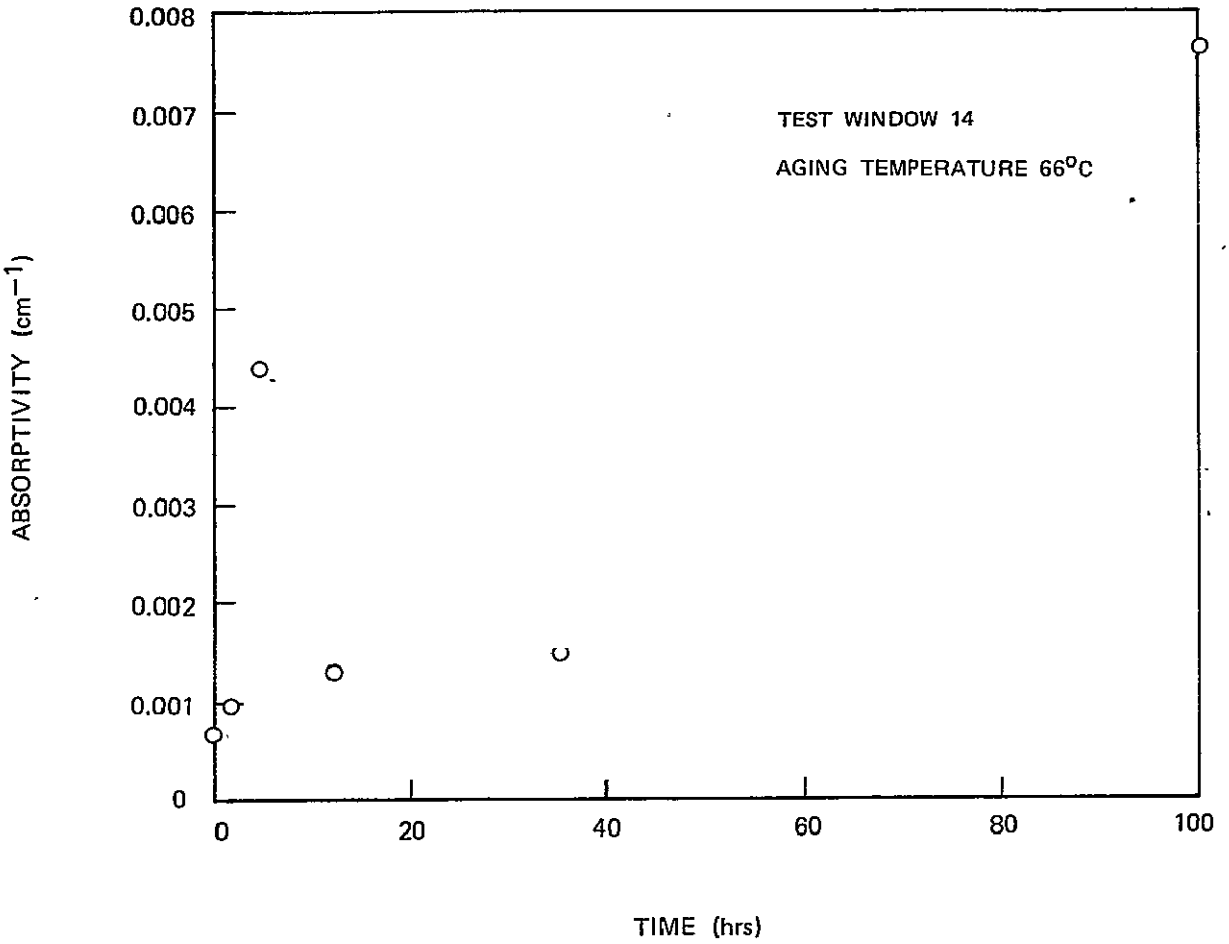

76–02–85–15

FIG. 29

SINGLE CRYSTAL KCL 10.6 MICROMETER ABSORPTIVITY
VS THERMAL AGING TIME.

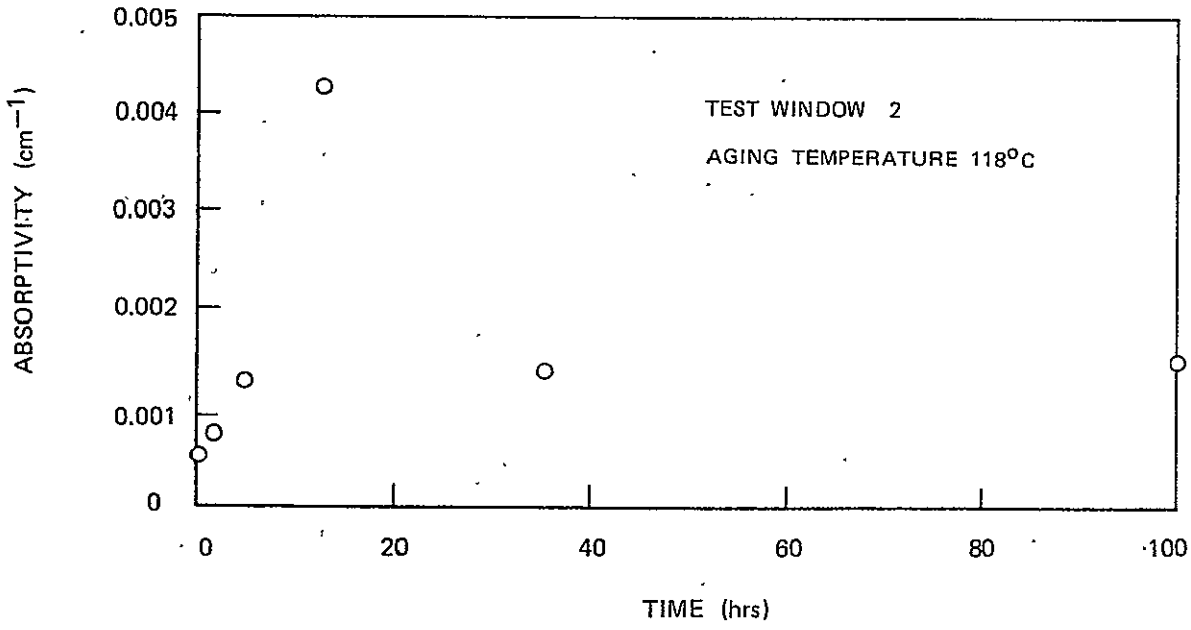

76–02–85–8

FIG. 30

SINGLE CRYSTAL KCL 10.6 MICROMETER ABSORPTIVITY VS THERMAL AGING TIME

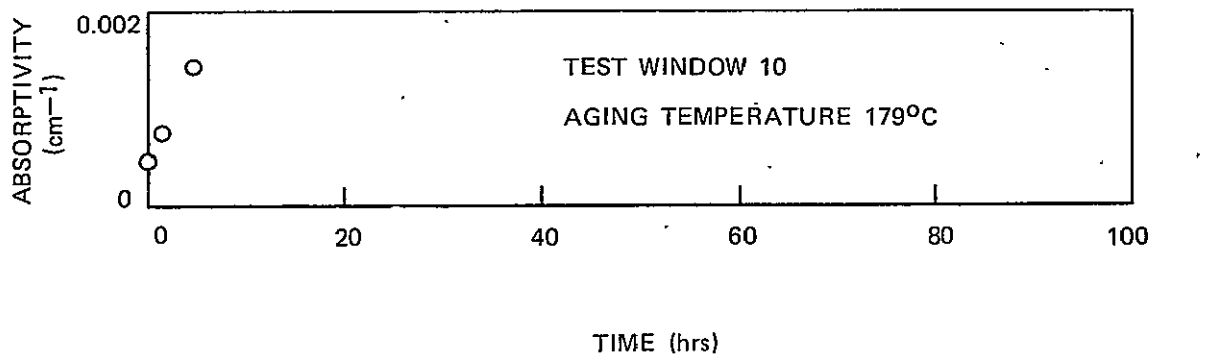

76–02–85–17

SINGLE CRYSTAL KCL 10.6 MICROMETER ABSORPTIVITY VS THERMAL AGING TIME

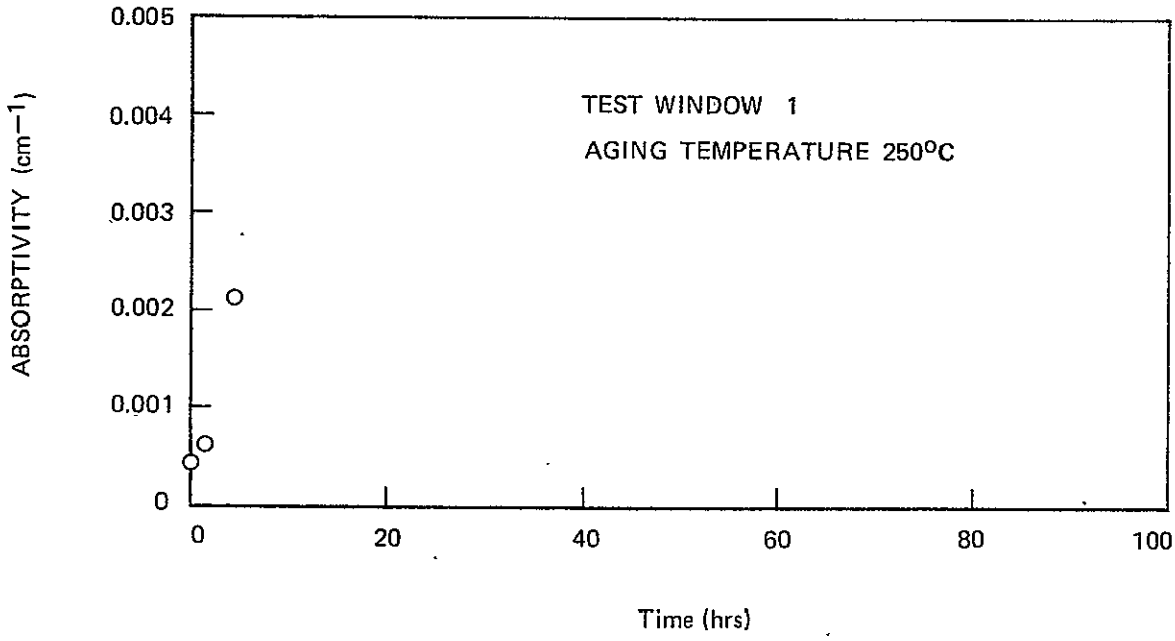

76–02–85–16

EUROPIUM DOPED POLYCRYSTAL KCL 10.6 MICROMETER ABSORPTIVITY VS THERMAL AGING TIME

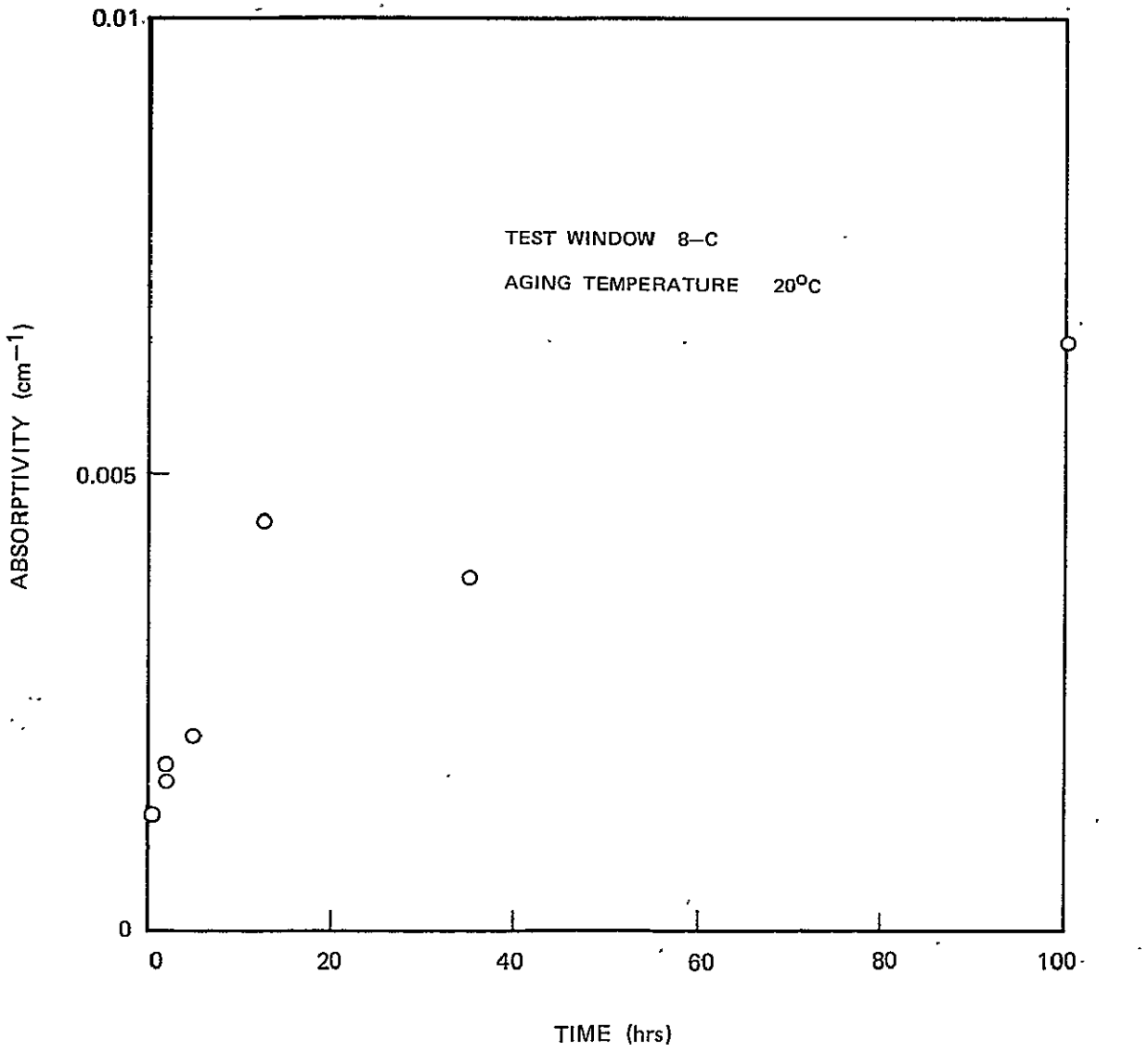

76-02-85-2

FIG. 33

EUROPIUM DOPED POLYCRYSTAL KCL 10.6 MICROMETER ABSORPTIVITY VS THERMAL AGING

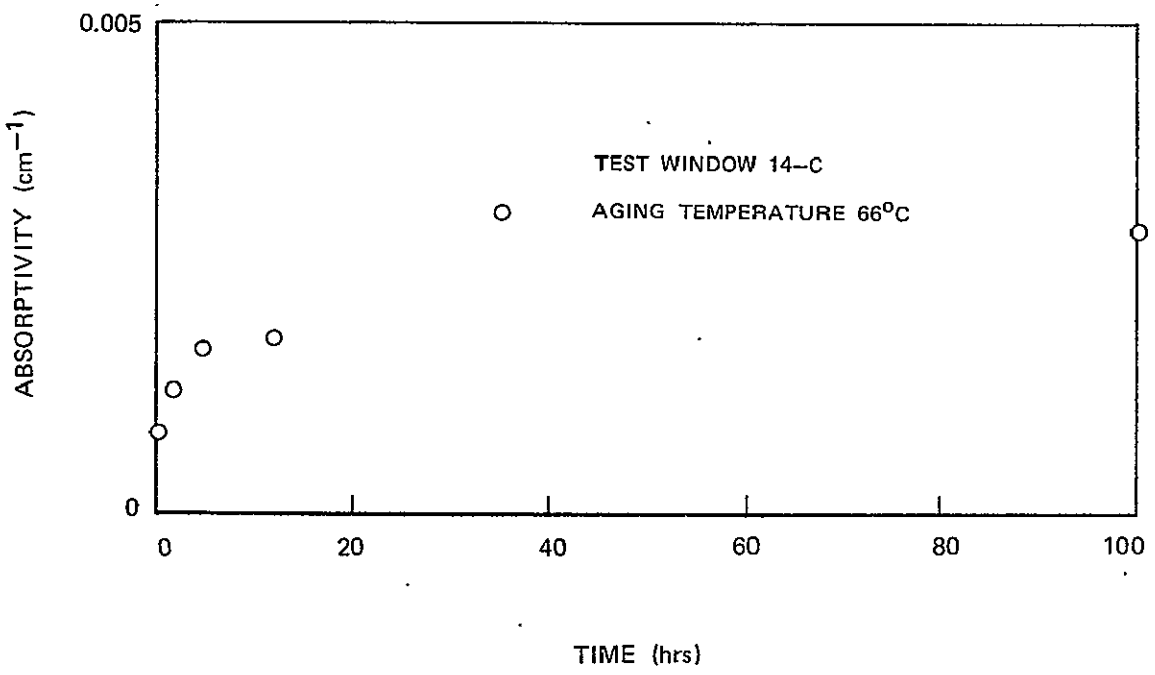

76–02–85–12

EUROPIUM DOPED POLYCRYSTAL KCL 10.6 MICROMETER ABSORPTIVITY VS THERMAL AGING TIME

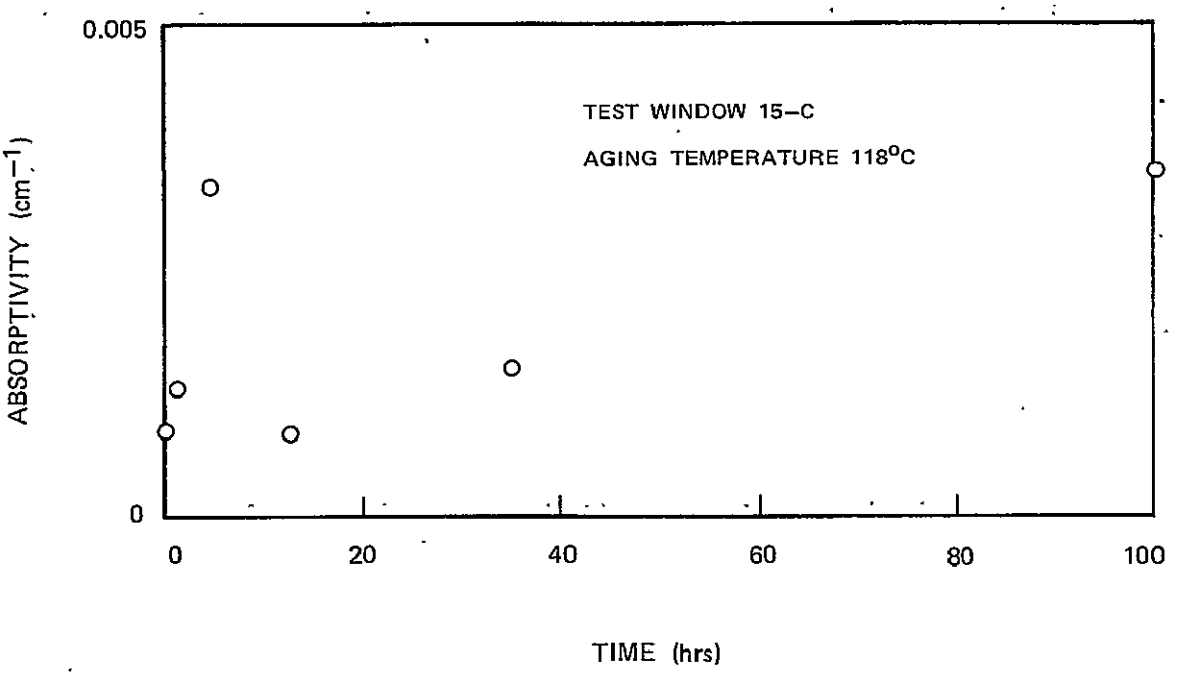

76–02–85–13

EUROPIUM DOPED POLYCRYSTAL KCL 10.6 MICROMETER ABSORPTIVITY VS THERMAL AGING TIME

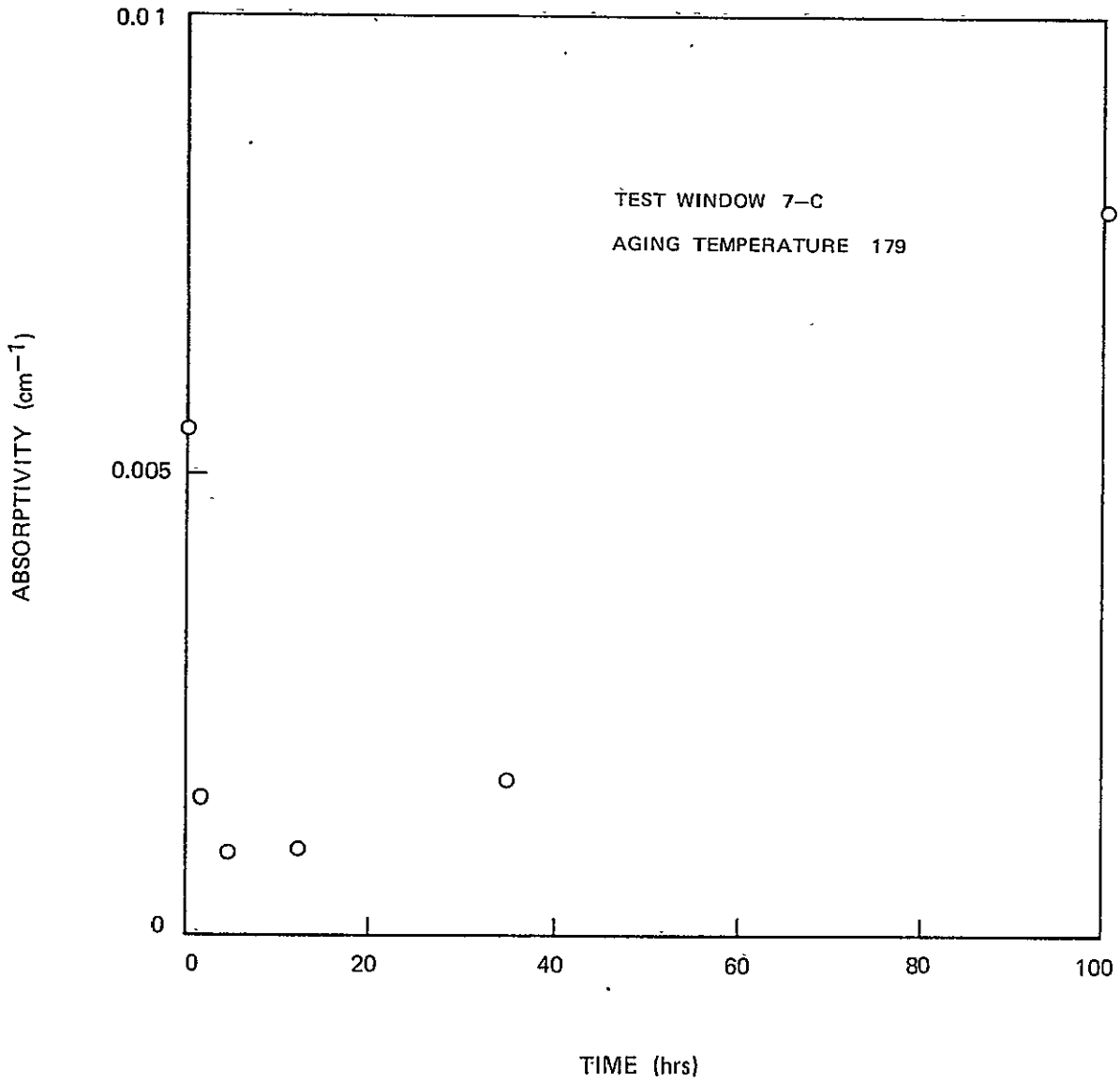

76–02–85–3

FIG. 36

EUROPIUM DOPED POLYCRYSTAL KCL 10.6 MICROMETER ABSORPTIVITY VS THERMAL AGING TIME

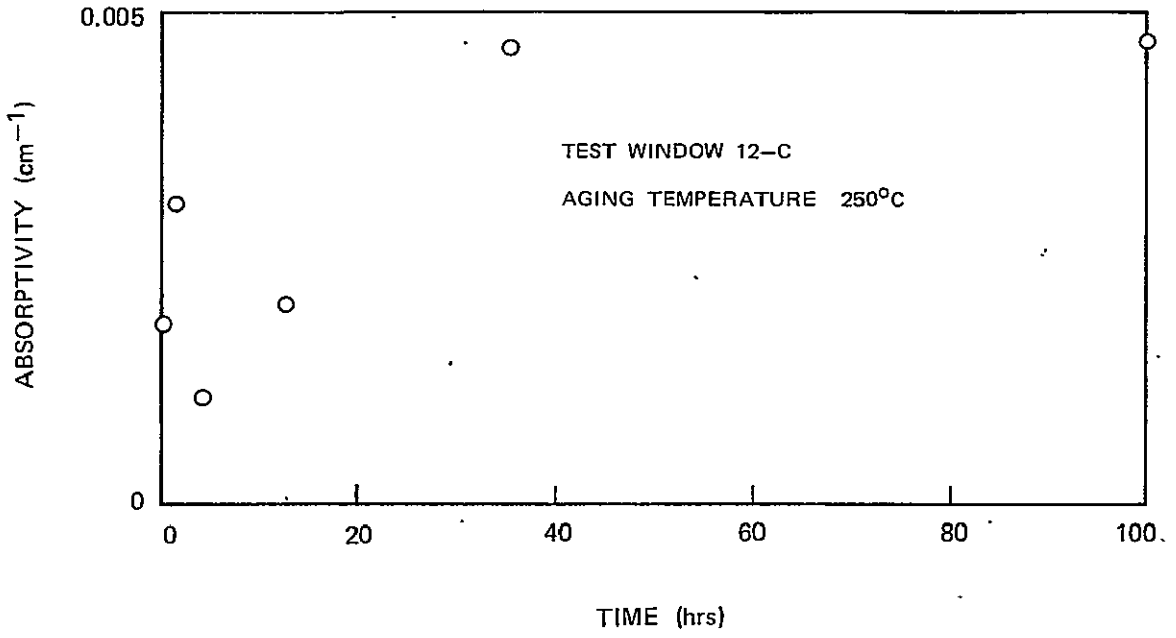

76–02–85–11

FIG. 37

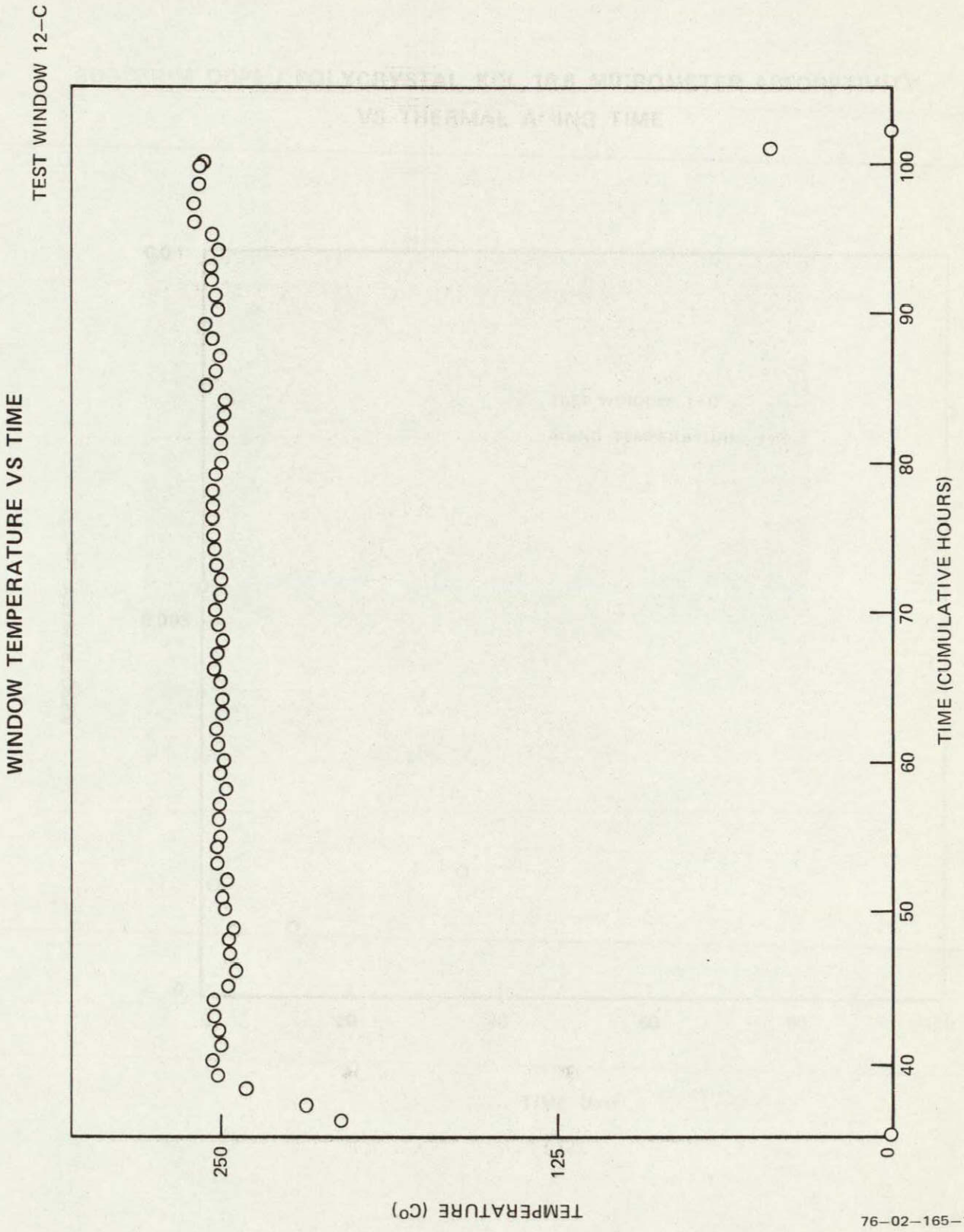
WINDOW TEMPERATURE VS TIME
TEST WINDOW 12–C
TEMPERATURE (C°)
250
125
0
40
50
60
70
80
90
100
TIME (CUMULATIVE HOURS)
76–02–165–1

FIG. 38

EUROPIUM DOPED POLYCRYSTAL KCl

TEST WINDOW 8–C

t = 100 HOURS

AGING TEMPERATURE 20C °

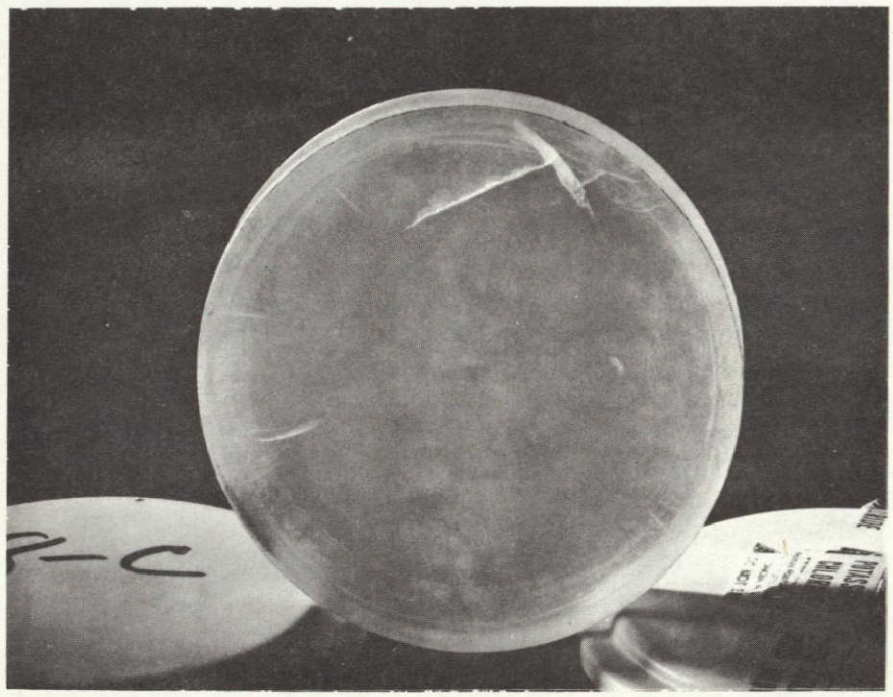

CRACKS ARE ON COMPRESSION SIDE OF WINDOW
AND DID NOT PENETRATE VACUUM SURFACE.
FAILURE OCCURED BETWEEN 35 HRS. AND 100 HRS.

76–02–102–2

EUROPIUM DOPED POLYCRYSTAL KCl

TEST WINDOW 12–C

t = 100 HOURS

AGING TEMPERATURE 250 C°

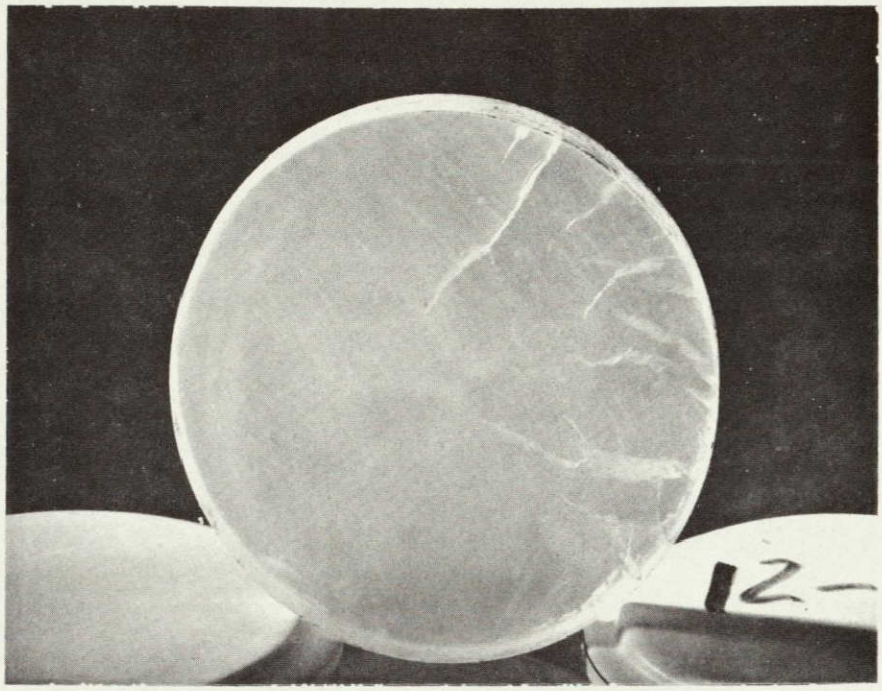

WINDOW CRACKED AT t = 96 HRS. WINDOW MAINTAINED MECHANICAL INTEGRITY TO 100 HRS AGAINST FULL DESIGN PRESSURE.

76–02–102–1

FIG. 40

SINGLE CRYSTAL KCl

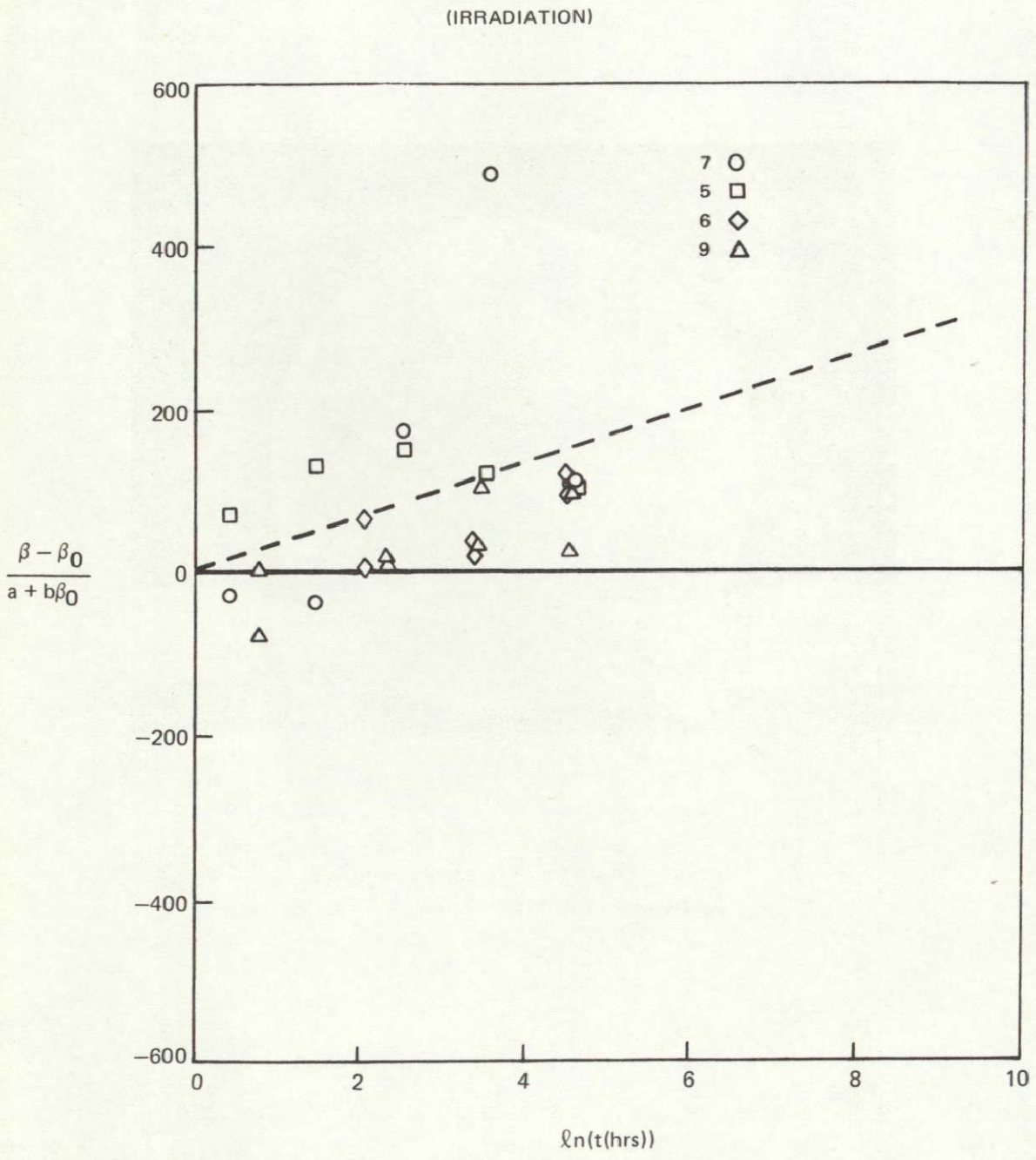

76–03–234–5

FIG. 41

EUROPIUM DOPED POLYCRYSTAL KCl

(IRRADIATION)

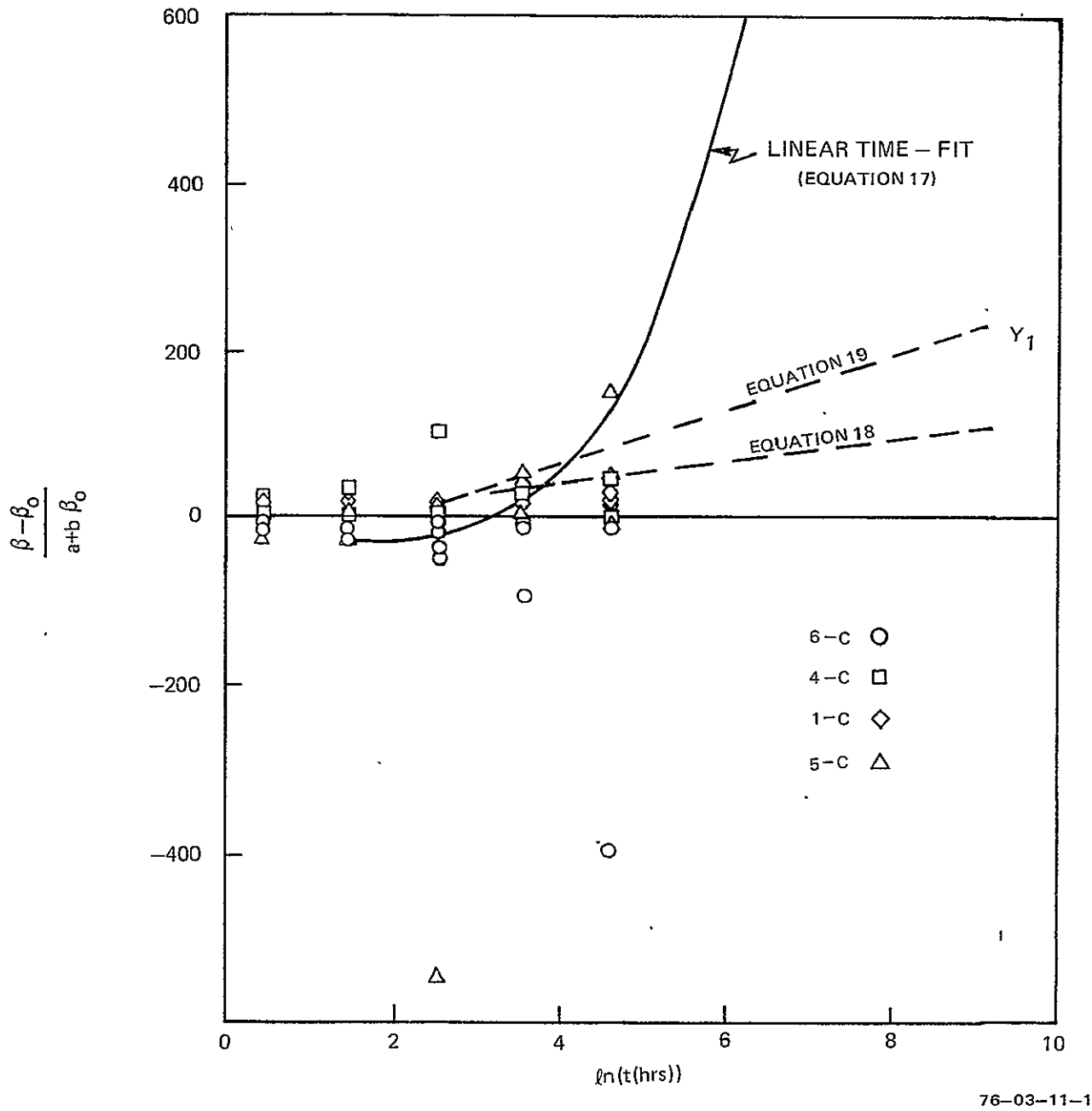

SINGLE CRYSTAL KCl IN THERMAL AGING

$$\ell n \left(\frac{\partial \beta}{\partial t} \times 10^6 \right) = 0.9903 + 0.00967T$$

$$\ell n \left(\frac{\partial \beta}{\partial t} \times 10^6 \right) = -0.2991 + 0.01077T$$

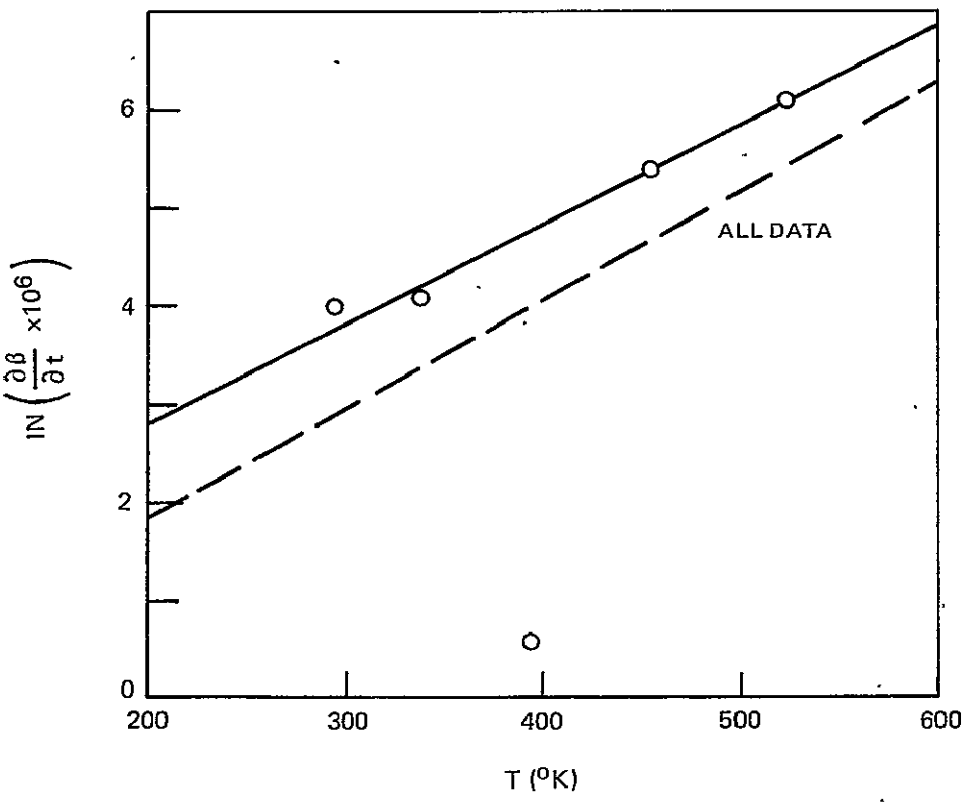

76-03-83-3

FIG. 43

SINGLE CRYSTAL KCl IN THERMAL AGING

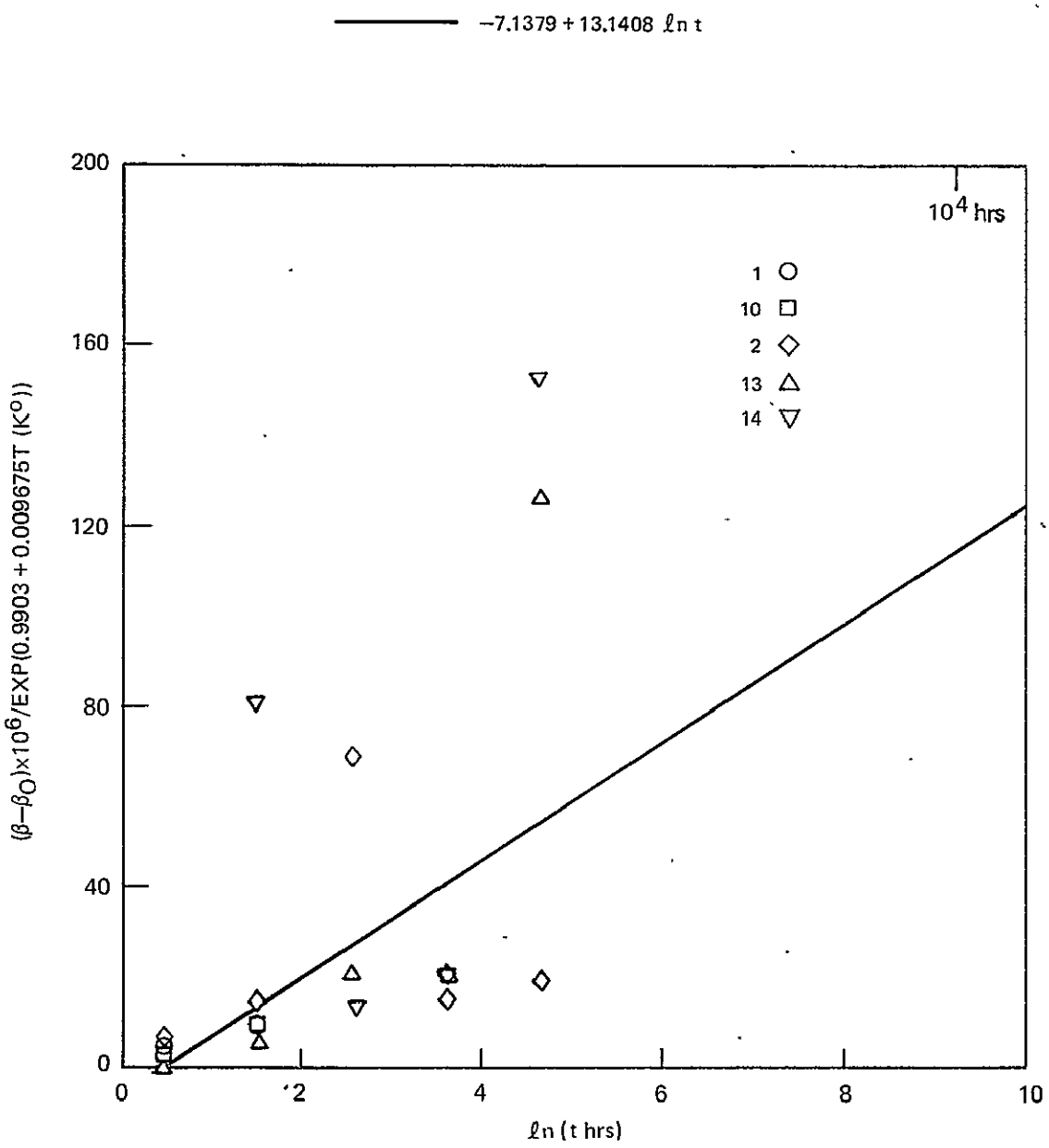

76–03–83–1

FIG. 44

EUROPIUM DOPED POLYCRYSTAL KCl IN THERMAL AGING

$$\frac{\beta-\beta_O}{\beta_O} = -0.050905 + 0.44507\,\ell n\,(t)$$

$$DF = 24 \qquad r_d^2 = 0.250$$

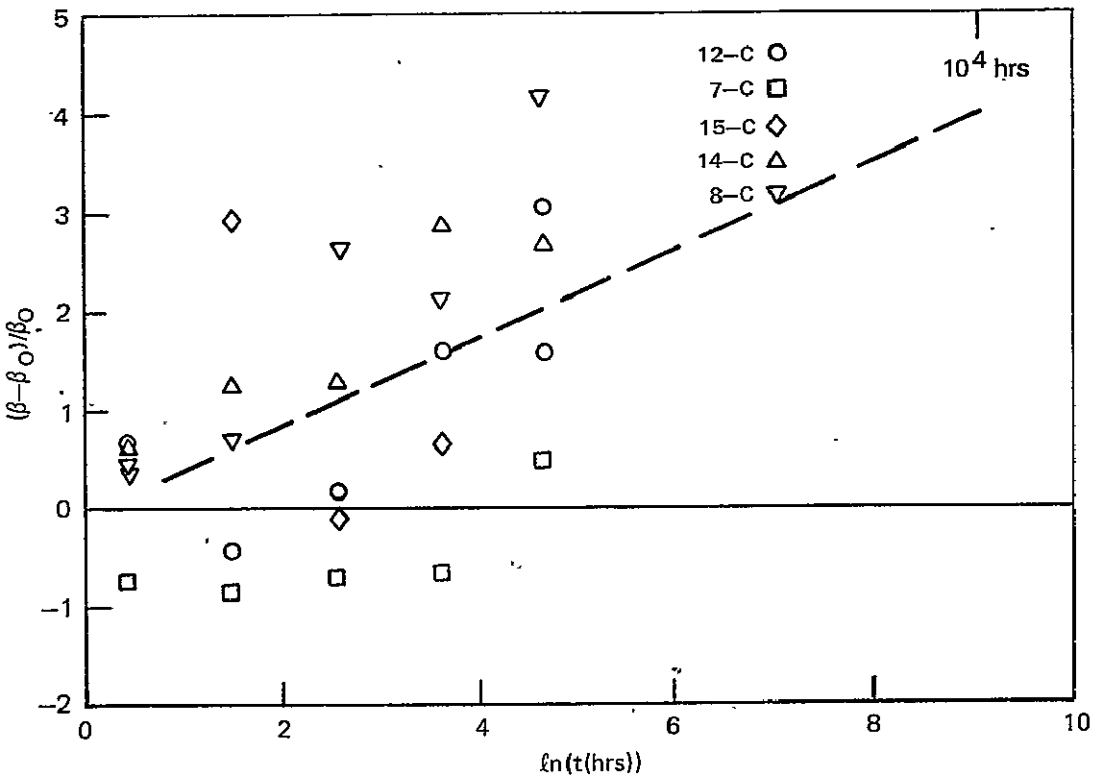

76–03–83–2

POISSON'S RATIO VS TEMPERATURE

EUROPIUM DOPED POLYCRYSTAL KCL

(AS RECEIVED MATERIAL)

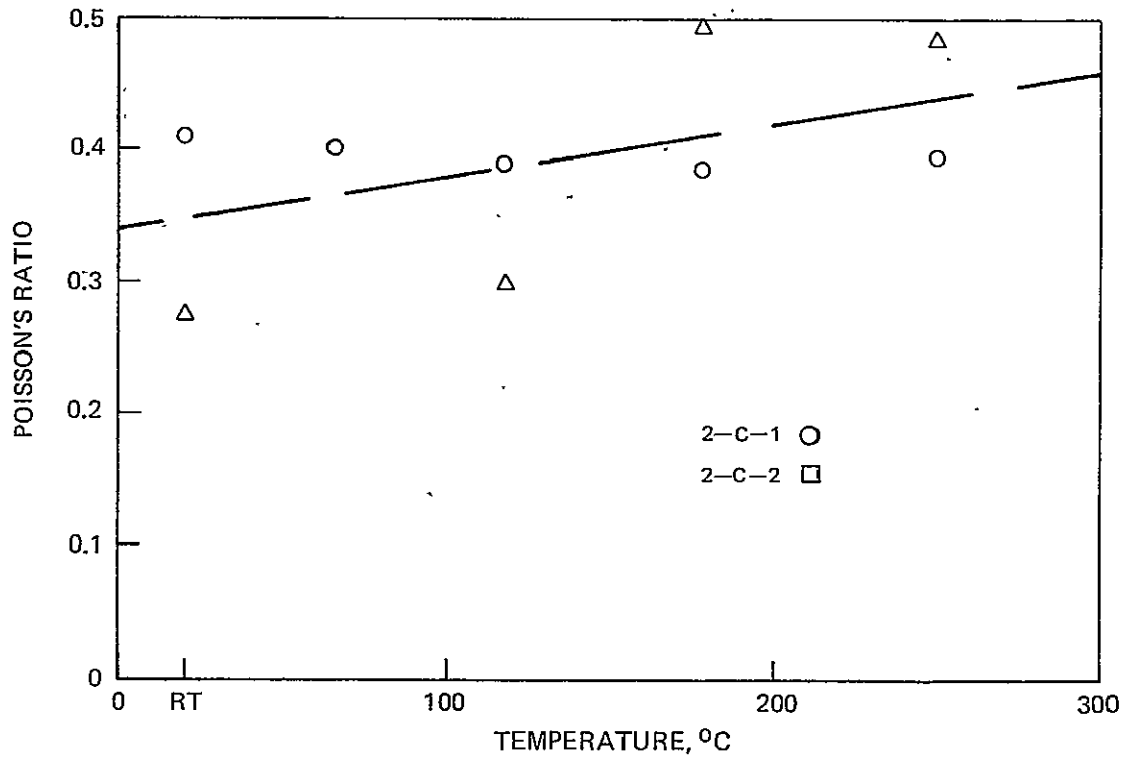

76–03–194–2

FIG. 46

YIELD STRESS VS TEMPERATURE

EUROPIUM DOPED POLYCRYSTAL KCL

(AS RECEIVED MATERIAL)

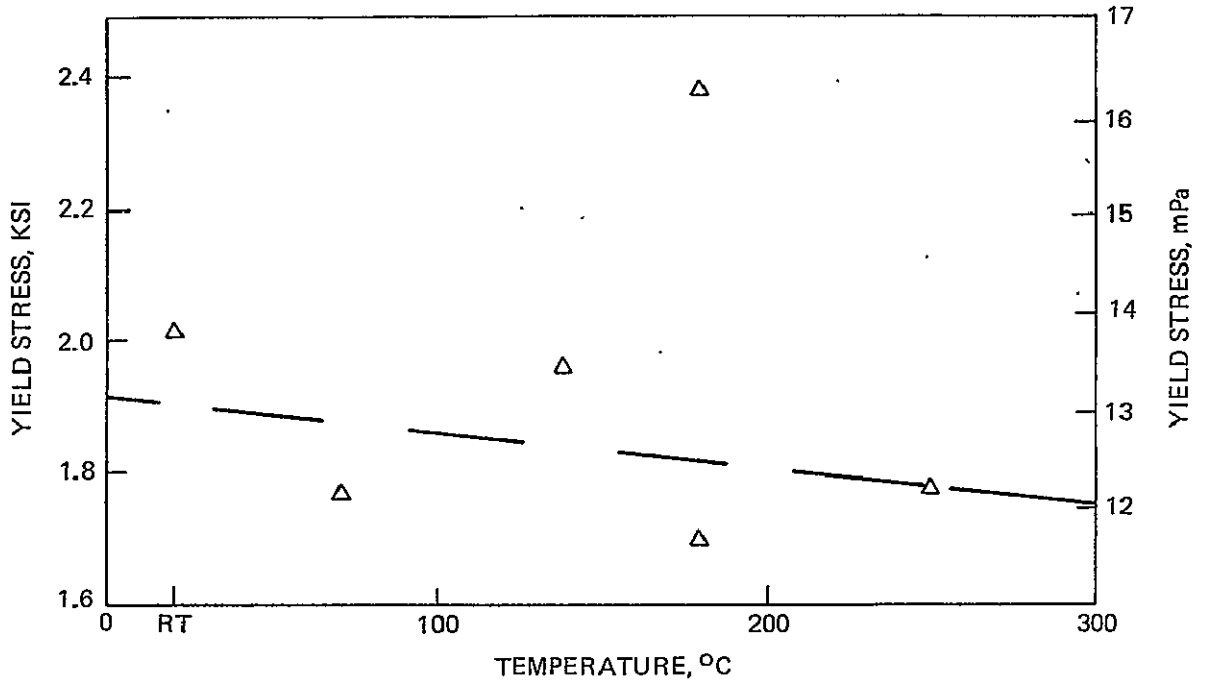

76–03–194–1

YOUNG'S MODULUS VS TEMPERATURE

EUROPIUM DOPED POLYCRYSTAL KCL

(AS RECIEVED MATERIAL)

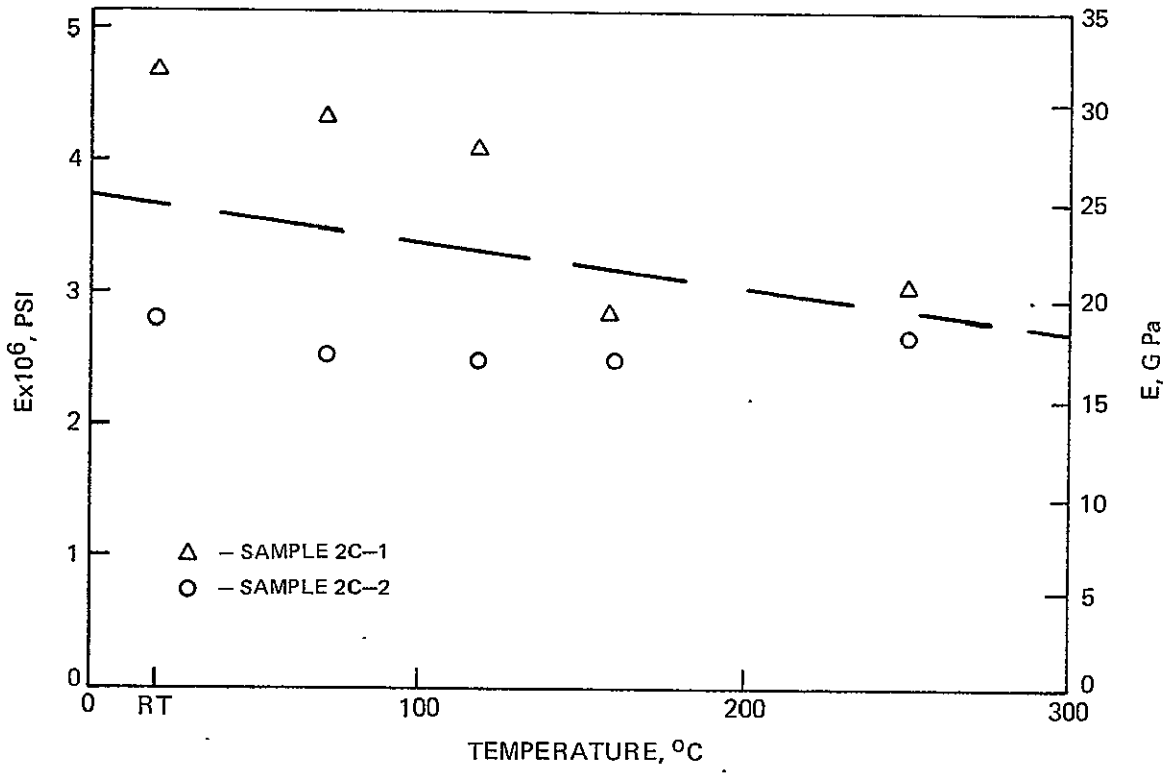

76–03–194–6

YOUNG'S MODULUS VS TEMPERATURE

SINGLE CRYSTAL KCL

(AS RECEIVED MATERIAL)

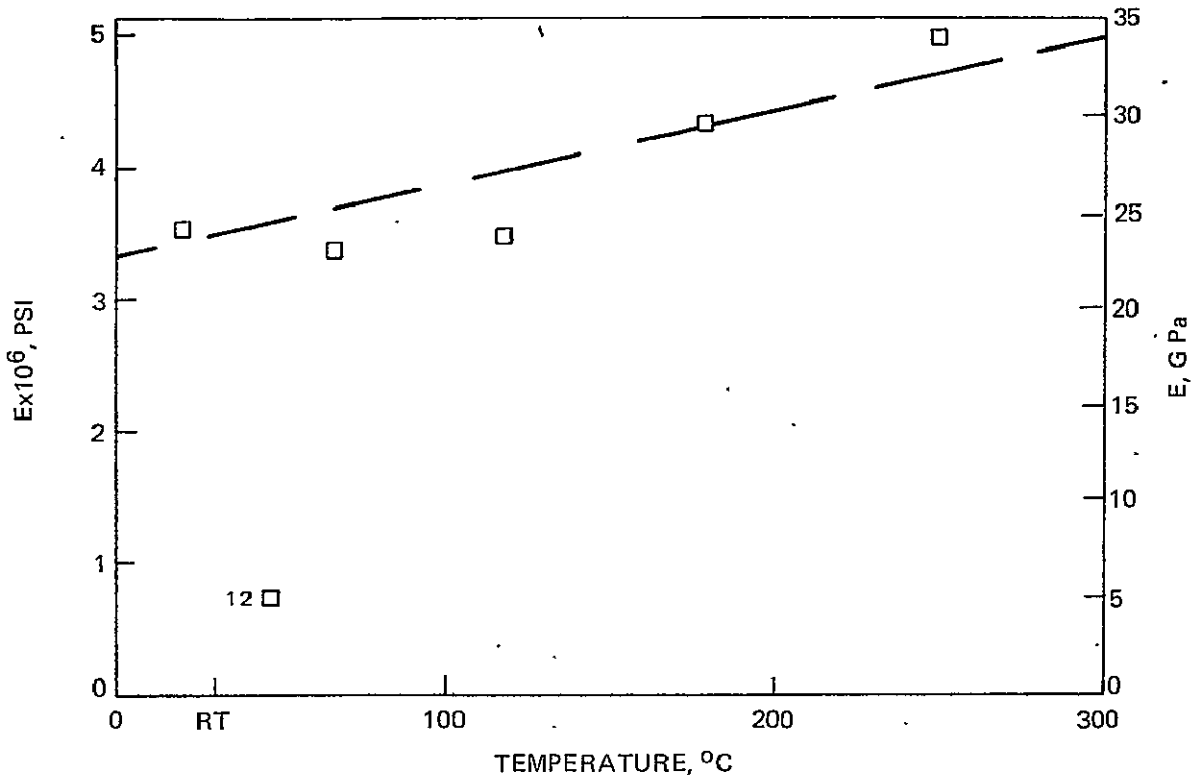

FIG. 49

POISSON'S RATIO VS TEMPERATURE

SINGLE CRYSTAL KCL

(AS RECEIVED MATERIAL)

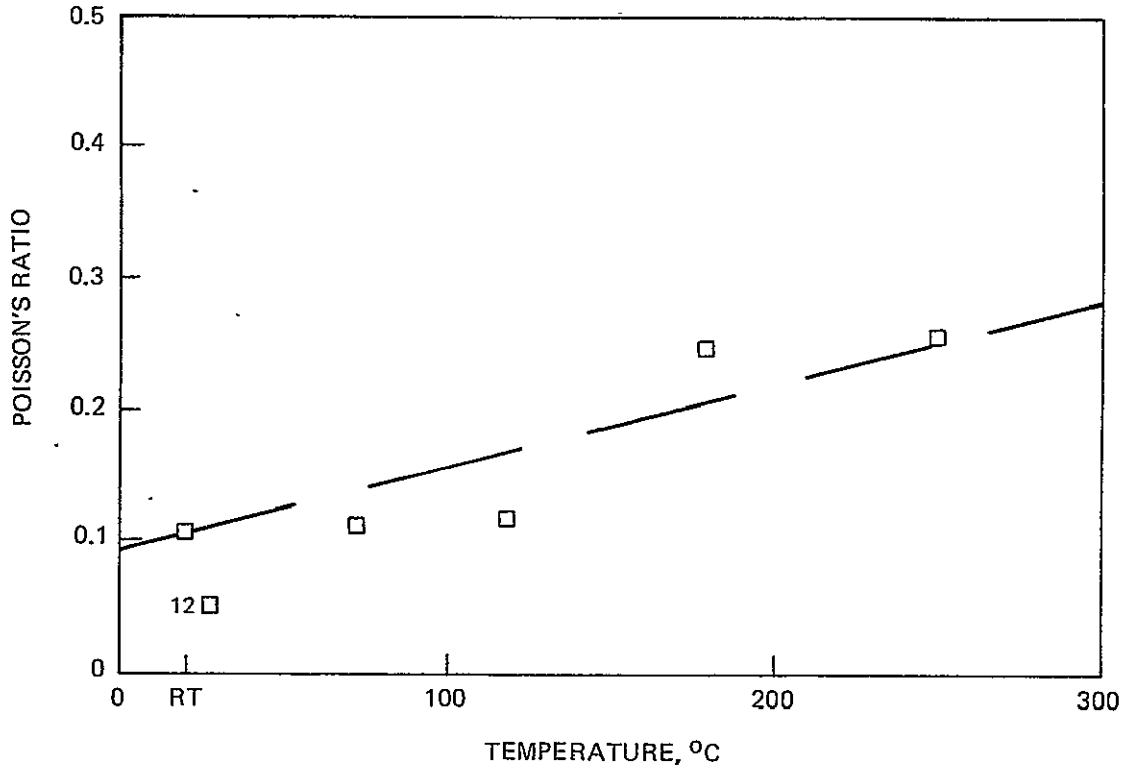

76–03–194–3

FIG. 50

YIELD STRESS VS TEMPERATURE

SINGLE CRYSTAL KCL

(AS RECEIVED MATERIAL)

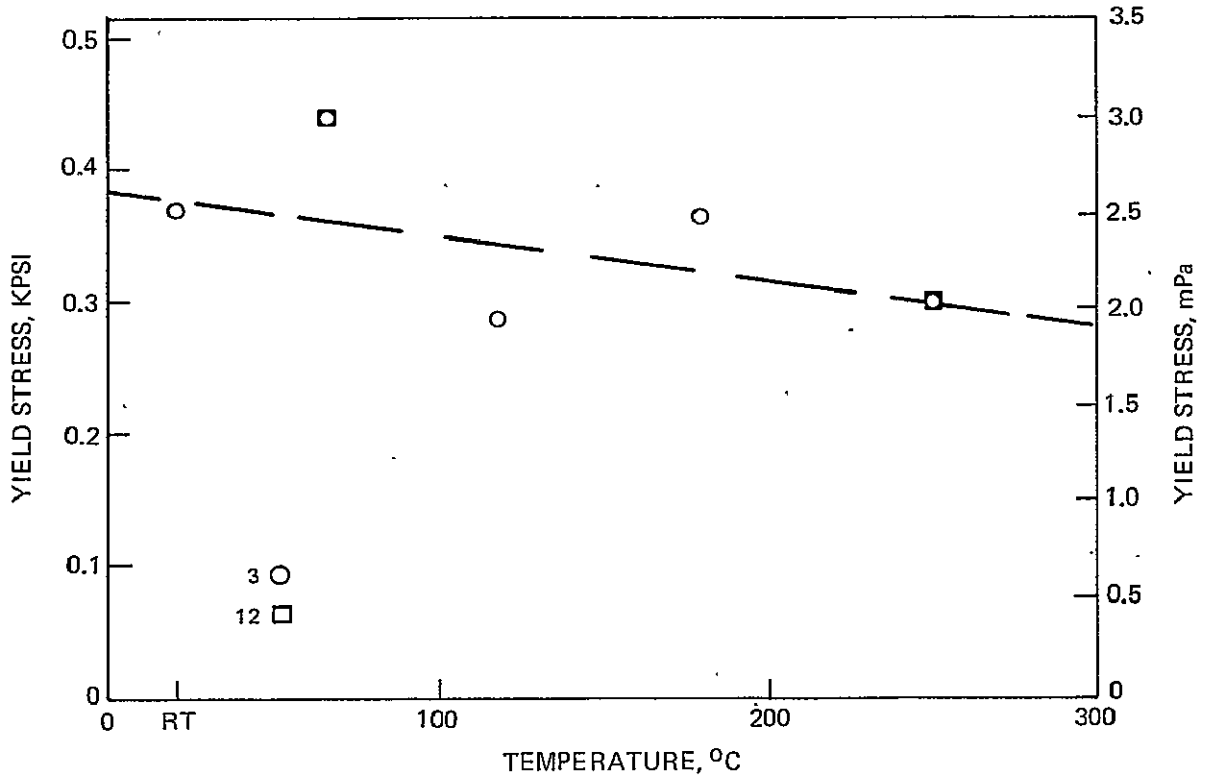

76–03–194–5

FIG. 51

EUROPIUM DOPED POLYCRYSTAL KCl

(AS RECIEVED MATERIAL)

WINDOW 2–C

100 μ

EUROPIUM DOPED POLYCRYSTAL KCl

WINDOW 12–C

AFTER 100 HRS AT 250° C

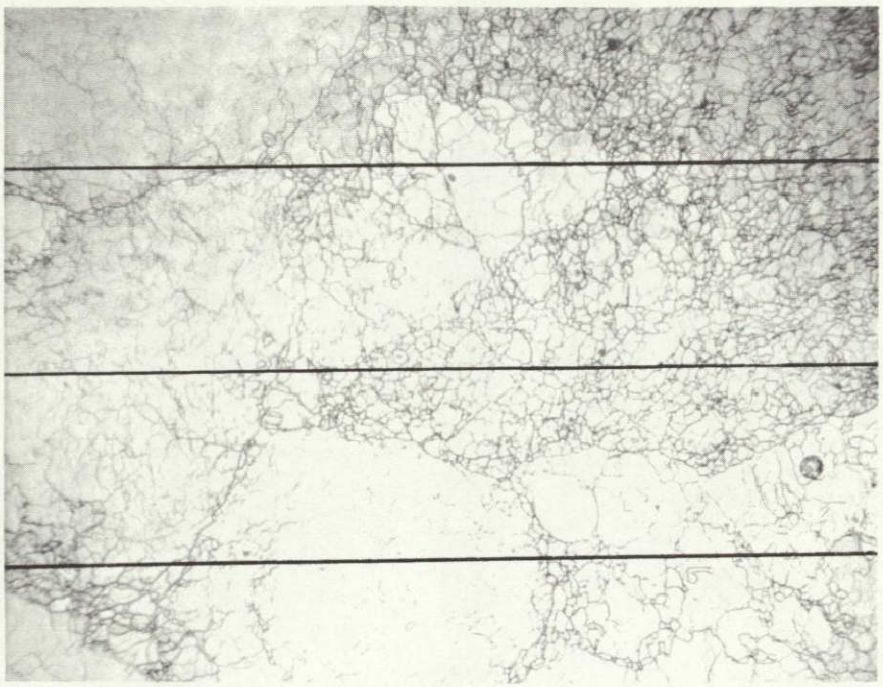

76–03–234–9

FIG. 53

EUROPIUM DOPED POLYCRYSTAL KCl AFTER IRRADIATION FOR 100 HRS

(GRAIN SIZE)

WINDOW 6–C

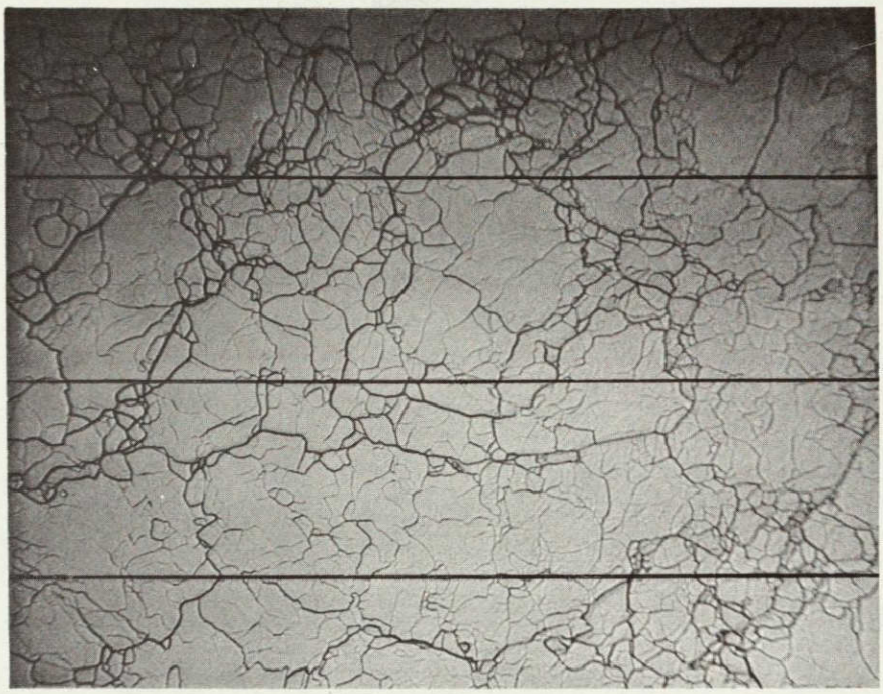

1000 W/cm^2

0.05 mm

WINDOW 5–C

1495 W/cm^2

0.05 mm

76–03–234–2

FIG. 54

EUROPIUM DOPED POLYCRYSTAL KCl AFTER IRRADIATION FOR 100 HRS

(GRAIN SIZE)

WINDOW 1—C

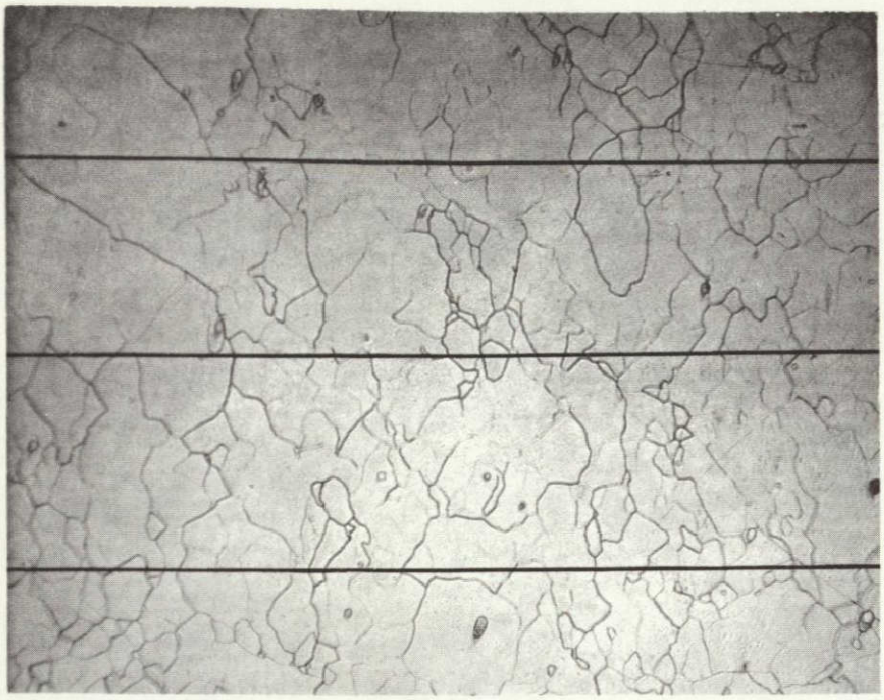

2236 W/cm^2

0.1 mm

WINDOW 4—C

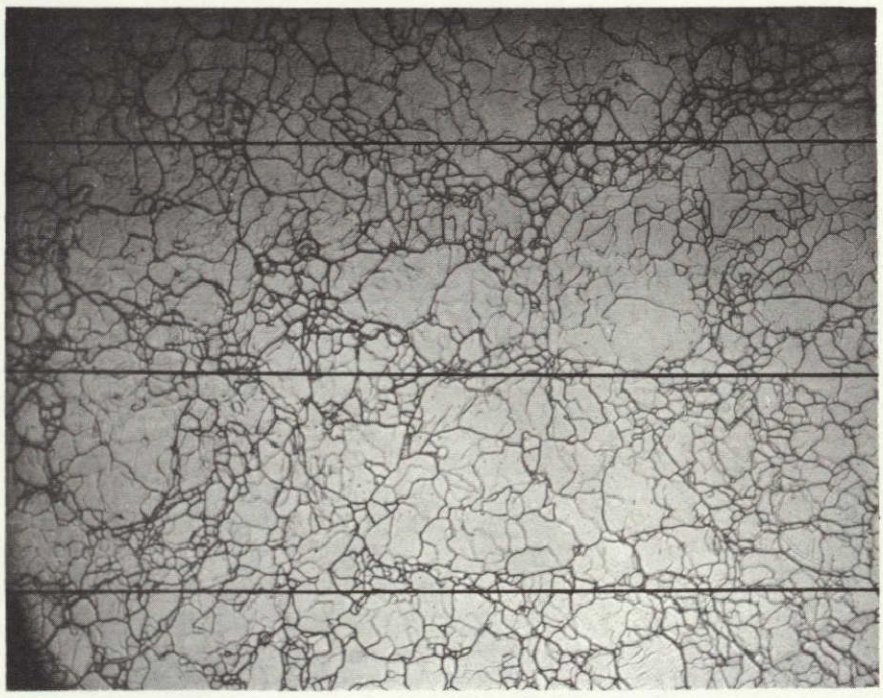

5000 W/cm^2

0.05 mm

76—03—234—7

FIG. 55

EUROPIUM DOPED POLYCRYSTAL KCl AFTER 100 HRS THERMAL AGING

(GRAIN SIZE)

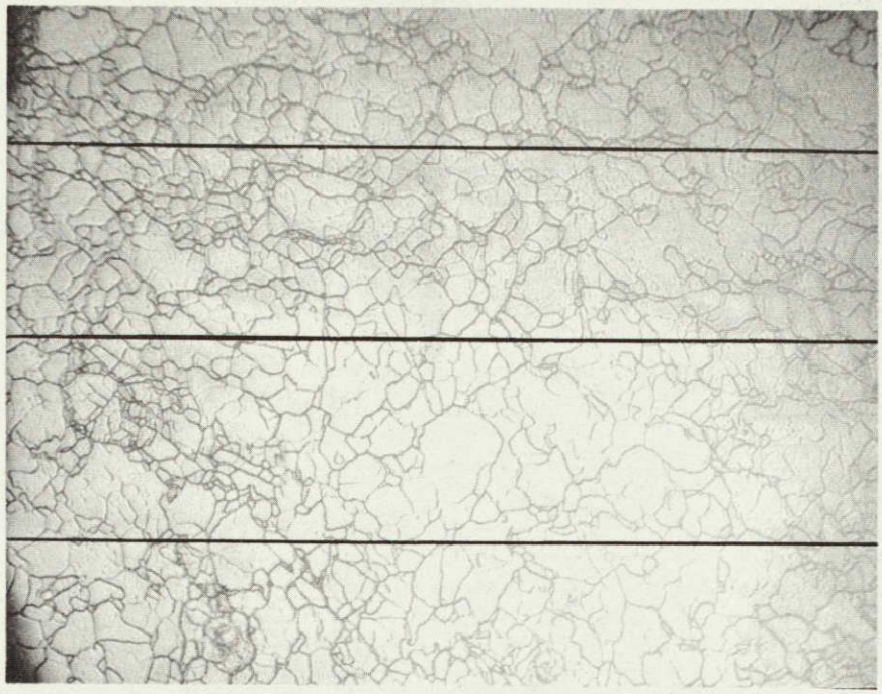

WINDOW 8–C

20°C

0.05 mm

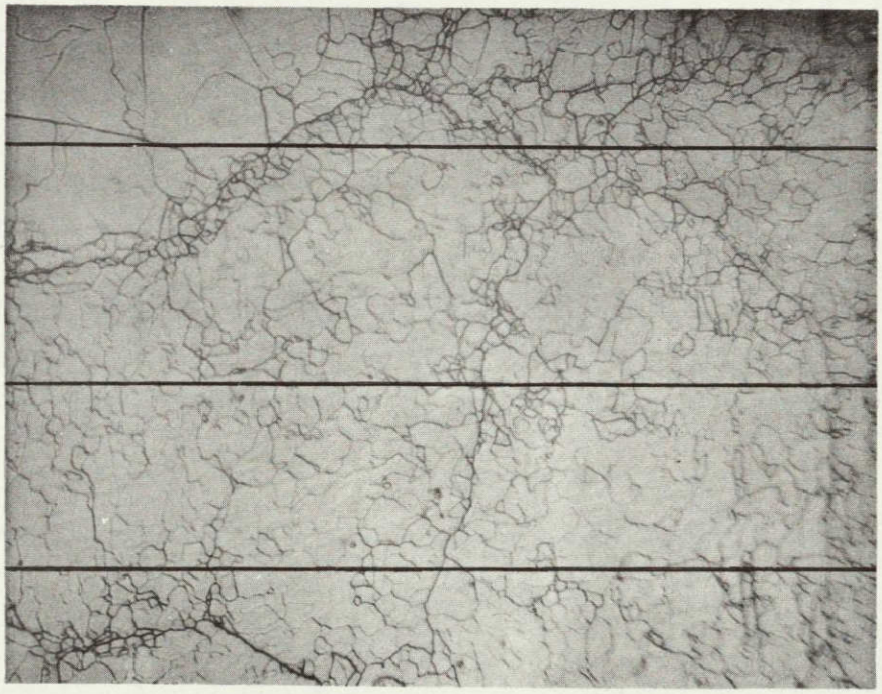

WINDOW 14–C

66°C

0.05 mm

76–03–234–4

FIG. 56

EUROPIUM DOPED POLYCRYSTAL KCl AFTER 100 HRS THERMAL AGING

(GRAIN SIZE)

WINDOW 15–C

118°C

0.05 mm

WINDOW 7–C

179°C

0.05 mm

76–03–234–1

FIG. 57

EUROPIUM DOPED POLYCRYSTAL KCl AFTER 100 HRS THERMAL AGING

(GRAIN SIZE)

WINDOW 12–C
250°C

0.05 mm

76–03–234–6

Thermal Stress Induced Failure of Alkali-Halide Windows

By P. R. Blaszuk

INTRODUCTION

The purpose of this effort was to attempt to validate our understanding of the mechanisms involved in the failure of alkali-halide windows subjected to CW laser irradiation with edge cooling being the principal method of heat removal. Initial consideration of this problem led to the concept that the windows were being stressed beyond the elastic limit, particularly at the outside edge. This plastic deformation was presumed to then lead to failure. In order to simulate the exposure of windows to high power irradiation, a scaling analysis is developed in the first two sections, which shows that for a fixed ratio of beam to window diameter the stress at window edge is linearly proportional to the product of power and absorptivity. On this basis an experiment was developed using windows with very high β at low power to simulate our conventional windows. Plastic deformation has been observed in these windows and the experimental results are summarized in the third section.

THERMAL ANALYSIS

The geometry considered was a right circular cylinder of length h, thermal conductivity κ, diameter $2\mathcal{R}$ being heated by a volume source $I\beta$. in a region between $\rho = 0$ and $\rho = b$. The heat flow equations in the region o-b becomes:

$$\frac{\partial^2 T}{\partial \rho^2} + \frac{1}{\rho}\frac{\partial T}{\partial \rho} + \frac{I\beta}{K} = 0 \qquad (31)$$

The resulting temperature distribution is

$$T = C - \frac{I\beta\rho^2}{4K} \qquad (32)$$

where C is yet to be determined.

In the source free region (1) reduces to:

$$\frac{\partial^2 T}{\partial \rho^2} + \frac{1}{\rho}\frac{\partial T}{\partial \rho} = 0 \tag{33}$$

and the temperature distribution becomes:

$$T = \frac{I\beta b^2}{2} \ln\left(\frac{R}{\rho}\right) \tag{34}$$

where we have set the temperature at $\rho = R$ to zero.

Matching boundary conditions at b on both (2) and (4) we obtain the value of the unspecified constant C in (2). The temperature variation in the disk is found to be:

$$T(\rho) = \frac{I\beta b^2}{4K} + \frac{I\beta b^2}{2K}\ln\left(\frac{R}{b}\right) - \frac{I\beta\rho^2}{4K}; \quad 0 \le \rho \le b \tag{35}$$

$$T(\rho) = \frac{I\beta b^2}{2K}\ln\left(\frac{R}{\rho}\right); \quad b \le \rho \le R \tag{36}$$

STRESS ANALYSIS

For a solid disk subjected to azimuthally symmetric heating the radial and azimuthal stress can be calculated directly from the temperature distribution. Pressure forces are ignored here since they can be added via linear superposition as long as the material is not stressed beyond yield. The radial and azimuthal stress components are (Ref. 1): where α is the expansion coefficient and ϵ is Young's modulus.

$$\sigma_{rr} = \alpha\epsilon\left[\frac{1}{R^2}\int_0^R T(\rho)\,\rho\,d\rho - \frac{1}{\rho^2}\int_0^\rho T(\rho)\,\rho\,d\rho\right] \tag{37}$$

$$\sigma_{\theta\theta} = \alpha\epsilon\left[\frac{1}{R^2}\int_0^R T(\rho)\,\rho\,d\rho - \frac{1}{\rho^2}\int_0^\rho T(\rho)\,\rho\,d\rho - T(\rho)\right] \tag{38}$$

Substituting the radial temperature distribution (5), (6) the azimuthal stress component at the outside edge becomes:

$$\sigma_{\theta\theta} = \alpha\epsilon\frac{I\beta b^2}{KR^2}\left[-\frac{b^2}{8} + \frac{R^2}{4}\right] \tag{39}$$

The calcualtion of σ_{rr} or $\sigma_{\theta\theta}$ at any arbitrary radius is perfectly straight forward since the necessary integrals reduce to algebraic expressions similar to the above.

EXPERIMENTAL RESULTS

The purpose of the experiment was to demonstrate in-situ plastic flow in a KCl window subjected to thermal stress caused by 10.6 micron radiation. The preceding theoretical section demonstrated that the basic scaling parameters for the azimuthal tensile stress at the window edge was the product of the power and β with a modifying factor that considers the intensity distribution and the window geometry. We have made use of this linear $P\beta$ scaling to construct an experiment that replaces our normal problem of a low β window subjected to high power radiation with a high β window operating at low power levels. The experiments have shown that permanent deformation of the KCl can occur with $P\beta$ loadings as small as 1 watt. The experimental apparatus consists of a forced water cooled mount which serves to maintain the outside edge of the test window at a constant temperature. Strain gauges are then mounted on the periphery of the window to determine the azimuthal strain induced by the irradiation. Figure 1 shows the results of a set of power irradiation cycles on a 1 1/2-inch diameter window with a β of 0.007 cm^{-1} (approximately 7 times that expected in a normal high quality window). The first irradiation cycle with a power level of 170 watts was sufficient to produce plastic flow in the material. The apparent limit for elastic behavior is about 130 micro inches/inch in strain. Using Young's Modulus, which is in range of 1.5×10^6 psi to 4×10^6 psi for this material, the stress at the elastic limit is in the range 195 psi-520 psi.

During the second irradiation cycle at 150 watts no plastic deformation was observed. This cycle and cycle 4 were run to insure that the strain gauge bonds to the substrate were still intact. Cycle 3 at the 300 watt level shows the plastic flow very clearly. The deformation rate at 300 watts was on the order of 25 micro inches per inch-minute. The particular sample was from Harshaw boule 25-6-12". Figure 2 shows data obtained with a window of identical size having a β of 0.005 cm^{-1} cut from Harshaw boule 3-27-10", which has an apparent elastic limit expressed in strain, of 500 micro inches/inch. Power levels in excess of 600 watts were necessary to produce plastic flow in this material. This corresponds to a yield stress of 750 psi to 2000 psi if Young's Modulus of this particular sample is within the expected range.

CONCLUSION

In the light of the experimental data and the theoretical analysis we can set approximate boundaries on the power capabilities of the various window materials using a criterion of max stress equal to 1/2 yield stress for presently available material. For a conduction cooled window these limits are: KCl single crystal (1 kW), KCl polycrystalline material (5 KW). These power estimates are based on a β of 0.001 cm^{-1} for the KCl. Needless to say, the present analysis does not consider problems such as grain growth in the polycrystalline material.

Operation of windows at power levels that raise the maximum stress above yield has been shown to produce plastic deformation. At the present time, we have no reliable means of predicting the time to failure of windows subjected to repetitive plastic deformation.

IRRADIATION INDUCED PLASTIC FLOW IN KCL

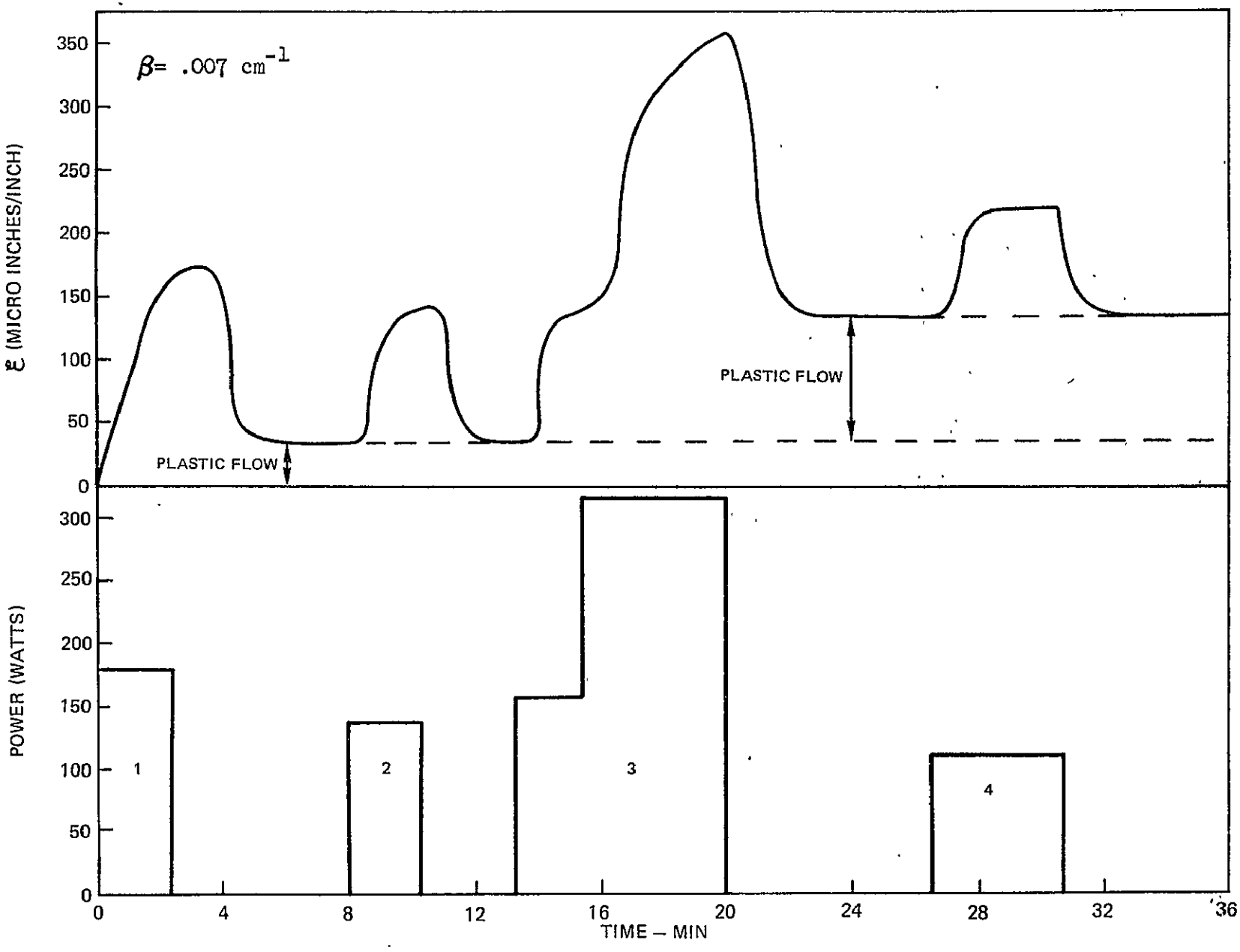

Fig. 1

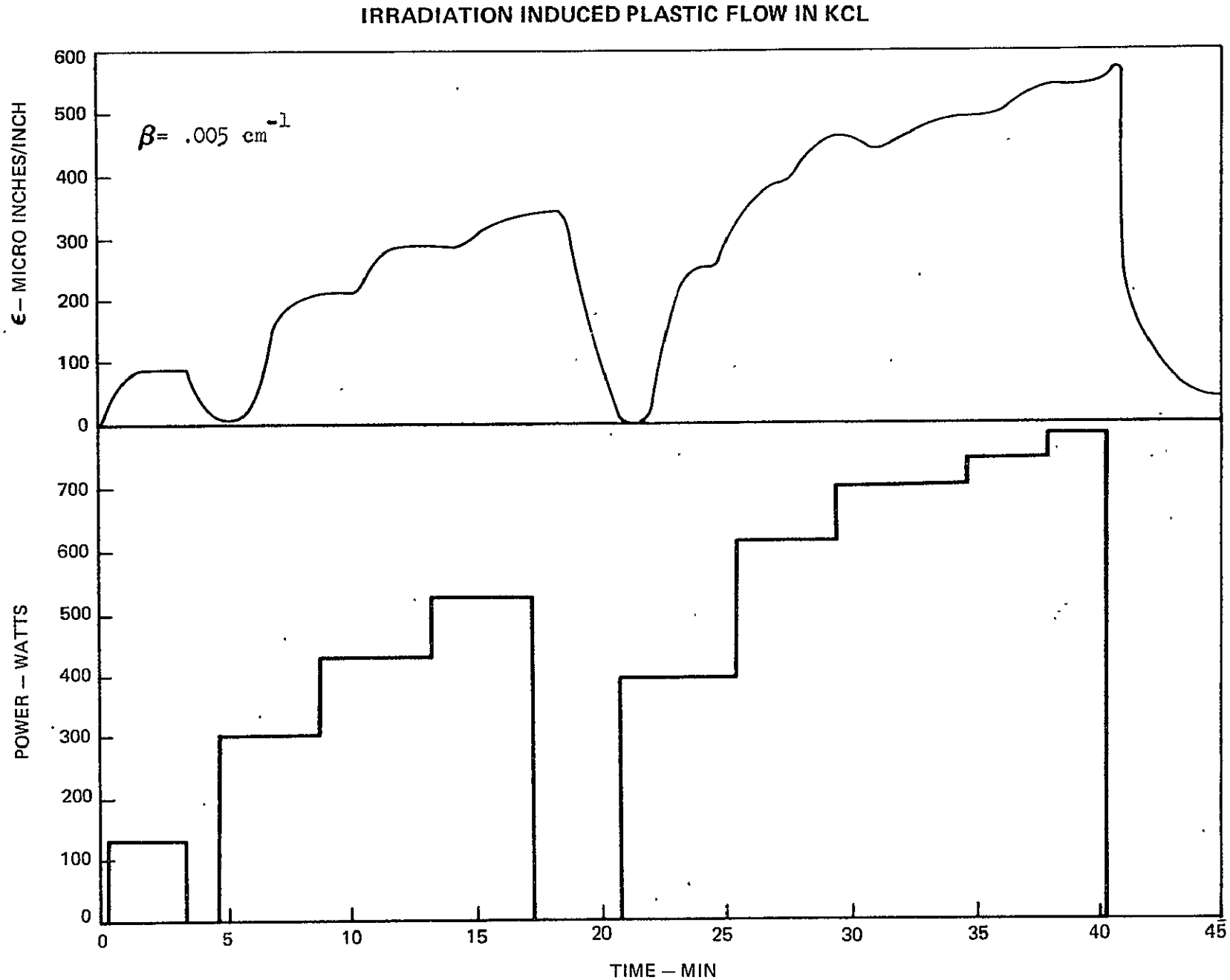
IRRADIATION INDUCED PLASTIC FLOW IN KCL
β= .005 cm⁻¹
ε – MICRO INCHES/INCH
600
500
400
300
200
100
0
POWER – WATTS
700
600
500
400
300
200
100
0
0
5
10
15
20
25
30
35
40
45
TIME – MIN

Fig. 2

Vacuum Evaluation of a New Perfluoroelastomer

M. F. Zabielski

and

P. R. Blaszuk

United Technologies Research Center

East Hartford, Connecticut 06108

Introduction

The elastomeric O-rings used in high vacuum valves and flanges generally limit system bake temperatures to a maximum of 200°C and, typically, to below 150°C. Above these temperatures, most elastomers have poor mechanical properties and outgas excessively. In order to bake a system at 300°C, gold, OFHC copper, or polyimide seals are required. The advantages and disadvantages of metal seals are well documented.[1] Polyimide has excellent outgassing properties at elevated temperatures if properly cured;[2] however, it does not have the desirable mechanical properties of an elastomer like Viton. In fact, polyimide is relatively brittle, subject to chipping and, typically, requires considerable stress to effect a seal.

High temperature, atmospheric pressure experiments conducted at this laboratory on a new fluorocarbon elastomer indicated that this elastomer might be a suitable replacement for metal and polyimide seals in systems bakeable to 300°C. This elastomer, developed by E. I. duPont de Nemours & Co., is sold under the name ECD-006 perfluoroelastomer. It possesses many of the mechanical properties of Viton, but with a significantly superior high temperature limit. Most of its mechanical and chemical properties at atmospheric pressure and high temperatures have

been documented.[3,4] However, there has been no effort, to date, to investigate its high vacuum properties. This brief communication presents some data on these properties.

Experimental Procedures and Results

Two types of measurements were made. The first was a simple comparison of the outgassing rates of Viton and ECD-006. The second was an evaluation of ECD-006 as an O-ring in a bakeable valve.

A. Outgassing

Figure 1 shows the apparatus used to compare the outgassing rates of Viton and ECD-006. The sample was placed in an enclosed volume on a stainless steel (Type 304) plate which was 1.27 cm (0.5 in.) on a side and .381 mm (.015 in.) thick. The temperature of the plate was monitored with a chromel-alumel thermocouple. The heater was constructed to minimize temperature gradients in the center of the plate. Heating of the plate was accomplished by radiation from tungsten filaments. Pressure within the enclosed volume was measured by a nude ionization gauge. A shield was interposed between this gauge and the sample plate to reduce charged particle bombardment of the sample. The only orifice connecting the sample volume with the main chamber was a 1.91 cm (0.750 in.) orifice through a 0.015 in. stainless steel removable

cover plate. The volume of the sample enclosure was 2.5 ℓ. The pressure in the main chamber was also determined by a nude ionization gauge. Thoriated iridium filaments were used on both gauges. Two separate ionization gauge control units were employed. With the cover plate removed, the gauges agreed to within 5% of reading. The output from each gauge control was recorded along with data from the thermocouple. The current provided to the heater came from a programmable power supply operated in a voltage programmed mode. The control voltage to this power supply was a slow ramp obtained from a commercial function generator. A dc power supply was also used when a particular temperature was to be maintained.

Each sample was 0.318 cm (1/8 in.) by 0.635 cm (1/4 in.) by 0.159 cm (1/16 in.). After the sample was placed on the plate and secured with a tungsten ribbon, the chamber was evacuated, and both ionization gauges were turned on. The radiation from the ionization gauge within the sample volume was sufficient to quickly bring the temperature of the sample to 120°C. The samples were baked at this temperature for four hours. After this bake, the pressure in the sample volume was typically 9.33 - 10.67 x 10^{-5} Pa (7-8x10^{-7} Torr) while the pressure in the main chamber was 6.67 - 8.00 x 10^{-5} Pa

($5\text{-}6\times10^{-7}$ Torr). The temperature of the sample plate was then elevated from 120°C to 400°C over approximately a 13 minute interval. Each sample tested experienced approximately the same heating rate because of the use of the programmable supply. The accuracy of the temperature measurement was estimated to be ±10°C. Since the rate of temperature rise with time was slow relative to the gas equilibrium times, the outgassing rate q_o was computed in terms of nitrogen equivalents using the relationship

$$q_o = S(P_2-P_1) \tag{40}$$

where P_2 was the pressure in the sample volume, P_1 was the pressure in the main chamber, and S was the speed of the pumpout orifice. A pumping speed of 11.6 l/sec-cm^2 was assumed which for this orifice yielded a speed of 33 l/sec. In Figure 2 are shown the outgassing rates as a function of temperature for ECD-006, Viton, and a stainless steel blank which was used as a reference.

B. Valve Test

In order to check the mechanical properties of ECD-006 at elevated temperatures in a typical high vacuum application, the following test was performed. A 1.5 in. right angle, high vacuum valve (Varian 951-5072) was attached to a 30 l/s VacIon pump. The valve was initially provided with polyimide gaskets on both

the bellows and main seals, so that the valve could be baked to 300°C. Because the VacIon pump had seen extensive service during which it was exposed to large quantities of hydrogen and noble gases, the terminal pressure after a 48 hour bake at 300°C was 5.33 - 6.66 x 10^{-6} Pa (4-5x10^{-8} Torr), even though the pump was capped and the only load was the polyimide valve. The pressure was determined from the current drawn by the pump. After this base pressure was established, the polyimide main seal was replaced with an O-ring cut from ECD-006 sheet stock (Compound 01018). The valve was reassembled and then baked at 300°C for 48 hours. The terminal pressure after this bake was again 5.33 - 6.66 x 10^{-6} Pa (4-5x10^{-8} Torr). The valve was then disassembled, and the O-ring was inspected. The cracking and thermal set normally encountered with Viton when operated at temperatures in excess of 200°C were not present. The ECD-006 was still pliable. The valve was opened and closed several times with no apparent leaks across the main seal.

Results and Discussion

Despite the uncertainties associated with the outgassing measurements, e.g., the nitrogen equivalence assumption, the limited sample preparation, etc., Figure 2 indicates that

ECD-006 has an outgassing rate at least comparable if not superior to Viton in the temperature range up to 200°C. It also shows that ECD-006 has an acceptable outgassing rate at 300°C where Viton literally decomposes, as indicated by violent pressure bursts observed on the gauges. ECD-006, even when heated at 400°C, did not decompose as violently as Viton at 300°C. It is also interesting to note that the initial outgassing rate of ECD-006 at 300°C is only 3-5 times greater than that of the stainless steel blank.

The valve test that was performed used a valve that was designed to have a maximum bake temperature of 125°C in the closed position and 200°C in the open position if Viton-A was used for the main seal. A later design of this valve (Varian 951-5012) can be baked to 200°C in both open and closed positions because of a mechanical modification to reduce the problems of expansion and thermal set. With the ECD-006, bakeout at 300°C in the old style valve was accomplished witnout difficulty. Also, within the precision of these measurements, the room temperature outgassing rate of ECD-006 was comparable to polyimide.

The evidence of this study indicates that the vacuum properties of ECD-006 are such that it can be used as a

substitute for polyimide in the room temperature to 300°C operating regime. The measurements also indicate that more accurate tests should be made of the outgassing rates of ECD-006 and that its helium permeability, water absorption, and radiation resistance should be determined along with chemical character of the outgassing.

Footnotes

1. C. M. Van Atta, Vacuum Science and Engineering, McGraw Hill, N.Y., 1965.

2. Kendall, B. R. F. and M. F. Zabielski, J. Vac. Sci. Tech., 3, 114 (1966).

3. Barney, A. L., Kalb, G. H., and A. A. Khan, Rubber Chem. Tech., 44, 660 (1971).

4. Kalb, G. H., Quarles, R. W., and R. S. Graff, Applied Polymer Symposium, 22, 127 (1973).

List of Captions

Fig. 1. Outgassing Measurement Apparatus.

Fig. 2. Outgassing Rates as Functions of Temperature After 4-Hour Bake (120°C).

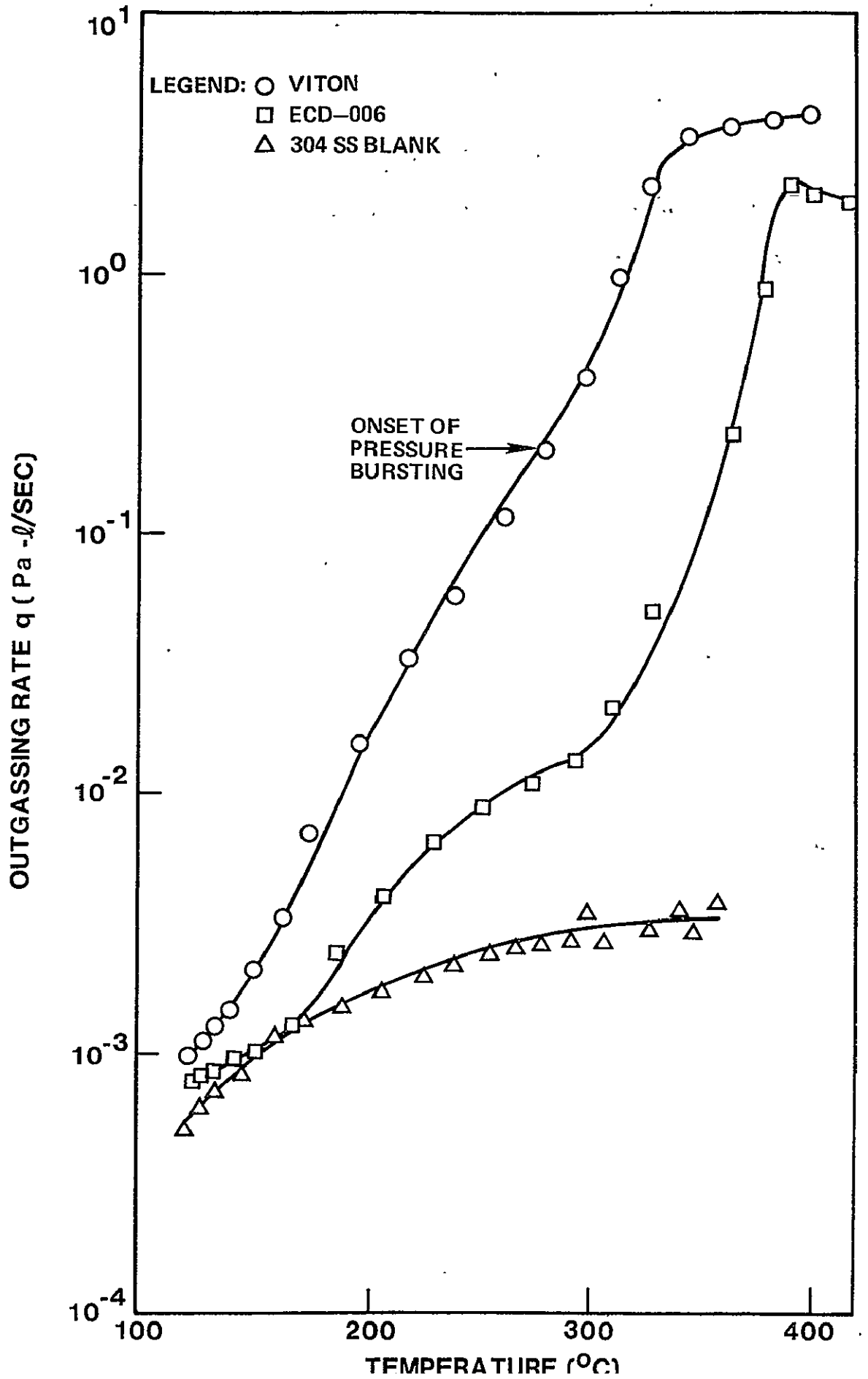
LEGEND: VITON
ECD–006
304 SS BLANK
ONSET OF PRESSURE BURSTING
OUTGASSING RATE q (Pa -ℓ/SEC)
10^{1}
10^{0}
10^{-1}
10^{-2}
10^{-3}
10^{-4}
100
200
300
400
TEMPERATURE (°C)

R05–206–3

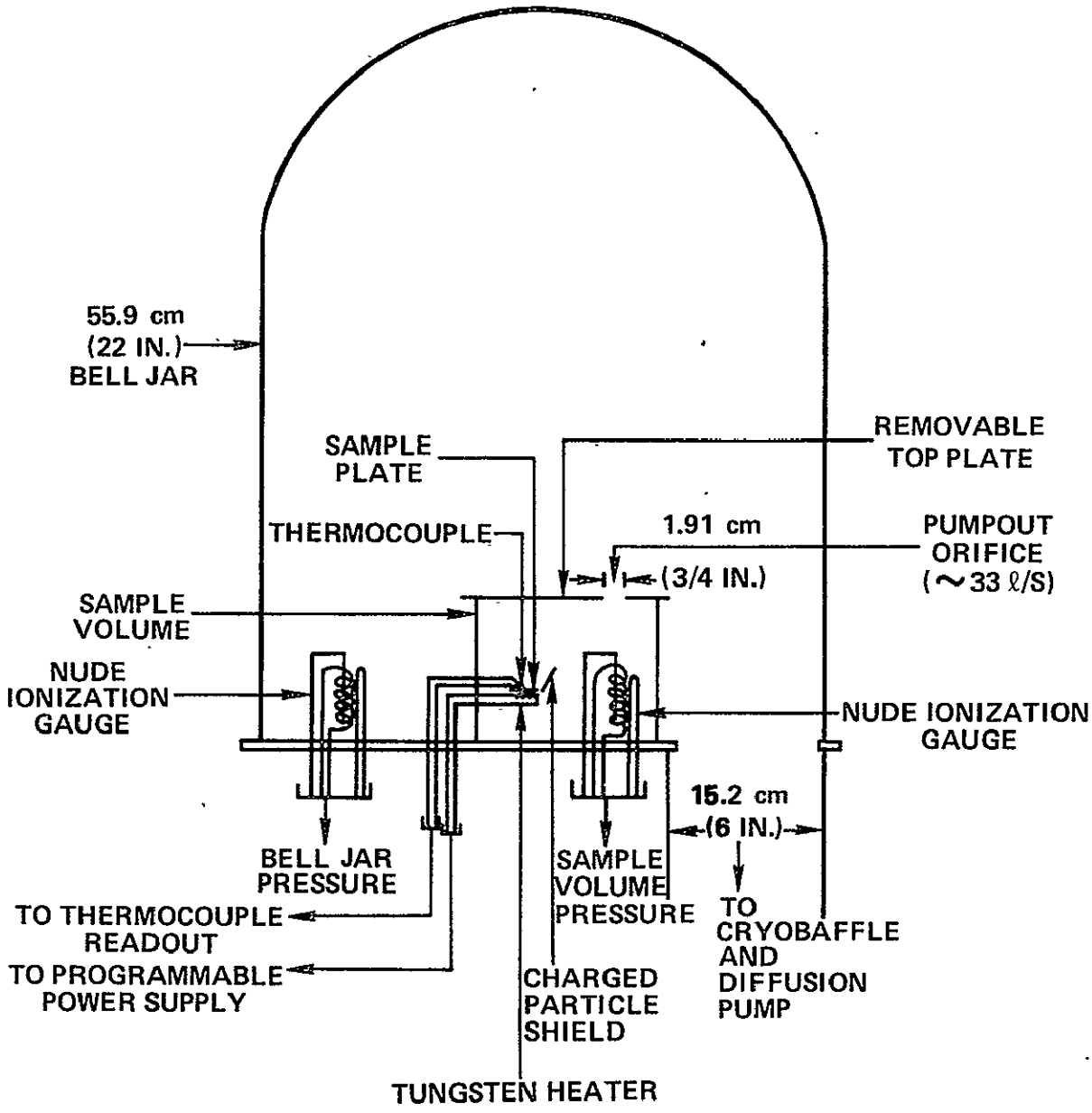
55.9 cm
(22 IN.)
BELL JAR
SAMPLE
PLATE
REMOVABLE
TOP PLATE
THERMOCOUPLE
1.91 cm
(3/4 IN.)
PUMPOUT
ORIFICE
(~33 ℓ/S)
SAMPLE
VOLUME
NUDE
IONIZATION
GAUGE
NUDE IONIZATION
GAUGE
15.2 cm
(6 IN.)
BELL JAR
PRESSURE
SAMPLE
VOLUME
PRESSURE
TO
CRYOBAFFLE
AND
DIFFUSION
PUMP
TO THERMOCOUPLE
READOUT
TO PROGRAMMABLE
POWER SUPPLY
CHARGED
PARTICLE
SHIELD
TUNGSTEN HEATER

R05–206–1

REFERENCES

1. Kulin, S. A.; Kreder, K.; Posen, H.; and Bowen, H. K.: Fabrication of Large Polycrystalline Infrared Windows. AFCRL-TR-73-0372 (II), Nov. 1973.

2. Posen, H.; Kulin, S. A.; Kreder, K.; and Bowen, H. K.: Properties of Large Polycrystalline KCl Windows. AFCRL-TR-73-0372 (II), Nov. 1973.

3. Rosette, K. H.; Swinehart, C. F.; and Shrader, E. F.: Divalent Ion Doping of Polycrystalline KCl. AFCRL-TR-73-0372 (II), No. 1973.

4. Rice, R. W.: High Energy Laser Windows. Semi-Annual Report #3, Naval Research Laboratory, ARPA Order 2031, Dec. 1973.

5. Deutsch, T. F.: Absorption Measurements on High-Power Laser Window Materials. AFCRL-TR-74-0085 (II), 1974.

6. Sparks, M.: Theoretical Studies of High-Power Infrared Window Materials. Technical Report, ARPA Contract No. DAHC15-73-C-0127, 30 June 1973.

7. Werner, A. J.: Methods in High Precision Refractometry of Optical Glass. Applied Optics, vol. 7, 1968, p. 837.

8. Bennett, H. E.: High Energy Laser Mirrors and Windows. Semi-Annual Report No. 5 under ARPA Order 2175, May 1974.

9. Hass, M.; Davisson, J. W.; Klein, P. H.; and Boyer, L. L.: Infrared Absorption in Low-loss KCl Single Crystals Near 10.6 μm. J. Appl. Phys., vol. 45, 1974, pp. 3959-3965.

10. Weil, R.: J. Appl. Phys., vol. 41, 1970, p. 3012.

11. Wolfe, W., ed.: Handbook of Military Infrared Technology. ONR Washington, D.C., 1965, cf p. 436.

12. Sherman, J. W.: Properties of Focused Apertures in the Fresnel Region. IRE Transactions on Antennas and Propagation, 1962, pp. 399-408.

13. McClintock, F. A.; and Matthews, J. R.: Design Strength of Polycrystalline KCl. Third Conference on High Power Infrared Laser Window Materials, vol. 2, Nov. 1973, p. 711.

14. Singh, R. N., et al: Strength and Fracture Behavior of Hot-Worked KCl. Third Conference on High Power Infrared Laser Window Materials, vol. 2, Nov. 1973, p. 693.

15. Soileau, M. J. et al: Polishing of Alkali-Halide Windows. Semi-Annual report #6. High Energy Laser Mirrors and Windows (ARPA Order 2175), Michelson Laboratory, Naval Weapons Center, China Lake, Calif., March 1975, p. 75.

16. Rice, R. W.: High Energy Laser Windows. Semi-Annual Report No. 6, ARPA Order 2031, Naval Research Laboratory, Washington, D. C.

17. Slack, G. A.: Thermal Conductivity of Potassium Chloride Crystals Containing Calcium. Physical Review, vol. 105, #3, p. 834 (1957).

18. Moran, P. R.: Dislocation Etch Techniques for Some Alkali Halide Crystals. J. Appl. Phys., vol. 29, #12, p. 1768 (1958).

19. Mendelson, M. I.: Average Grain Size in Polycrystalline Ceramics, J. Am. Ceram. Soc., vol. 52, #8, pp. 443-46 (1969).

20. Volk, W.: Applied Statistics for Engineers. McGraw-Hill Book Co., Library of Congress Card No. 6911710. (1969).

DISTRIBUTION LIST
Contract NAS3-18928

NASA-Lewis Research Center
21000 Brookpark Rd.
Cleveland, OH 44135

Atten: Contracting Officer, John Dilley, M.S. 500-313 (1)
Atten: Library, M.S. 60-3 (2)
Atten: Project Manager, R.A. Lindberg M.S. 105-1 (10)
Atten: W. D. Klopp, M.S. 105-1 (1)
Atten: N. T. Saunders, M.S. 105-1 (1)
Atten: R. L. Ashbrook, M.S. 49-3 (1)
Atten: W. F. Brown, M.S. 105-1 (1)
Atten: R. H. Kemp, M.S. 49-3 (1)
Atten: S. J. Grisaffe, M.S. 49-3 (1)
Atten: F. B. Garrett, M.S. 105-1 (1)
Atten: H. B. Probst, M.S. 49-3 (1)
Atten: J. C. Freche, M.S. 49-1 (1)
Atten: H. H. Grimes, M.S. 106-1 (1)
Atten: R. M. Stubbs, M.S. 500-318 (1)
Atten: Jack G. Slaby, M.S. 500-318 (1)
Atten: S. M. Cohen, M.S. 500-318 (1)

NASA-Scientific and Technical Information Facility
P.O. Box 8757
Balt/Wash International Airport
MD 21240
Atten: Accessioning Dept. (40)

National Aeronautics & Space Admin.
Headquarters,
Washington, D.C. 20546
Atten: Office of Aeronautics & Space Tech., Director, Space Prop. & Power/R.P. (1)
Atten: F. C. Schwenk/R.R. (1)
Atten: Dr. J. G. Lundolum, Jr./R.R. (1)
Atten: N. J. Mayers/RWS (1)
Atten: G. C. Deutsch/RW (1)

National Aeronautics & Space Admin.
Flight Research Center
P. O. Box 273
Edward, CA 93523
Atten: Library (1)

National Aeronautics & Space Admin.
George C. Marshall Space Flight Cntr.
Huntsville, Alabama 35912
Atten: Library (1)

National Aeronautics & Space Admin.
Goddard Space Flight Center
Greebelt, MD 20771
Atten: Library (1)

National Aeronautics & Space Admin.
John F. Kennedy Space Center
Cocoa Beach, Florida 32931
Atten: Library (1)

National Aeronautics & Space Admin.
Lyndon B. Johnson Space Center
Houston, Texas 77001
Atten: Library (1)

National Aeronautics & Space Admin.
Langley Research Center
Langley Station
Hampton, VA 23365
Atten: Library (1)

Jet Propulsion Laboratory
4800 Oak Grove Dr.
Pasadena, CA 91103
Atten: Library (1)

Air Force Geophysics Laboratory
Hanscom AFB, MA 01731
Atten: C. Sahagian (1)
Atten: H. Posen (1)
Atten: Library (1)

DISTRIBUTION LIST (Cont'd.)

Air Force Materials Laboratory
AFML/LPO
Wright-Patterson AFB, OH 45433
Atten: Major Paul Elder(LPJ) (1)
Atten: Library (1)

Air Force Weapons Laboratory
Kirtland AFB, NM 87117
Atten: AFWL/LR Col. D. L. Lamberson(1)
Atten: AFWL/AR Col. R. K. Parsons (1)
Atten: AFWL/AL Col. R. D. Rose (1)
Atten: John C. Schultz (PG) (1)
Atten: Lt. Col. John C. Rich (AL) (1)
Atten: Lt. Col. R. F. Prater (1)
Atten: Dr. D. R. Dean/ALO (1)
Atten: Major L. T. James/ALO (1)

Defense Advanced Research Projects Agency
Director of Materials Science (707)
1400 Wilson Blvd.
Arlington, VA 22209 (1)

Defense Documentation Center
Cameron Station
Bldg. 5
5010 Duke St.
Alexandria, VA 22314
Atten: TISIA (1)

ODDR & E
Pentagon
Washington, D.C. 20301
Atten: Dr. Robert Greenberg (1)

Superintendent
Naval Postgraduate School
Monterey, CA 93940
Atten: Library (1)

U. S. Naval Weapons Center
China Lake, CA 93555
Atten: E. B. Niccum (Code 5114) (1)

Naval Research Laboratory
Washington, D.C. 20375
Atten: Dr. P. Livingston
(Code 5560) (1)
Atten: Dr. J. L. Walsh
(Code 5503) (1)
Atten: Dr. J. T. Schriempf
(Code 6410) (1)
Atten: Dr. J. Davisson (1)
Atten: R. Rice (1)
Atten: M. Hass (1)
Atten: F. Patten (1)
Atten: H. Rosenstuk (1)
Atten: John C. Kershenstein (1)

Headquarters Electronics Sys. Div.
Hanscom AFB, MA 01731
Atten: Capt. Allen R. Tobin(XRE)(1)

Hughes Research Laboratories
3011 Malibu Canyon Rd.
Malibu, CA 90265
Atten: Arthur N. Chester (1)
Atten: Dr. Viktor Evtuhov (1)
Atten: Dr. A. L. Gentile (1)
Atten: Dr. Susan Allen (1)
Atten: Dr. R. C. Pastor (1)
Atten: Dr. A. C. Pastor (1)
Atten: Library (1)

Itek Corporation
Optical Systems Div.
10 Maguire Rd
Lexington, MA 02173
Atten: R. J. Wollensak (1)

Perkin Elmer Corp.
Norwalk, CT 06856
Atten: Dr. D. A. Dooley (1)
Atten: Jack Callahan (1)

DISTRIBUTION LIST (Cont'd.)

Raytheon Co.
Research Division
28 Seyon Street
Waltham, MA 02154
- Atten: Dr. Frank A. Herrigan (1)
- Atten: A. Levine (1)
- Atten: J. Burns (1)
- Atten: F. Petri (1)
- Atten: Library (1)

W. J. Schafer Associates, Inc.
Lakeside Office Park
607 N. Avenue, Door 14
Wakefield, MA 01880
- Atten: Francis W. French (1)

Westinghouse Research Laboratories
Beulah Rd., Churchill Boro.
Pittsburgh, PA 15235
- Atten: Mr. R. L. Hundstad (1)

Harshaw Chemical Co.
6801 Cochran Rd.
Solon, OH 44139
- Atten: Mr. E. C. Stewart (1)
- Atten: Dr. E. Shrader (1)
- Atten: Dr. K. Rosette (1)
- Atten: Dr. O. Nestor (1)
- Atten: Dr. C. Swinehart (1)
- Atten: Mr. D. J. Krus (1)
- Atten: Mr. H. Williams (1)
- Atten: D. R. Lesli (1)
- Atten: D. Cope (1)
- Atten: K. Brumbergs (1)

General Electric Corporation
Re-Entry and Environmental Systems
Product Division
Advanced High Energy Electronic Systems
3198 Chestnut St.
Philadelphia, PA 19101
- Atten: Manager. Jacob B. Gilsden (1)

Westinghouse Electric Corp.
Systems Development Div.
(S.D.D.)
Post Office Box 746;
Baltimore, MD 21203
- Atten: Mngr. William F. List (1)

National Bureau of Standards
Gaithersburgh, MD 20760
- Atten: H. Bennett (1)
- Atten: M. Dodge (1)
- Atten: J. Malitson (1)

Honeywell Ceramic Center
1885 North Douglas
Golden Valley, Minn. 55422
- Atten: W. Harrison (1)
- Atten: G. Hendrickson (1)
- Atten: J. Starling (1)

Honeywell Corporate
Research Center
Honeywell Plaza
Minneapolis, Minn. 55408
- Atten: E. Bernal (1)

University of Alabama
Huntsville, Alabama 35807
- Atten: Prof. J. Harrington (1)

University of Arizona
Tuscon, Arizona 85721
- Atten: J. Loomis (1)

University of Dayton
Research Institute
Dayton, OH 45409
- Atten: J. Wurst (1)
- Atten: G. Graves (1)
- Atten: C. Robert Andrews (1)

M.I.T.
Cambridge, MA 02139
- Atten: Prof. H. Bowen (1)